

ABSTRACT

Title of Thesis: COMPUTATIONAL SCREENING FOR NOVEL
INHIBITORS OF PROTEINS IN THE MAST CELL
DEGRANULATION PATHWAY

Team CASCADE, 2021

Thesis directed by: Dr. Kenneth Frauwirth
Department of Cell Biology & Molecular Genetics

Allergies are a pervasive issue and require novel ways of alleviating symptoms. Existing treatments focus on symptom management and immunotherapy in response to an allergic reaction. However, there is also the potential for prophylactic treatment that inhibits molecules involved in the mast cell degranulation pathway, which causes allergic symptoms. We identified potential target proteins downstream of this pathway including PKC, PLC γ , and PI3K isoforms, the activation of which results in the degranulation of mast cells. We computationally modeled protein-inhibitor binding interactions and identified inhibitors with the predicted highest binding affinity to the target pathway proteins. For the most efficient inhibitors, we extended our analysis by construction of analogs to determine which chemical properties of the inhibitors contributed to the highest binding affinity. The identified possible inhibitors have the potential to hinder mast cell degranulation, limit histamine and cytokine release, and therefore prevent allergic symptoms, making them ideal targets for future pharmacology research.

COMPUTATIONAL SCREENING FOR NOVEL
INHIBITORS OF PROTEINS IN THE MAST CELL
DEGRANULATION PATHWAY

by

Team CASCADE

Naja Fadul, Zachary Kasica, Kyeisha Laurence, Stephanie Moy, Sindhu Murugan,
Chinmayi Pamala, Morgan Robinson, Rohan Shah, Mansu Shrestha, Marcus Smith,
Bhavya Vashi

Mentor: Dr. Kenneth Frauwirth

Librarian: Celina McDonald

Thesis submitted in partial fulfillment of the requirements of the Gemstone Honors
Program, University of Maryland, College Park 2021

Advisory Committee:
Dr. Kenneth Frauwirth
Dr. Paul Pakustelis
Dr. Silvina Matysiak
Dr. Nicole LaRonde

© Copyright by

Team CASCADE

Naja Fadul, Zachary Kasica, Kyeisha Laurence, Stephanie Moy, Sindhu Murugan,
Chinmayi Pamala, Morgan Robinson, Rohan Shah, Mansu Shrestha, Marcus Smith,

Bhavya Vashi 2021

Acknowledgements

We would like to thank our incredible mentor Dr. Kenneth Frauwirth, our librarian Celina McDonald, and Dr. David Mosser and Kajal Hamidzadeh for the generous use of their laboratory space. Thank you to our discussants, Dr. Paul Paukstelis, Dr. Silvina Matysiak, and Dr. Nicole LaRonde for their useful critique and expert guidance. We'd also like to thank our LaunchUMD Donors for their generosity, as well as the Gemstone staff for their support: Dr. Coale, Dr. Lovell, Dr. Skendall, Dr. Hill, and Dr. Tobin.

Table of Contents

Acknowledgements.....	i
Table of Contents.....	ii
Introduction.....	1
Literature Review.....	4
Overview of Immune Responses.....	4
Allergic Response Mechanism.....	6
Immunoglobulin G and Immunoglobulin E.....	8
B Cell Activation.....	9
FcεR1.....	10
Signaling Pathways.....	11
Lipid Rafts, LYN, FYN, GAB2, PI3K.....	11
PLCγ and PLD Pathways.....	14
Sphingosine Kinase Pathway.....	15
PKA and cAMP.....	16
Current Treatments.....	17
Symptom Management.....	17
Allergy Immunotherapy.....	18
Anti-Cytokine Drug Therapy.....	19
Anti-IgE Drug Therapy.....	20
Adenine in Cell Signaling.....	21
Potential Targets.....	21
State of Current Research in Protein Modeling.....	22
Materials and Methods.....	25
Refining Macromolecules.....	25
Preparing Ligands for Docking.....	25
Analogues.....	26
Results.....	28
Protein Structure Analysis.....	28
Binding Energy of Established Inhibitors.....	29
Analogues of Selected Inhibitors.....	31
PI3K Inhibitor: Wortmannin.....	32
PI3K Inhibitor: ZSTK474.....	34
PKCβ1 Inhibitor: Enzastaurin.....	36
PKCβ1 Inhibitor: Ruboxistaurin.....	38
PKCβ1 Inhibitor: Midostaurin.....	41
PKCβ2 Inhibitor: Enzastaurin.....	44
PKCβ2 Inhibitor: Sotrastaurin.....	45
PKCδ Inhibitor: Sotrastaurin.....	47
PKCδ Inhibitor: Rottlerin.....	49
PKCη Inhibitor: Sotrastaurin.....	52
PLCγ1 Inhibitor: U73122.....	55
PLCγ2 Inhibitor: U73122.....	57
Discussion.....	59
Future Directions.....	69

Equity Impact Report.....	74
Defining Equity in Healthcare.....	74
Who Our Research Serves: Identifying Stakeholders	75
Examining the Causes of Inequities and Considering Adverse Impacts.....	77
Recommendations.....	78
Appendices.....	81
Appendix A - Glossary	81
Appendix B - Supplemental Figures.....	85
Appendix C - Structure Analysis and Comparison.....	87
References.....	124

Introduction

An allergy is a chronic condition due to an adverse reaction to an otherwise harmless environmental substance within the immune system. Allergies impede both the dietary and social lives of those affected as well as the families and communities surrounding each person. The allergic response is characterized by a range of symptoms from sneezing, runny nose, coughing, and itching to life-threatening reactions such as anaphylactic shock (Centers for Disease Control and Prevention, 2017). According to the World Health Organization (2011), the percentage of persons with sensitivity to allergens is 40% and climbing; it is the most pervasive disorder globally. In the United States, allergies are the sixth leading cause of chronic illness (Centers for Disease Control and Prevention, 2017).

Generally, allergies are the product of repeated reactions within the immune system to a specific allergen. In every reaction, the immune cells known as mast cells are activated, triggering a cascade of molecules to bind, activate, or recruit each other in a complex signaling pathway. This leads to degranulation, a process in which the cells release cytotoxic molecules and other inflammatory mediator molecules resulting in the manifestation of allergic reactions. (Metcalf et al., 2009). Currently, the most common therapeutics can be characterized in three ways: avoidance of the allergen, medication to treat symptoms, and immunotherapy. These current therapeutics involve significant lifestyle changes and treatment upkeep for the patients. Additionally, although inexpensive treatments are available, many patients find them insufficient for symptom

management. Therefore, there exists the opportunity to research novel allergy therapeutic options.

This research focuses on the intracellular signaling pathway within mast cells to screen for novel drug targets and identify inhibitors with the best binding affinity to signaling proteins. Previous treatments have targeted extracellular binding of antibodies and downstream release of inflammatory molecules, but not the signaling pathway. The identified inhibitors could then be synthesized by pharmaceutical companies and this allergy medication could be taken prophylactically.

To determine which inhibitors had the lowest binding energies, signaling protein structures were modeled in Pyre2 and refined using Modrefiner; these 3D structures were then modeled with different known inhibitors using PyRx, which outputted binding energies. The inhibitors that demonstrated protein-inhibitor interactions with the lowest binding energies were selected, and analogues of these inhibitors were derived from the ZINC database and modeled against signaling molecules. This analysis demonstrates proof of concept of the modeling procedure to identify effective inhibitors against biological signaling molecules, which can be refined and utilized in future drug screening procedures.

There are a few limitations to this study. These include the use of *in silico* modeling, which cannot entirely simulate the conditions in the human body. There might be unintentional effects on other biological processes due to the ubiquity of the target proteins in the human body. Furthermore, the modeling software is giving a best estimation of the binding energies, but these values are not exact, and may also differ

when done *in vitro* and *in vivo*. Therefore, further experimentation should be done in mast cell lines and murine models to verify these findings.

Literature Review

This section provides an overview of published works on the basic functions of the immune system, key components of the allergic response from the binding of antibodies to mast cells to the signaling pathway leading to degranulation, current treatments for allergic disease, and potential drug targets.

Overview of Immune Responses

In an adaptive immune response, the body utilizes many cell types to combat foreign substances known as antigens. When an antigen enters the body, it is detected and phagocytized by antigen-presenting cells (APCs). The engulfed antigen is broken up into peptide fragments by acid hydrolases in phagolysosomes which are then presented on surface proteins on the exterior of the APC (Warrington et al., 2011). These surface proteins, known as the major histocompatibility complex 2 (MHC2), work in conjunction with a second signal known as co-stimulation in order to induce T cell maturation and differentiation (Bonilla & Oettgen, 2010). If the T cell matures into a helper T cell, it can use the specificity of the original antigen to prompt B cells into producing antigen-specific antibodies. In different pathways, the B cell acts as an APC itself, and can use the antigen fragments to make specific antibodies (Bonilla & Oettgen, 2010). This is the mechanism of antibody-mediated immunity.

Due to DNA rearrangements within the B cell, every antibody made by a specific B cell is unique to that antigen and to its B cell (Alberts et al., 2002). This allows the B cells to make many antibodies to combat a specific antigen. After the encounter of an antigen, the B cell can clonally expand and differentiate into antibody-secreting effector

cells. Other B cells do not become effector cells, but function to retain the genetic memory for producing that specific antibody in order to ensure that a second exposure will trigger a more effective attack on the foreign substance (Warrington et al., 2011).

Most commonly in a normal immune response, effector B cells produce the immunoglobulin G (IgG) antibodies. Once bound to their specific antigen, the antibody can enact the antibody-mediated immune response, also known as the humoral immune response. Antibodies coat the antigen, which can block many of the pathogenic mechanisms of an antigen such as adhering to host tissues or binding to other mechanistic structures needed to carry out infection (Forthal, 2014). In other cases, opsonization occurs when the antibody coating of antigens promotes phagocytosis (Janeway et al., 2001). The presence of antibodies coating the antigens can cause phagocytes of the immune system to recognize protein sequences within the Fc region of the IgG antibodies and bind to Fc γ receptors found on the surface of the phagocytes (Hiemstra & Daha, 1998). This binding increases phagocytosis by pulling the membrane of the phagocyte around the antigen (Hiemstra & Daha, 1998). A final aspect of the humoral response occurs in the form of complement activation, which can lead either to enhanced opsonization or pathogen cell lysis (Noris & Remuzzi, 2013). In summary, the normal humoral immune response is largely dictated by the activity of immunoglobulin G and results in the neutralization of pathogenic substances to the body. This greatly differs from the allergic response, which is dictated by IgE rather than IgG.

Allergic Response Mechanism

In the allergic response mechanism, the naive T helper cell recognizes the antigen and the co-stimulatory molecule, it becomes a mature T Helper 2 cell (TH2). When interacting with the B cell, cytokines such as Il-4, Il-5, and Il-13 trigger the B cell to start producing Immunoglobulin E (IgE) instead of IgG (Bubnoff et al., 2001). The IgE then binds to the FcεR1 receptor on the mast cell. If there is another exposure of this same antigen, the specific IgE antibody is already produced and bound to the mast cell (Warrington et al., 2011). Once it recognizes the antigen, the Fab region of the IgE binds to the antigen. This causes the mast cell to degranulate and release proinflammatory mediators such as histamines, prostaglandins, and leukotrienes (Galli et al., 2008). Depending on the proinflammatory mediator released, the body expresses different reactions, as shown in Figure 1.

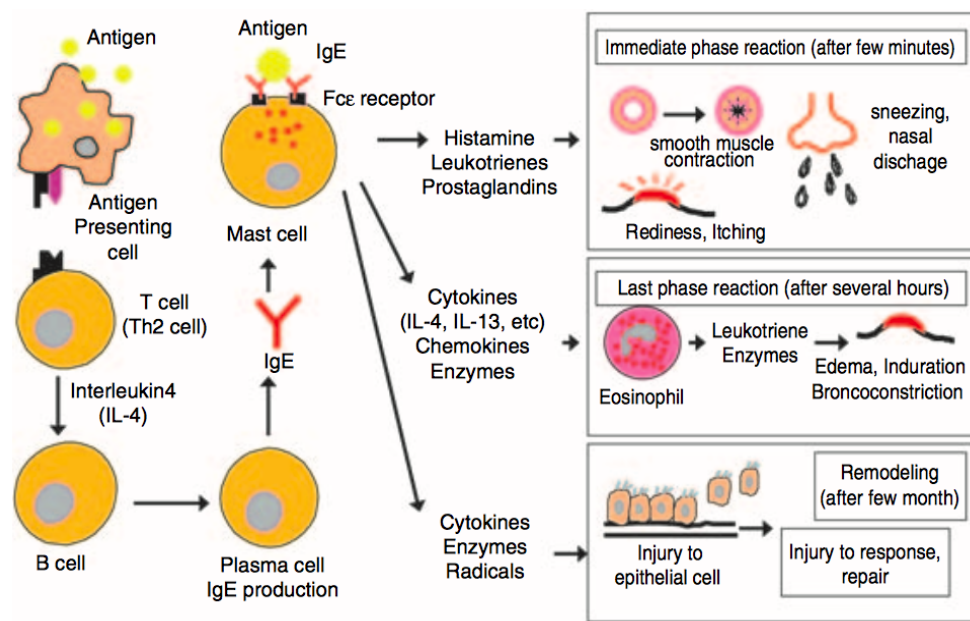


Figure 1. *The mechanism of IgE mediated allergic reaction. (Nagai,, Teramachi, & Tuchiya 2006)*

Many proinflammatory mediators have overlapping effects, which can cause symptoms such as coughing, sneezing, wheezing, hives, mucus secretion, and anaphylaxis. In most cases, these symptoms are a result of acute inflammation in which the body is working to heal itself and are temporary (Galli et al., 2008). Allergic diseases such as eczema, hay fever, sinusitis, and asthma, however, are the result of chronic inflammation (Galli et al., 2008). The specific mechanisms leading to this kind of chronic inflammation are still not completely understood.

One of the major proinflammatory mediators released are histamines, which bind to H1 receptors and cause the smooth muscles of the bronchi to contract (Faustino-Rocha et al., 2017). This makes breathing difficult as the airways start to close. In addition, histamines cause blood vessel dilation and increase permeability of the blood vessel walls. In severe cases of allergic responses, rapid onset of histamine release can cause a combined attack of oral, skin, respiratory, cardiovascular, gastrointestinal, and neurologic systems known as anaphylactic shock, which can be life-threatening (Kim & Fischer, 2011).

Prostaglandins are important in both early and late immune responses. They can also cause the smooth muscle to contract, causing coughing, wheezing, and shortness of breath (Sato et al., 2006). Persistent bronchial hyperreactivity can lead to the diagnosis of asthma. Six hours after the exposure to the allergen, it is also involved in the

pathogenesis of urticaria, allergic rhinitis, and allergic bronchial asthma (Satoh et al., 2006).

Leukotrienes are seen to have a role in many chronic inflammatory diseases (Liu & Yokomizo, 2015). For example, they are correlated with eczema, asthma, and hay fever. The molecules are also related to some more acute symptoms such as bronchoconstriction, mucus secretion, and anaphylaxis.

Immunoglobulin G and Immunoglobulin E

Human immunoglobulin (Ig) is a Y-shaped protein produced by plasma cells to aid the immune system in destroying foreign bacteria (Schroeder & Cavacini, 2010). Of the five antibody classes, IgG and IgE are the two isotypes directly involved in allergy mechanisms (Warrington et al., 2011). All immunoglobulin are composed of two heavy (H) and two light (L) chains, and a combination of variable (V) and constant (C) regions. The light chains are made up of one V region and one C region. The heavy chains are made up of one V region and three C regions (Schroeder & Cavacini, 2010). The variable regions of the heavy and light chain are paired together at the top of the antibody to create an antigen binding site. The constant regions specify effector functions, such as binding to the Fc regions of mast cells, and determine the specific isotype of the immunoglobulin (Schroeder & Cavacini, 2010).

Immunoglobulin G (IgG) is the most abundant immunoglobulin within the blood and lymph nodes. IgG has a large role in the opsonization of pathogens (Warrington et al., 2011). IgG also engages in agglutination in which the antibody can connect multiple antigen particles in order to create large clumps for easier and more efficient recognition

and degradation (Warrington et al., 2011). Finally, IgG is the only immunoglobulin that can pass through the placenta. This is very important because mothers can pass their IgG into their offspring, therefore passing certain immunities onto their offspring (Warrington et al., 2011).

Immunoglobulin E (IgE) is the antibody most directly related to allergies (Stone et al., 2010). When the immune system produces an allergic mechanism, the B cells switch from producing IgG to producing IgE. IgE binds to the FcεR1 receptor on mast cells in order to induce an immune response to a foreign substance. Once the IgE is bound to the Fc portion of the FcεR1 receptor, it can capture antigens, causing the mast cell to release its granules which contain proinflammatory mediators (Galli et al., 2008).

B Cell Activation

In the immune response, naive B cells undergo a process known as class switch recombination in which the class of antibody is changed from IgM to either IgG, IgE, or IgA by means of a chromosomal deletion along the locus for the antibody's heavy chain (Stavnezer et al., 2008). There are two main components to class switching in T-dependent B cell activation. The first component is the binding of the CD40L molecule on a T cell with the B-cell surface receptor CD40, and the second is the release of cytokines by that T cell (Maddaly et al., 2010). Once the B cell is activated, enzyme activation induced cytidine deaminase (AID) oversees the deletion along two splice sites known as switch (S) regions (He et al., 2015). The first S region is fixed just upstream of the coding sequences for IgM and IgD (Stavnezer et al., 2008). The second S region to be cut is determined by cytokines produced by helper T cells. Cytokine interferon- γ (IFN- γ)

causes a splice site just before the gene sequence for IgG to be cut, excising the sequence for IgM and IgD (Kawano et al., 1995). Cytokine interleukin 4 (IL-4) is responsible for the deletion resulting in the generation of IgE antibodies (Stavnezer & Schrader, 2014). Thus, the specific isotype of antibody produced by a B cell is dependent on the cytokines produced by the helper T cell.

FcεR1

_____FcεR1 is expressed on mast cells and basophils and has a high affinity for IgE (Metz et al., 2008). Structurally, FcεR1 is tetrameric and is composed of, an α , β , and 2 disulfide-linked γ subunits. The β and γ chains are involved in signal transduction after binding of IgE in order to mediate the cell's response to IgE binding, and dictate subsequent signal cascades and histamine release. The FcεR1 receptor is present in its complete form and expressed at a constitutive level only on basophils and mast cells (Metz et al., 2008). However, it is also present in a reduced form $\alpha\gamma_2$, in which the β signaling subunit is not present, in cells like dendritic cells, eosinophils, and platelets. IgE binding to FcεR1 causes its upregulation.

Signaling Pathways

The binding of IgE to FcεR1 on mast cells and basophils results in a cascading web of signaling pathways between a complex array of adaptor proteins, kinases, and other molecules. These events lead to two events specific to the allergic mechanism symptom manifestation: mast cell degranulation and cytokine production, as depicted in Figure 2.

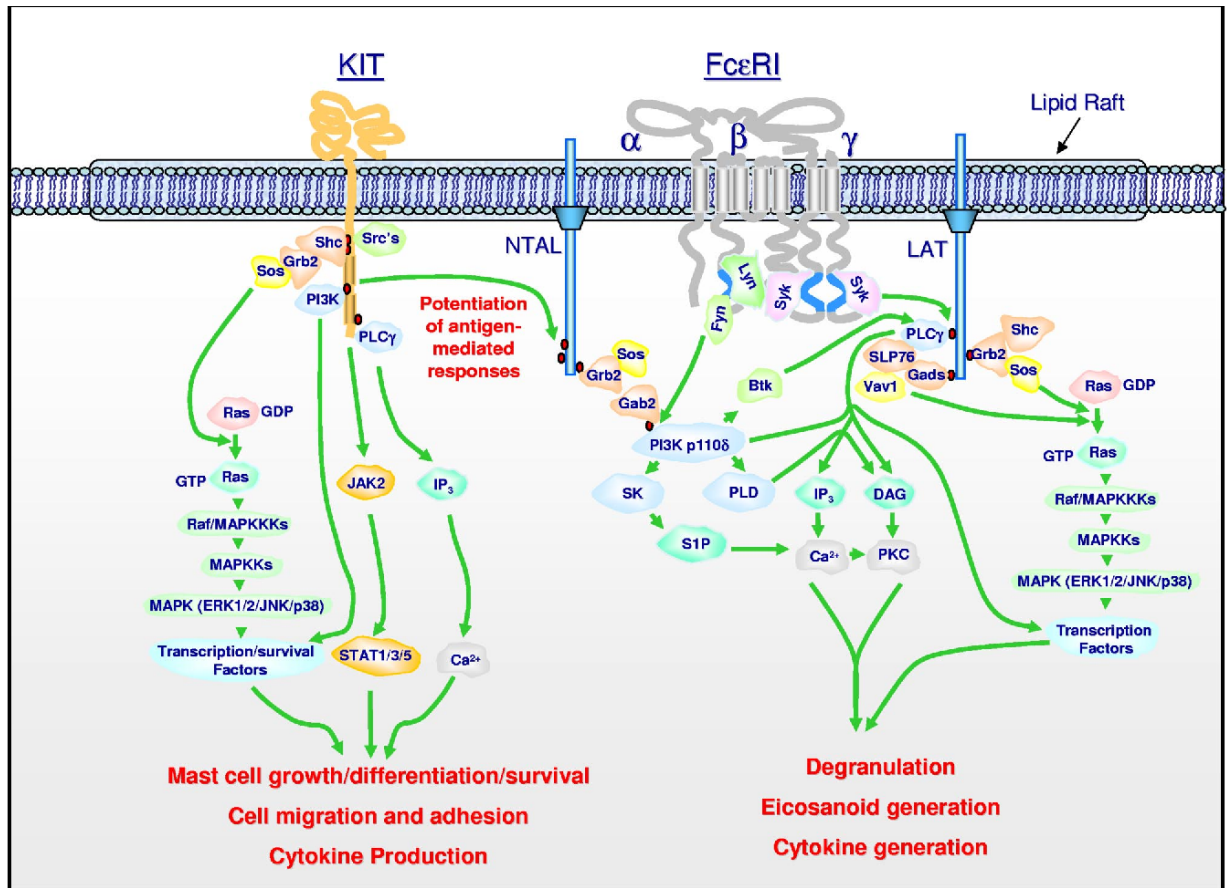


Figure 2: Overview of cell signaling pathways within mast cells. (Gilfillan, & Tkaczyk 2006)

Lipid Rafts, LYN, FYN, GAB2, PI3K

In the early part of the signaling pathway, IgE-antigen complexes bind to the FcεR1 receptor (Oettgen & Burton, 2015). Before this binding, FcεR1 receptors have a low affinity to insert into lipid rafts, regions of the cell membrane where certain glycolipids cluster to form microdomains useful in signaling (Dykstra et al., 2003). After IgE-antigen binds to FcεR1, however, oligomeric antigens cross-link IgE bound to FcεR1 just long enough to assemble a “signalosome” made of adaptor proteins and other signaling proteins that promote raft clustering and bind to the actin cytoskeleton to

stabilize the receptors in the lipid raft (Dykstra et al., 2003). Then, tyrosines in immunoreceptor tyrosine-based activation motif (ITAM) sequences, found in the cytosolic domains of the FcεR1 β and γ chains, become phosphorylated by Src kinase Lyn (Metcalf et al., 2009). Lyn kinase is preferentially found in these membrane microdomains and shifts the equilibrium from most inactive to mostly phosphorylated and active FcεR1 (Gilfillan & Tkaczyk, 2006).

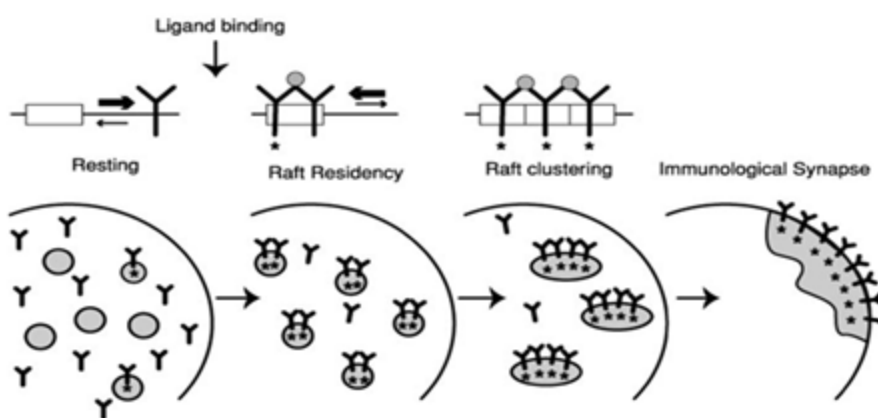


Figure 3. Process of creating lipid raft with IgE-antigen and FcεR1 oligomers

(Dykstra et al., 2003)

Fyn kinase is also found in these lipid rafts and binds more tightly to the β subunit of FcεR1 when the receptor is activated (Parravicini et al., 2002). It is responsible for phosphorylating GRB2-associated binding protein 2 (Gab2). Gab2, like its analogs of Gab1 and Dos, is a scaffold adaptor protein that signal molecules can bind to. Gab^{-/-} mice were found to have both impaired mast cell degranulation and cytokine expression (Gu et al., 2001). Phosphorylation of Gab2 causes a conformational change to recruit molecules like Src-homology domain 2-containing protein tyrosine phosphatase 2 (SHP2) and phosphatidylinositol-3-OH kinase (PtdIns-3K or PI3K).

PI3K is a family of lipid kinases known to be involved in many cellular functions such as cell growth, development, proliferation, and survival (Hemmings & Restuccia, 2012). They are involved in pathways leading to endocytosis, vesicle trafficking, autophagy, signaling, cortical remodeling, secretion, and cytokinesis. Deregulation of PI3K can lead to tumorigenesis (Jean & Kiger, 2014). Here we will focus on the immediate involvement of PI3K within the pathway previously described as activated by Gab2.

In the mast cell degranulation signaling pathway, PI3K is activated by the adaptor molecule Gab2. When recruited, the regulatory subunit of PI3K in conjunction with a tyrosyl phosphorylated SHP binds to sites on Gab2 (Gu et al., 2001). Once bound, class 1A PI3K containing p85 and p110 subunits convert the membrane lipid phosphatidylinositol-(4,5)-bisphosphate (PIP₂) to phosphatidylinositol-(3,4,5)-trisphosphate (PIP₃) (Kim et al., 2008). PIP₃ has docking sites that are made available to associating proteins at domains called pleckstrin-homology domains (Gilfillan & Tkaczyk, 2006). Some associating proteins called to PIP₃ include PLC γ , VAV, PLD, SK, and BTK.

There are two well established inhibitors of PI3K: wortmannin and LY294002. Wortmannin is a fungal toxin which binds to the p110 subunit of PI3K (Barker et al., 1995). Wortmannin has been shown to reduce levels of degranulation when tested in the rat basophil leukemia cell line RBL-2H3 (Gilfillan & Tkaczyk, 2006). The second inhibitor of PI3K is known as LY294002. LY294002 is a more stable alternative to wortmannin in solution with a tradeoff of requiring a much higher concentration in order

to reach the same level of inhibition (Walker et al., 2000). Other inhibitors such as quercetin, myricetin, and staurosporine have also been tested as PI3K inhibitors, providing proof of concept for allergic therapy in the inhibition of PI3K (Walker et al., 2000).

PLC γ and PLD Pathways

Syk tyrosine kinase activates adaptor molecules that lead to the activation of phospholipase C γ (PLC γ), a critical molecule for B cell activation (Peng & Beaven, 2005). There are two forms of PLC γ with PLC γ -1 mainly expressed in mast cells and T cells and PLC γ -2 mainly involved in B-cells (Kim, 2000). PLC γ is the signaling enzyme that catalyzes the hydrolysis of phosphatidylinositol 4,5-bisphosphate (PIP₂), a phosphoinositide on the plasma membrane, into the second messengers DAG and inositol 1,4,5-trisphosphate (IP₃) (Kim, 2000). These two cleavage products have important and independent roles in subsequent signaling that ultimately results in calcium release and PKC activation (Gericke, 2013). PLC inhibitor U-73122 has been previously tested in inhibiting PI hydrolysis and IP₃ synthesis in neutrophils, neuroblastoma cells, and platelets, and has been cited as a possible inhibitor of PLC (MacMillan & JG McCarron, 2010).

IP₃ production induces calcium release in the endoplasmic reticulum, that in turns causes calcium to flow in from extracellular channels (Rivera & Gilfillan, 2006). This influx of calcium leads to steps initiating transcription and differentiation. Internal calcium is also involved in a number of other activating processes, such as in the activation of Protein Kinase C (PKC).

PKC is a group of lipid dependent kinases that phosphorylate protein structures and serve as effector molecules (Becker, 2005). DAG generation recruits PKC to migrate to the plasma membrane, during the path in which it attaches to and activates PLD (Becker, 2005). DAG competes with phorbol esters to bind to the C1 site on PKC (Becker, 2005). This could possibly become an area of interest for cascade inhibition. There are several different subgroups of PKC, some of which are dependent on DAG and calcium, some DAG alone, and some on neither (Singer et al., 1996). Of the calcium dependent groups, DAG generally binds to the C1 unit and calcium to the C2 unit, while in the calcium-independent groups, only DAG binds to the C1 unit (Huang 1989). PKC inhibitors such as staturosporine and calphostin C have been seen to block PLD activation. However, there are some studies that suggest that calphostin may act directly upon PLD (Peng & Beaven, 2005).

Production of DAG is what triggers PKC to bind and interact with PLD, though this pathway is less understood. It has direct contact with kinases such as Protein Kinase C (PKC), ERK, and Tyrosine Kinase 2 (TYK). DAG is produced by PLC, which then induces PLD to produce its own DAG in a much greater amount in order to activate PKC (Peng & Beaven, 2005). Activation of PLD has been linked to the production of phosphatidic acid (PA), diacylglycerol (DAG), and choline. PA itself also targets and regulates PKC (Peng & Beaven, 2005).

Sphingosine Kinase Pathway

Sphingosine kinase (SphK) is another enzyme found in the mast cell pathway. The role of SphK is to catalyze the phosphorylation of sphingosine to form

sphingosine-1-phosphate (S1P) (Sun & Bonder, 2012). S1P is known to have a role in the signaling processes of various diseases from cancers, to diabetes, osteoporosis, and allergies and asthma (Maceyka et al., 2011). In the allergic response, SphK and S1P are involved in survival, differentiation, migration, and activation (Sun & Bonder, 2012).

There are two isoenzymes which form S1P, the SphK1 and the SphK2. These enzymes catalyze the phosphorylation of sphingosine to form S1P. SphK1 regulates cell growth and survival, but when overexpressed SphK2 induces cell death (Olivera et al., 1999). Both SphK1 and SphK2 were found to have increased activity when the FcεRI receptor was activated in mast cells (Mizugishi et al., 2005).

S1P has two receptors, S1P₁ and S1P₂, which are both expressed on the surface of mast cells. (Oskeritzian et al., 2007). S1P₁ regulates migration of mast cells towards antigens. S1P₂ is known to mediate mast cell activation and degranulation, which makes it a better target for this research. (Oskeritzian et al., 2007). The S1P that is secreted by the mast cell is able to bind to these receptors.

PKA and cAMP

Protein kinase A (PKA) is an enzyme that phosphorylates other proteins to regulate their function. Its two catalytic subunits are responsible for the phosphorylation activity, while its two regulatory subunits are able to detect and properly react to levels of cyclic AMP (cAMP). When cAMP levels are low, the catalytic subunit is inactive, and when cAMP levels are high, the catalytic subunit is active. Research suggests that administering a treatment using an antagonist of cAMP or shRNA down-regulation of PKA reversed the EP2-mediated inhibitory effect on MC degranulation (Serra-Pages,

Olivera, Torres, Picado, de Mora, & Rivera, 2012). A molecule called PGE2 can mediate the suppression of mast cell degranulation, which researchers found could be modulated to vary from activating to suppressing, depending on the relative ratio of EP2 to EP3 (two types of G protein coupled receptors) expression on these cells with suppression evident only in cells having increased EP2 to EP3 expression. (Serra-Pages et al., 2012).

Current Treatments

Symptom Management

Currently, there is no cure for allergies. Relatively common and established treatment recommendations for allergies are focused on avoidance measures and pharmacotherapy-based symptom management (Lanser et al., 2015). Although the recommendation of avoiding allergens will certainly lessen allergen exposure and thus the subsequent allergic response, the measure is impractical and inconvenient in daily practice (Marple et al., 2007).

Some treatments, such as decongestants and corticosteroids, focus on treating the symptoms of allergies. Decongestants relieve the nasal congestion associated with allergies by reducing swelling in nasal tissues and blood vessels (AAAAI, 2018). Corticosteroids also work to reduce inflammation in addition to ameliorating stuffiness, sneezing, and runny nose. There are also a number of over-the-counter treatments such as eye drops and nasal saline spray that can also help to alleviate some of the symptoms. In emergency cases, epinephrine can be administered to stop the serious allergic reaction of anaphylaxis (AAAAI, 2018).

Other treatments aim to stop or limit the allergy symptoms from occurring by interfering with a step in the molecular pathway of the allergic response. These include antihistamines, mast cell stabilizers, and antileukotriene agents (AAAAI, 2018).

Antihistamines such as loratadine (Claritin) and cetirizine hydrochloride (Zyrtec) block histamine from attaching to its receptor after it has been released from the mast cells.

Mast cell stabilizers can stop the histamine from being released from the mast cells in the first place. Antileukotriene agents work to limit the effects of leukotrienes, which are known to play an important role in some severe allergic symptoms. Some of these agents work by blocking the production of leukotrienes while others stop leukotrienes from ever binding to their receptors (AAAAI, 2018).

Although avoidance and symptom management treatments are able to reduce the effects of allergic responses, they are insufficient for many and are not measures working towards a curative or long-lasting therapy. Researchers have been seeking new and improved therapeutics such as through immunotherapy to better target the foundational mechanisms initiating allergic reactions which can even work in conjunction with the aforementioned treatments to increase the efficacy and endurance of treatment.

Allergy Immunotherapy

_____Allergy-specific immunotherapy (SIT) is a curative method of treatment for certain allergies as it is able to induce long-term allergen-specific tolerance through multiple mechanisms and routes of administration (Akdis, 2014). Desensitization with SIT involves a process similar to vaccinations in which increasing doses of extracts of the specific allergen are administered followed by maintenance doses for several years. This

process is hoped to trigger immunological change for sustained desensitization (Orengo et al., 2018). Immunotherapy, specifically allergy shots or desensitization, is one of the most effective treatments for those who experience chronic allergies. Currently, there are even oral tablets such as Grastek and Oralair that can be taken at home (AAAAI, 2018).

SIT focuses on inducing an increase in IgG production to outcompete IgE in binding to effector cell receptors. Orengo et al. (2018) tested this method in mice and cat-allergic patients, finding that an increase in the blocking IgG/IgE ratio reduces the allergic response. Although SIT can provide lasting treatment, it has variable efficacy among patients. Some patients have no response to treatment, and others have adverse side effects. Side effects are most commonly associated with food allergies, and therefore SIT is only available for environmental aeroallergens (Orengo et al., 2018). To address some of the issues of this technology, more research is emerging on dosing schedules, routes of administration, and advanced vaccines (Akdis, 2014). While there are established methods of immunotherapy, improvements can be made for more effective actions that can be applied to all types of allergens.

Anti-Cytokine Drug Therapy

There is research underway in the vein of genetic exploration among the genes behind antibody production and class switch recombination. In a 2016 study, the effects of anti-IL-4 were investigated to combat asthma with variable changes among asthmatic symptoms across asthma types (Bagnasco et al., 2016). In 2001, clinical trials began testing anti-IL-4 drug pascalizumab against the effects of allergic asthma with mixed results that ultimately concluded inefficacy (Hart et al., 2002). Often, therapies with

action to block IL-4 act in conjunction with inhibitors of IL-13 due to the redundancy that the two cytokines possess in expressing many of the same pathways, functioning similarly (Kau & Korenblat, 2015). Several dual-blocking anti-IL-4 and anti-IL-13 drugs are in the process of testing yet are thus far ineffective in entirely blocking allergic asthma due to functional differences of various subtypes of asthma which complicate the efficacy of the drugs (Kau & Korenblat, 2015). Overall there is a lack of consistent efficacy in asthma studies and even less so within the scope of more complicated allergies, rendering anti-cytokine therapy unpromising.

Anti-IgE Drug Therapy

Anti-IgE drugs mediate the allergic response by binding to the Cε3 region within the Fc region of the IgE antibody (Holgate, 2014). One example of this type of drug is omalizumab, a recombinant humanized monoclonal antibody. It works by binding two of its molecules to the Fc region of the free-floating IgE so that it is unable to bind to FcεR1. This reduces the levels of free-floating IgE in the body as over time they are recycled. This reduction of IgE over time allows the drug to be effective against a long-term allergy such as allergic rhinitis (Easthope & Jarvis, 2001). Other allergies have been tested against the effects of omalizumab with varying degrees of success. In a review done in 2014, omalizumab was reported to have anecdotal or limited evidence against allergies such as Churg-Strauss Syndrome, bronchopulmonary allergic aspergillosis (fungal sensitivity), and eosinophilic otitis media (Holgate, 2014).

MEDI4212 is an anti-IgE monoclonal antibody that has the potential to eliminate IgE-expressing B cells and neutralize soluble IgE in asthma prone patients (Nyborg et al.,

2015). This occurs through cell-mediated cytotoxicity, a type of immune reaction in which the target is coated with antibodies and killed by white blood cells. MEDI4212 variants also inhibited IgE-induced signaling and demonstrated enhanced cell killing. (Incorvaia & Mauro, 2015). MEDI4212's advantage over omalizumab is its ability to neutralize high amounts of soluble IgE as well as remove the IgE expressing B cells. (Incorvaia & Mauro, 2015). The authors suggest that this drug is not likely to replace omalizumab, which has been brought to market, but could potentially be used as an additional treatment (Nyborg et al., 2015). More research needs to be done on this novel high-affinity anti-IgE monoclonal antibody, such as testing its abilities to reduce other allergies other than asthma.

Adenine in Cell Signaling

Adenine has a variety of biological functions other than being a component of DNA and RNA. A 2015 study shows that adenine possess anti-allergic effects by inhibiting FcεRI-mediated signaling events (Silwal et al., 2015). Findings by Silwal et al. testing the effects of adenine is valuable in the search for finding a medication that prevents the allergic response from occurring. Rather than antihistamines which merely alleviate symptoms caused by the degranulation of mast cells, administering adenine could terminate the allergic response earlier in its pathway.

Potential Targets

After conducting the literature review, including the background on the immune response as well as current and potential treatments available, the team decided to target the mast cell degranulation pathway. There are extensive therapeutic options that target

processes after degranulation occurs; thus, we focused our research on inhibiting the release of inflammatory molecules. Based on the literature findings for parts of the pathway, we chose which enzymes to focus our research on based on three factors: the availability of previously-identified inhibitors for the protein, the protein having a critical role in the signalling pathway, and a gap in the research on its impact in mast cells. Three enzymes fit these requirements and warranted further research on their inhibitors: Protein Kinase C (PKC), Phospholipase C gamma (PLC γ), and Phosphoinositide-3-Kinase (PI3K). Next, we will examine these known inhibitors and their analogs to optimize their binding to these target proteins. In this project, we explore how proteins within the downstream mast cell signaling pathway can be inhibited in order to reduce degranulation and thus reduce the allergic response. To examine this, the team decided to focus on computational methodologies.

State of Current Research in Protein Modeling

Virtual screening is a computational method by which binding between ligands and their macromolecule is simulated. This technique is often used in the context of drug discovery due to its ability to screen libraries by way of sequential filters to target ligands with appropriate affinities to a molecule's binding site (Lavecchia & Di Giovanni, 2013). There are two main types of virtual screening methods: ligand-based and structural-based. In ligand-based virtual screening, the properties of known active ligands are evaluated according to their similarity to new ligands. To operate in a ligand-based method, an efficient similarity measure and a reliable scoring method are utilized (Hamza et al., 2012) This method is useful when there is no available structure of the target

protein molecule. Structure-based virtual screening operates by scoring the affinity of a known ligand with a known protein target. This predicted ligand-protein complex is evaluated by calculating the free energy of the docking site when involved by the ligand in the protein (Lionta et al., 2014). Many computational softwares use both ligand- or structure-based screening techniques to approximate novel ligand-protein complexes.

PyRx is an open-source virtual screening software that contains Autodock Vina, a program used for computational docking to simulate receptor-ligand interactions (Trott & Olsen, 2010). Computational docking software relies on a number of approximations to predict the confirmation and binding affinity between a target receptor and its ligand. Autodock Vina assumes a rigid receptor and fixed bond angles and bond lengths in the ligand to reduce the size of the conformational search space (Cosconati et al., 2010). An empirical free energy force field with terms for hydrogen bonding potentials, electrostatics, and torsional entropy predicts the binding affinity between the ligand and receptor at different conformations. Autodock Vina uses a scoring function based on predictions from the empirical force field to determine the best binding conformations and their respective free energies of binding. Since the conformational search methods are stochastic, the lowest reported binding affinity is not guaranteed to be a global minimum. The estimated free energies of binding are accurate within 2-3 kcal/mol (Forli et al., 2016).

Identification of more inhibitors in the pathway through computational modeling could lead to more effective treatment after in depth study. Thus, the aim of this project is to identify drug candidate molecules similar in structure to these lead inhibitors from a

vast library of compounds and to screen them using virtual modeling. Specifically, by modeling protein-inhibitor interactions using PyRx, we can predict the effectiveness of different molecules in reducing degranulation.

Materials and Methods

Refining Macromolecules

The protein sequences (FASTA sequences) of the macromolecules tested—PI3K, PKC-beta1 (β 1), PKC-beta2 (β 2), PKC-delta (δ), PKC-eta (η), PLC-gamma1 (γ 1), PLCgamma2 (γ 2)—were derived from the National Center for Biotechnology Information (NCBI) database or Research Collaboratory for Structural Bioinformatics (RCSB) database. These protein sequences were then modeled using Phyre2, a 3D protein modeling software (Kelley et al., 2015). Putting the resulting protein models through Modrefiner, an algorithm for atomic-level, high-resolution protein structure refinement, provided a more reliable model of the signaling molecule, as we determined using the following protein structure analysis programs: ProSA, ProCheck, and ERRAT server (Xu & Zhang, 2011). ProSA determined local quality of sections of the protein so that it can be seen if any areas specifically are incorrectly modelled (Wiederstein & Sippl, 2007). ProCheck created Ramachandran plots to check accuracy of bond angles (Laskowski et al., 1996). ERRAT server measured the accuracy of nonbonded intermolecular forces (Colovos & Yeates, 1993). All of these analysis programs together provided a comprehensive picture of the accuracy of the protein models made by Phyre2 and ModRefiner.

Preparing Ligands for Docking

These refined models were then screened in PyRx, a virtual molecular screening software which predicts binding affinity, against known inhibitors whose structures were

derived from PubChem (Dallakyan & Olson, 2014). The chosen proteins were imported into PyRx as .pdb files and converted into AutoDock macromolecules.

The established inhibitors for the selected pathway were designated as the ‘ligands’ within PyRx and were screened against the signaling molecules, termed ‘macromolecules’ in the software. ‘Ligands’ were imported into PyRx from PubChem in the form of SDF files. Intramolecular forces within the ligands were then minimized through OpenBabel by setting the total number of steps to 10,000 and the stop criterion at an energy difference of less than 0.01. These parameters were modified in the PyRx software in order to optimize the orientation of the ligand for binding interactions. The ligand was then converted into an AutoDock ligand to begin virtual screening. For the screening process, we used the Vina Wizard program within PyRx. We selected the macromolecule and ligand whose binding was to be modeled and maximized the region of protein to be analyzed for potential binding sites, although not necessarily the ATP binding pocket of the kinases modeled, as well as increased exhaustiveness of binding site identification to 12 before starting the run. A list of binding affinities was generated, and we recorded the most favorable ΔG value, indicative of the highest predicted affinity between the ligand and the macromolecule.

Analogs

Several ligands were selected to be run with each protein specified. Eleven simulation trials were run in PyRx modeling affinity software for each ligand-protein pair. Out of 34 known inhibitors, the average binding affinity was calculated across eleven trials. Out of 15 selected inhibitors, analogs were derived from the ZINC database.

Analogs tested had similarity thresholds above 0.3, by ZINC standards. These analogs were then tested for binding energy to the signaling molecules in PyRx using a similar methodology as described above; however, exhaustiveness was set to 16 and an average of predicted ΔG values was taken across 5 trials.

Results

We were interested in identifying novel inhibitors that might point to new therapeutic avenues for treating allergies. In order to investigate this, we took a computational approach.

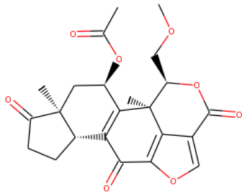
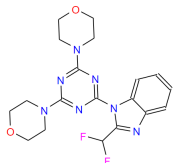
Protein Structure Analysis

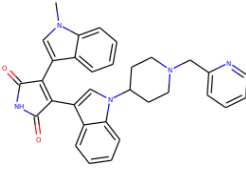
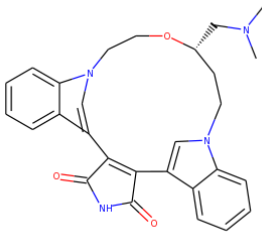
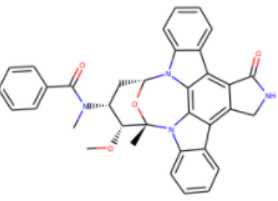
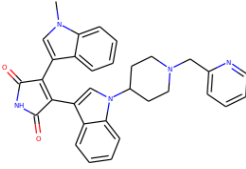
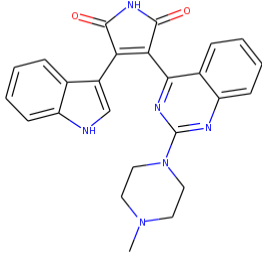
We began by using Phyre2 and Modrefiner to develop and refine 3D models of the signaling molecules involved in the degranulation pathway, as many of the selected molecules did not have reliable existing file type PDBs of the selected molecules; in order to maintain consistency in our modeling, we chose to create 3D models for all selected signaling molecules. The Phyre2 server, a protein structure prediction web portal, was used to predict the 3D structure of a single submitted protein sequence (Kelley et al., 2015). The 3D structures were subsequently put through Modrefiner, which aimed to enhance the models by altering them to be closer to their native states by altering hydrogen bonds, backbone topology, and side chain positioning (Xu & Zhang, 2011). Models were then evaluated through ProCheck, ProSA, and ERRAT—which determine the validity of the 3D protein models through evaluation of local quality of sections of the protein, accuracy of bond angles, and accuracy of nonbonding intermolecular forces, respectively—and indicated that ModRefiner greatly increased the quality of the protein model PDB files in relation to the models that were only made with the Phyre2 software. This made the signaling protein models more valid for binding studies. The results of the protein structure analysis programs are shown in Appendix C.

Notably, many of the Ramachandran plots generated from the 3D models of the signaling molecules, even after refinement, indicated regions of error above acceptable levels. However, despite this limitation in our models, we proceeded forward with modeling as proof of concept of the modeling procedure due to time limits and lack of computational power for modeling.

Binding Energy of Established Inhibitors

We then identified known inhibitors for signaling proteins in the selected pathway and predicted the binding energy using PyRx, a virtual molecular screening software (See Appendix B for complete list). This screening allowed us to establish a baseline for finding novel inhibitors. Shown in Table 1 are the average ΔG values of the established inhibitors with the highest affinities to the signaling molecules across eleven trials. For each signaling macromolecule, the best one or two inhibitors were selected for further study in order to determine what, if any, changes to the structure would lead to a stronger binding energy. We then converted averaged binding energies to K_d using the equation: $dG = RT\ln(K_d)$.

Binding Site (macromolecule)	Known Inhibitors (ligand)	Structure	Average Binding Energy (kcal/mol)	K_d
PI3K	Wortmannin		-7.62 ± 0.36	1.35E-06
PI3K	ZSTK474		-8.41 ± 0.18	4.89E-07

PKC- β 1	Enzastaurin		-10.15 ± 0.38	$3.54E-08$
PKC- β 1	Ruboxistaurin		-9.50 ± 0.06	$8.54E-08$
PKC- β 1	Midostaurin		-9.63 ± 0.06	$8.54E-08$
PKC- β 2	Enzastaurin		-9.40 ± 0.31	$1.27E-07$
PKC- β 2	Sotrastaurin		-8.90 ± 0.46	$6.44E-08$

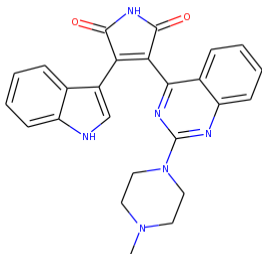
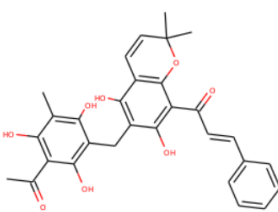
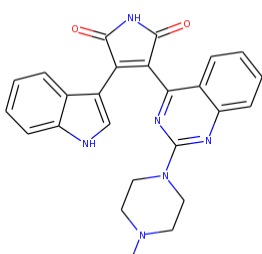
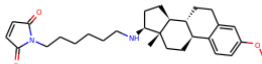
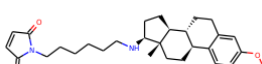
PKC δ	Sotrastaurin		-10.00 ± 0.67	1.41E-08
PKC δ	Rottlerin		-9.36 ± 0.54	1.27E-07
PKC η	Sotrastaurin		-9.03 ± 0.25	2.38E-07
PLC- γ 1	U73122		-8.60 ± 0.45	1.78E-07
PLC- γ 2	U73122		-8.20 ± 0.31	4.89E-07

Table 1. The binding energy of known inhibitors to macromolecules in the mast cell signalling pathway

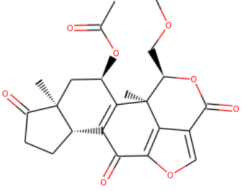
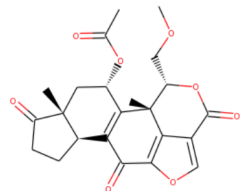
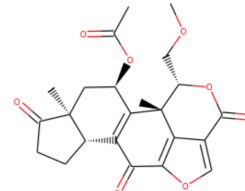
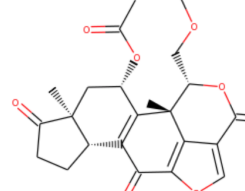
Analogs of Selected Inhibitors

In order to identify novel inhibitors that could serve as potential therapeutics against the signaling molecules of the degranulation pathway, we utilized the ZINC Database to search for analogs of the established inhibitors we selected. We searched for

analogs that had a similarity-30 by ZINC database standards, which means ZINC database defined them to be at least 30% similar to the ligand. When we did this, we increased the exhaustiveness for binding from 12 to 16 in the PyRx software to ensure that we were truly identifying the best binders.

PI3K Inhibitor: Wortmannin

We examined 30 analogs of Wortmannin from the ZINC Database. Of these 30 analogs, there were four analogs that had better binding affinities than Wortmannin.

Inhibitor	Structure	Binding Energy (kcal/mol)
Wortmannin		-7.62±0.36
Analog		
ZINC8035078		- 8.08 ± 0.38
ZINC257519889		- 8.18 ± 0.16
ZINC144119389		- 8.26 ± 0.05

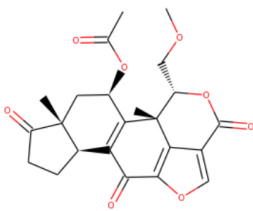
ZINC71789745		-7.90 ± 0.42
--------------	---	------------------

Table 2. Average binding affinities after molecular docking of Wortmannin and analogs to PI3K. An average of five trials was taken for the binding affinities of each analog with corresponding standard deviation values.

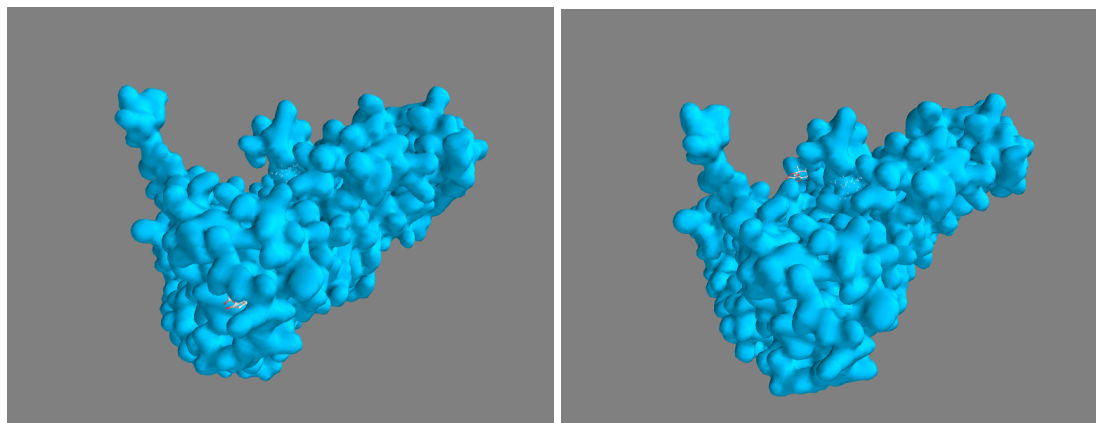
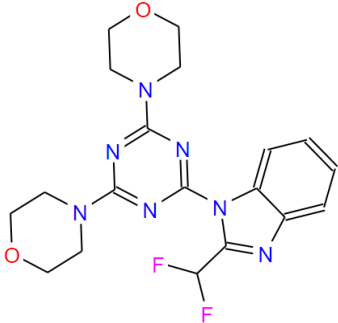
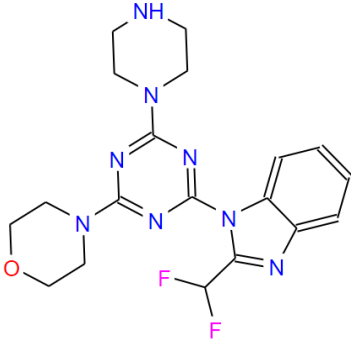
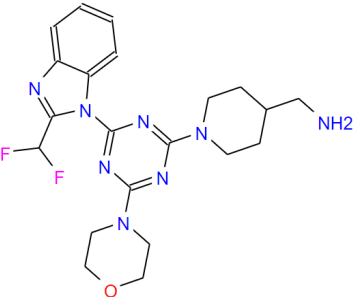


Figure 4. Image to the left shows binding of ZINC144119389 which had the lowest binding energy and image to the right shows binding of ZINC257519889 to PI3K.

The binding energy of Wortmannin to PI3K was measured to be -7.62 kcal/mol over five trials. The analog that decreased binding energy the most was ZINC144119389 with an increase of about 0.94 kcal/mol from that of Wortmannin. Another analog with a strong binding energy was ZINC257519889 with an increase of 0.86 . The figure above shows the binding site for the two analogs with the lowest binding energy. When comparing the values we found in the literature, wortmannin had a binding energy of -10.9 and -11.7 kcal/mol.

PI3K Inhibitor: ZSTK474

We examined 17 analogs of ZSTK474 from the ZINC Database. Of these 17 analogs, there were 5 analogs with higher binding affinities upon docking with PI3K than that of ZSTK474.

Inhibitor	Structure	Binding Energy (kcal/mol)
ZSTK474		-8.41±0.18
Analog		
ZINC113914670		-8.60± 0.00
ZINC1772626092		-8.50±0.00

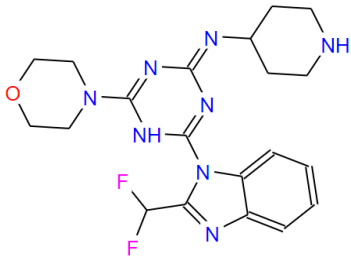
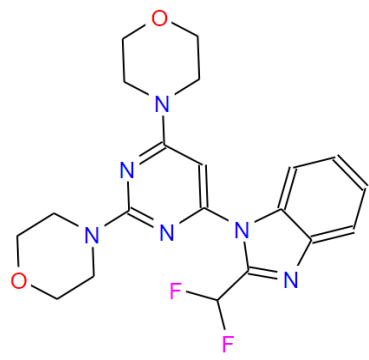
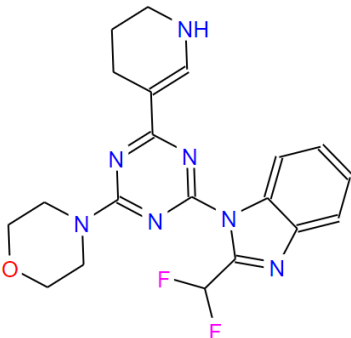
ZINC1772653009		-8.66 ± 0.06
ZINC73160255		-8.70 ± 0.00
ZINC1243947389		-8.82 ± 0.19

Table 3. Average binding affinities after molecular docking of ZSTK474 and analogs to PI3K. An average of five trials was taken for the binding affinities of each analog with corresponding standard deviation values.

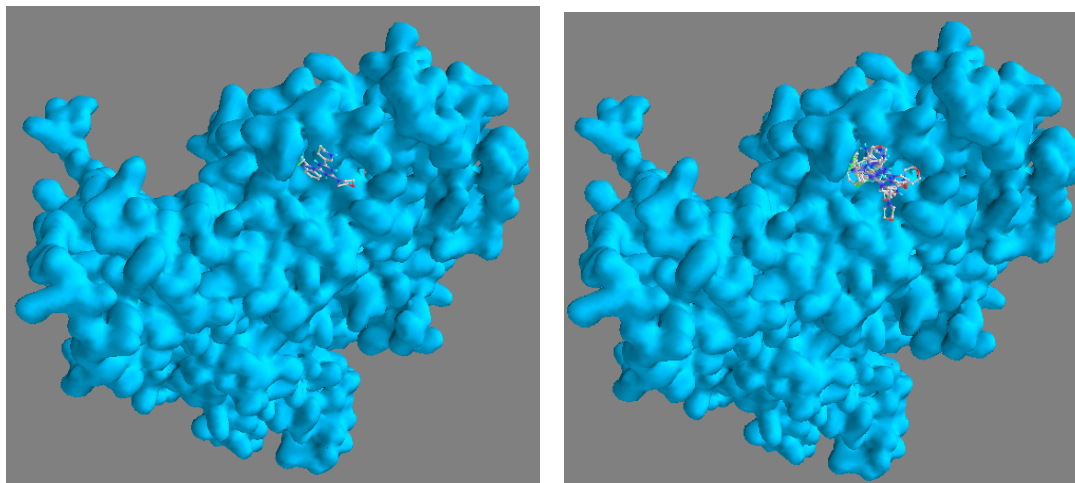


Figure 5: Image to the left shows the binding of ZINC1243947389, which had the lowest binding energy, on to PI3K. Image to the right shows the binding of all the six compounds, ZSTK474 and its examined analogs, on to PI3K.

The binding energy of ZSTK474 to PI3K was measured to be -8.41 kcal/mol over five trials. Figure 5 shows that all examined analogs of ZSTK474, as well as ZSTK474 itself, bind to the same area on the PI3K molecule. The ZSTK474 analogs with better binding affinities differed in structure through changes to the triazine ring or its substituents, which may have led to their higher binding affinities. The analog that decreased binding energy the most was ZINC1243947389 with an increase of about 0.41 kcal/mol from that of ZSTK474.

PKC β 1 Inhibitor: Enzastaurin

We examined six analogs of Enzastaurin from the Zinc Database. Of these six analogs, there were three analogs that had a binding energy that was at least as strong as Enzastaurin itself.

Inhibitor	Structure	Binding Energy (kcal/mol)
------------------	------------------	----------------------------------

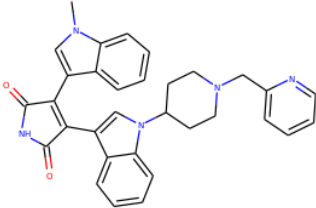
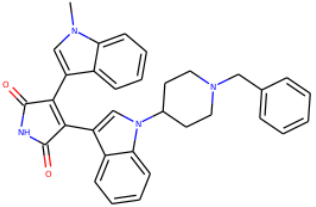
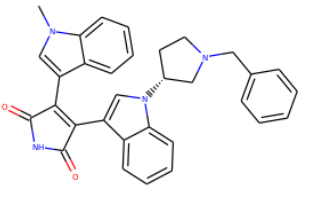
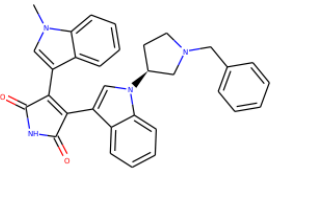
Enzastuarin	 <p>The chemical structure of Enzastuarin features a central pyrazole ring substituted with a methyl group, a benzimidazole ring, and a 2-phenylpiperidine ring. The benzimidazole ring is further substituted with a 2-oxo-1,2,3,4-tetrahydro-1H-imidazole-5-yl group.</p>	- 10.16 ± 0.40
Analog		
ZINC13489985	 <p>The chemical structure of ZINC13489985 is similar to Enzastuarin, but the 2-phenylpiperidine ring is replaced by a 2-phenylpiperazine ring.</p>	- 10.36 ± 0.05
ZINC13489986	 <p>The chemical structure of ZINC13489986 is similar to Enzastuarin, but the 2-phenylpiperidine ring is replaced by a 2-phenylpyrrolidine ring.</p>	- 10.16 ± 0.31
ZINC13489987	 <p>The chemical structure of ZINC13489987 is similar to Enzastuarin, but the 2-phenylpiperidine ring is replaced by a 2-phenylpyrrolidine ring, and the methyl group on the pyrazole ring is highlighted in red.</p>	- 10.42 ± 0.54

Table 4. Average binding energies after molecular docking of enzastaurin and analogs to PKC β 1. An average of five trials was taken for the binding energies of each analog with corresponding standard deviation values.

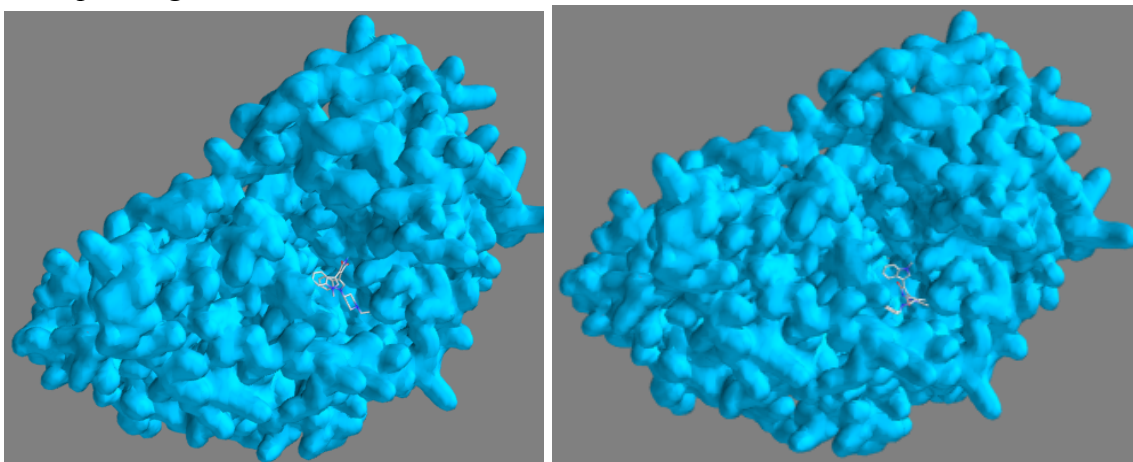


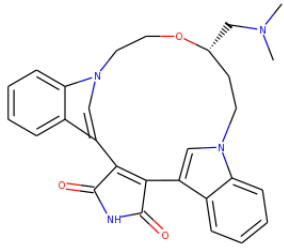
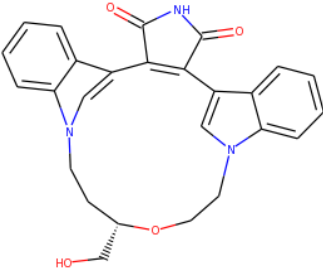
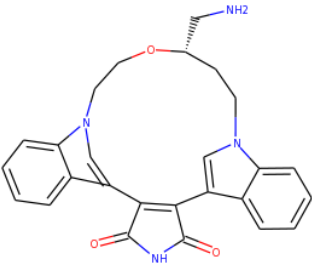
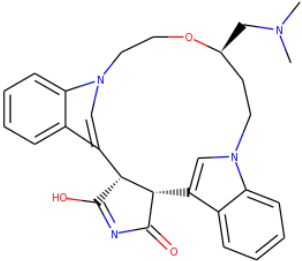
Figure 6. The image on the left shows Enzastaurin (shown in the molecular surface model) interacting with PKC β 1 (in the ball and stick model). The image on the right shows the analog ZINC13489987 interacting with PKC β 1.

Binding of PKC β 1 to ZINC13489987 had the lowest energy of -10.42 kcal/mol, which is a 0.26 kcal/mol increase compared to the binding energy of enzastaurin. This analog has a carbon instead of a nitrogen in the benzene ring. It also has a wedge stereochemistry change at one position, where the six carbon ring is replaced with a five carbon ring. As depicted in Figure 6, the analog does bind in the active site, and it likely interacts with a different orientation, therefore possibly different residues within that site that allow it to have a lower binding energy..

PKC β 1 Inhibitor: Ruboxistaurin

We examined 15 analogs of Ruboxistaurin from the Zinc Database, with five trials each. Of these fifteen analogs, there were five analogs that had a negative binding energy that was significantly stronger than Ruboxistaurin itself.

Inhibitor	Structure	Binding Energy (kcal/mol)
------------------	------------------	----------------------------------

Ruboxistaurin		-9.5 ± 0.00
Analog		
ZINC3825435		-10.1 ± 0.00
ZINC13604307		-10.02 ± 0.18
ZINC95569944		-9.84 ± 0.05

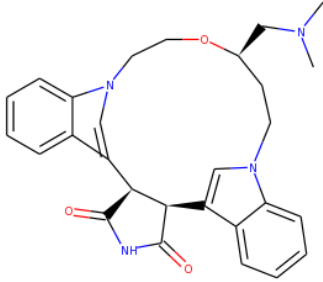
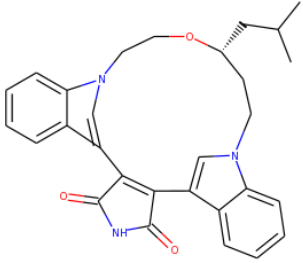
ZINC195440759	 The chemical structure of ZINC195440759 is a complex macrocyclic molecule. It features a large ring system containing two indole-like rings and a central amide group. The structure is colored with blue for nitrogen atoms, red for oxygen atoms, and black for carbon and hydrogen atoms.	-9.82 ± 0.13
ZINC575440512	 The chemical structure of ZINC575440512 is similar to ZINC195440759 but with a different substituent on the macrocyclic ring. It also features a large ring system with indole-like rings and an amide group, colored with blue, red, and black.	-9.78 ± 0.04

Table 5. Average binding affinities after molecular docking of Ruboxistaurin and analogs to PKC β 1. An average of five trials was taken for the binding affinities of each analog with corresponding standard deviation values.

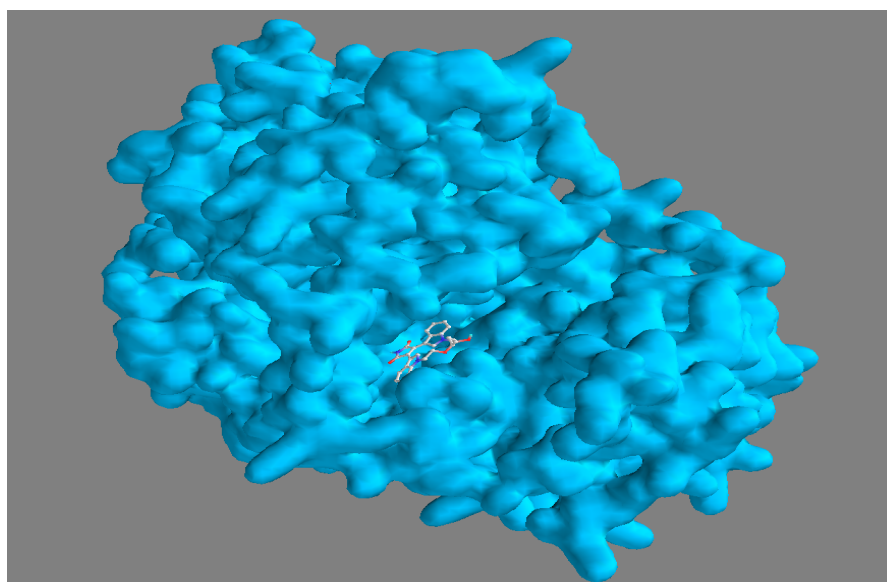
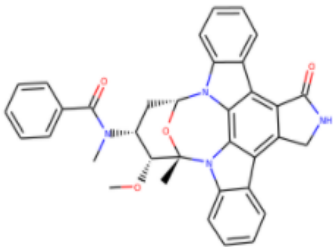
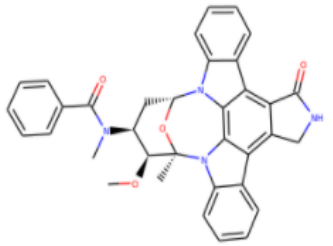


Figure 7. This image above shows the binding of ZINC3825435, which had the lowest binding energy, on to PKC β 1.

Binding of PKC β 1 to ZINC3825435 had the lowest energy of -10.1 kcal/mol, which is a 0.6 kcal/mol increase compared to the binding energy of ruboxistaurin. This analog has a hydroxyl group instead of a tertiary amine attached to the cyclic ring next to the oxygen. The stereochemistry of the hydroxyl group is conserved as it remains on the dashes.

PKC β 1 Inhibitor: Midostaurin

We examined 15 analogs of midostaurin binding to PKC β 1. Below are the 5 analogs that caused the greatest decrease in binding energy compared to base midostaurin.

Inhibitor	Structure	Binding Energy (kcal/mol)
Midostaurin		-9.44 \pm 0.34
Analog		
ZINC253614774		-10.58 \pm 0.12

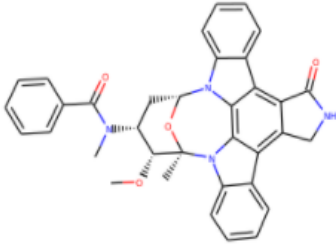
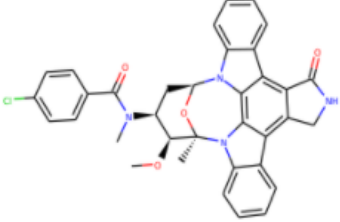
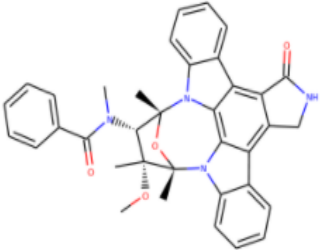
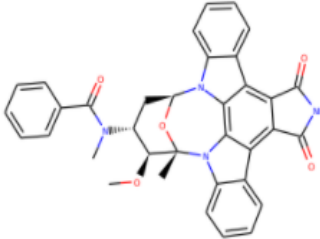
ZINC100080802		-10.42 ± 0.12
ZINC27326075		-10.92 ± 0.15
ZINC1569989194		-10.32 ± 0.15
ZINC584567048		-10.40 ± 0.25

Table 6. Average binding affinities after molecular docking of Midostaurin and analogs to PKC β 1. An average of five trials was taken for the binding affinities of each analog with corresponding standard deviation values.

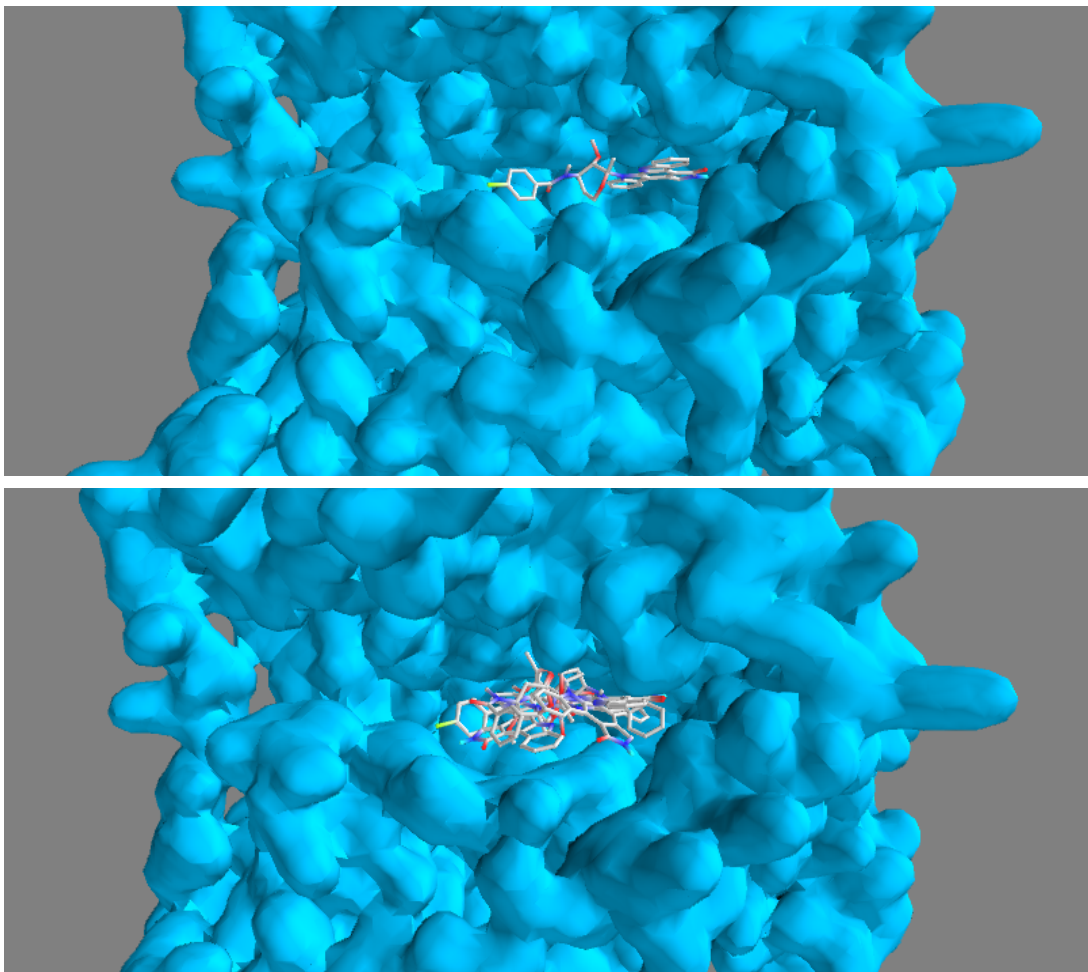


Figure 8. Image at the top shows the binding of ZINC27326075, which had the lowest binding energy, on to PI3K. Image at the bottom shows the binding of all the compounds, Midostaurin and its examined analogs, on to PKC β 1.

Binding of midostaurin to PKC β 1 was measured with a ΔG of -9.44 kcal/mol over 5 trials. Each analog of midostaurin, as well as midostaurin itself, bind to the same area on the PKC β 1 molecule. The analog that decreased binding energy the most was ZINC27326075, which differs from base midostaurin in that it has an extra chloride group coming off one of its aromatic rings, as seen in Figure 8. This leads to a binding energy increase of about -1.48 kcal/mol, from -9.44 kcal/mol for midostaurin to -10.92 kcal/mol for the analog.

PKC β 2 Inhibitor: Enzastaurin

We examined the same six analogs of Enzastaurin from the Zinc Database, however this time they were tested with PKC β 2. Two analogs, ZINC13489985 and ZINC13489987, were found to bind better to PKC β 2 than enzastaurin itself.

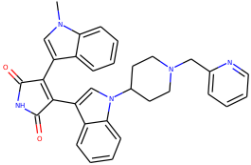
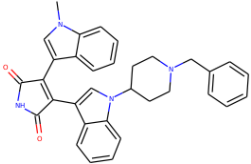
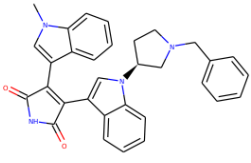
Inhibitor	Structure	Binding Energy (kcal/mol)
Enzastaurin		$- 9.40 \pm 0.31$
Analog		
ZINC13489985		$- 10.34 \pm 0.25$
ZINC13489987		$- 10.16 \pm 1.14$

Table 7. Average binding affinities after molecular docking of Enzastaurin and analogs to PKC β 2. An average of five trials was taken for the binding affinities of each analog with corresponding standard deviation values.

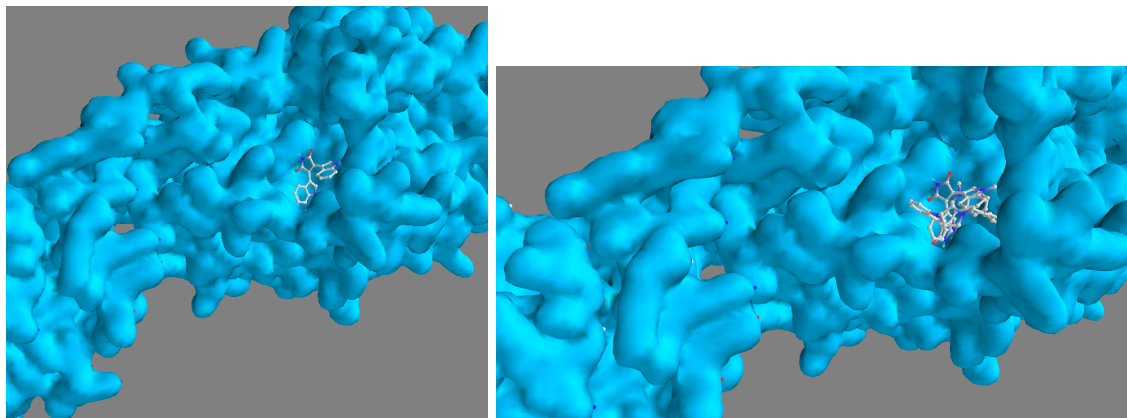


Figure 9. Image to the left shows the binding of ZINC13489985, which had the lowest binding energy, on to PKC β 2. Image to the right shows the binding of both analogs of enzastaurin, ZINC13489985 and ZINC13489987, on to PKC β 2.

The binding energy of enzastaurin to PKC β 2 was measured to be -9.40 kcal/ mol over five trials. Each analog of enzastaurin binds the site on the PKC β 2 molecule. The analog that had the best binding energy was ZINC13489985, with an increase of about -0.94 kcal/ mol from enzastaurin. The change made to enzastaurin to create this analog is replacing a nitrogen with a carbon in the benzene ring.

PKC β 2 Inhibitor: Sotrastaurin

We examined 9 analogs of Sotrastaurin from the ZINC Database, with five trials for each. Of these analogs, there were two molecules with significantly greater binding affinities upon docking with PKC β 2 than that of sotrastaurin.

Inhibitor	Structure	Binding Energy (kcal/mol)
Sotrastaurin		- 8.74 \pm 1.80

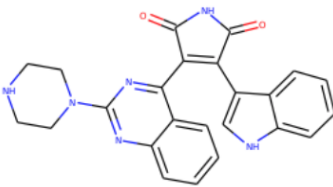
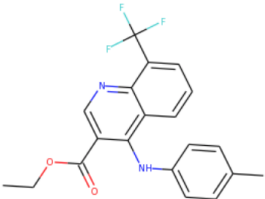
Analog		
ZINC36477833	 <p>The chemical structure of ZINC36477833 is a complex heterocyclic molecule. It features a central benzimidazole ring system. One of the imidazole nitrogens is substituted with a piperidine ring. The benzimidazole core is further substituted with a benzimidazole-2-thione group and a benzimidazole-5-yl group.</p>	- 11.16 ± 0.32
ZINC955736	 <p>The chemical structure of ZINC955736 is a substituted benzimidazole. It has a benzimidazole core with a trifluoromethyl group (-CF₃) at the 2-position, an ethyl ester group (-COOCH₂CH₃) at the 4-position, and a 4-methylphenylamino group (-NH-C₆H₄-CH₃) at the 5-position.</p>	- 9.28 ± 0.39

Table 8. Average binding affinities after molecular docking of Sotrastaurin and analogs to PKC β 2. An average of five trials was taken for the binding affinities of each analog with corresponding standard deviation values.

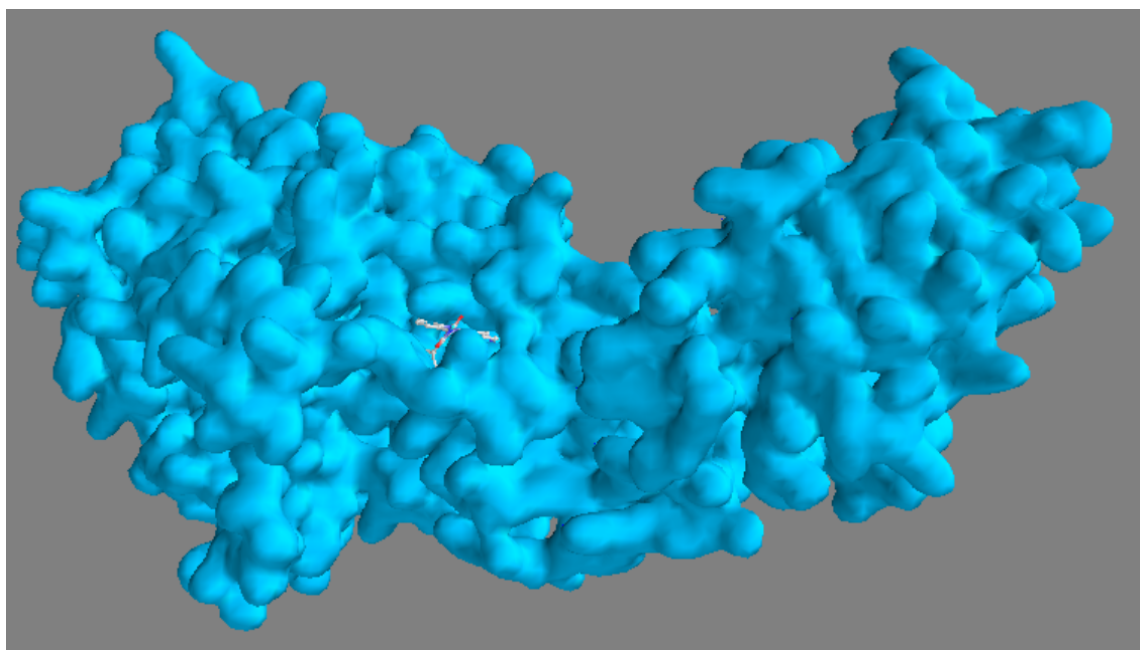
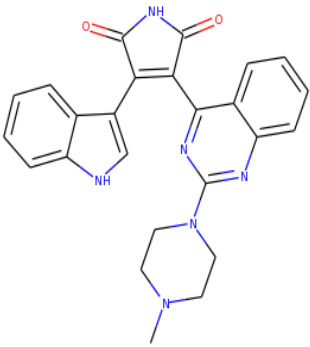


Figure 10. This image shows the analog ZINC36477833 (in the ball and stick model) interacting with PKC β 2 (shown in the molecular surface model).

Binding of sotrastaurin analogs to PKC β 2 were measured across five trials. ZINC36477833 has the lowest binding energy to PKC β 2 with a value of -11.16. This analog differs from sotrastaurin in its lack of a methyl group on a cyclic nitrogen, resulting in a 2.42 kcal/mol binding increase. The analog with the second lowest binding energy is ZINC955736, which differs from Sotrastaurin within many aspects of its structure, resulting in an increase of 0.54 kcal/mol. The major changes in the molecule include the addition of three fluorines, the removal of two cyclic structures, and the addition of an ester.

PKC δ Inhibitor: Sotrastaurin

We examined the binding energy of sotrastaurin and 10 of its analogues to PKC δ . Among these analogues, ZINC95573621 and ZINC36477833 had higher binding affinities to PKC δ compared to sotrastaurin. Another sotrastaurin analogue, ZINC95571944, exhibited a slightly lower but comparable binding affinity to PKC δ . We confirmed that sotrastaurin and all three reported sotrastaurin analogues have the same binding site on PKC δ .

Inhibitor	Structure	Binding Energy (kcal/mol)
Sotrastaurin		-10.00 \pm 0.67

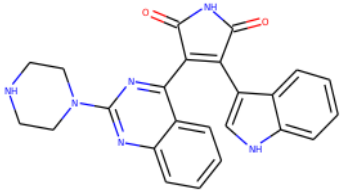
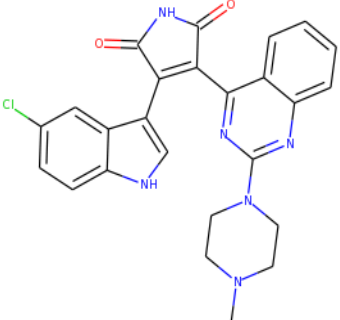
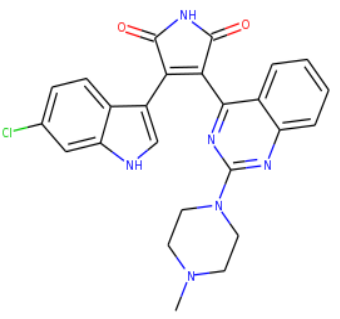
Analog		
ZINC36477833	 <p>The chemical structure of ZINC36477833 features a central benzimidazole ring system. It is substituted with a piperazine ring at the 2-position, a benzimidazole ring at the 5-position, and a 2,4-dioxo-1H-imidazole ring at the 7-position.</p>	-10.16 ± 0.09
ZINC95573621	 <p>The chemical structure of ZINC95573621 consists of a central benzimidazole ring system. It is substituted with a 4-chlorophenyl ring at the 2-position, a benzimidazole ring at the 5-position, and a 2,4-dioxo-1H-imidazole ring at the 7-position. Additionally, a piperazine ring is attached to the 2-position of the central benzimidazole ring.</p>	-10.18 ± 0.01
ZINC95571944	 <p>The chemical structure of ZINC95571944 is similar to ZINC95573621, featuring a central benzimidazole ring system. It is substituted with a 4-chlorophenyl ring at the 2-position, a benzimidazole ring at the 5-position, and a 2,4-dioxo-1H-imidazole ring at the 7-position. A piperazine ring is also attached to the 2-position of the central benzimidazole ring.</p>	-9.72 ± 0.04

Table 9. Average binding affinities after molecular docking of Sotrastaurin and analogs to PKC δ . An average of five trials was taken for the binding affinities of each analog with corresponding standard deviation values.

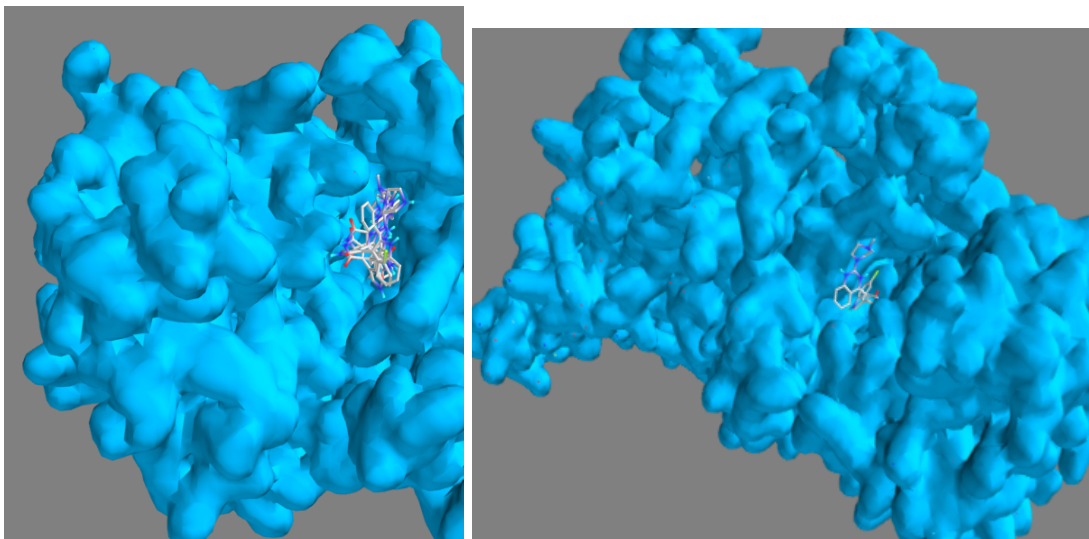


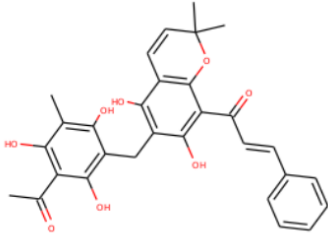
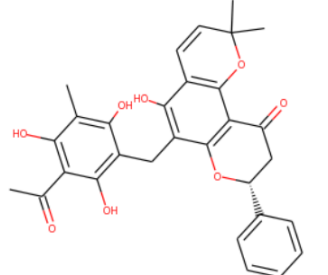
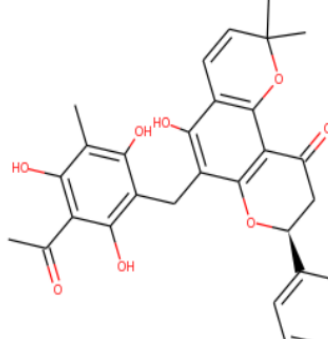
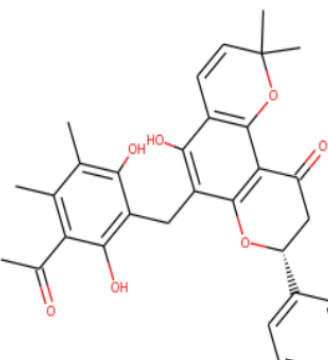
Figure 11. Image to the left shows the sotrastaurin analog ZINC95573621 interacting with PKC δ . Image to the right shows sotrastaurin and its three examined analogs bind to the same site on PKC δ .

The binding energy of sotrastaurin to PKC δ was measured to be -9.78 kcal/mol over five trials. The lowest binding energy was observed to be ZINC95573621 with a measured binding energy of -10.18 kcal/mol. The structure of ZINC95573621 differs from the structure of sotrastaurin by the addition of a chlorine substituent.

PKC δ Inhibitor: Rottlerin

We examined 13 analogs of Rottlerin from the ZINC Database. Of these 13 analogs, there were 5 analogs with higher binding affinities upon docking with PKC δ than that of Rottlerin.

Inhibitor	Structure	Binding Energy (kcal/mol)

Rottlerin	 <p>The chemical structure of Rottlerin is a complex molecule. It features a central chromane ring system. At the 2-position, there is a 3,4,5-trihydroxyphenyl group. At the 3-position, there is a 2,4,6-trihydroxyphenyl group. At the 4-position, there is a 2,4,6-trihydroxyphenyl group. At the 6-position, there is a 2,4,6-trihydroxyphenyl group. At the 7-position, there is a 2,4,6-trihydroxyphenyl group. At the 8-position, there is a 2,4,6-trihydroxyphenyl group. At the 9-position, there is a 2,4,6-trihydroxyphenyl group. At the 10-position, there is a 2,4,6-trihydroxyphenyl group.</p>	-9.30 ± 0.09
Analog		
ZINC33832042	 <p>The chemical structure of ZINC33832042 is a complex molecule. It features a central chromane ring system. At the 2-position, there is a 3,4,5-trihydroxyphenyl group. At the 3-position, there is a 2,4,6-trihydroxyphenyl group. At the 4-position, there is a 2,4,6-trihydroxyphenyl group. At the 6-position, there is a 2,4,6-trihydroxyphenyl group. At the 7-position, there is a 2,4,6-trihydroxyphenyl group. At the 8-position, there is a 2,4,6-trihydroxyphenyl group. At the 9-position, there is a 2,4,6-trihydroxyphenyl group. At the 10-position, there is a 2,4,6-trihydroxyphenyl group.</p>	-9.90 ± 0.00
ZINC33832041	 <p>The chemical structure of ZINC33832041 is a complex molecule. It features a central chromane ring system. At the 2-position, there is a 3,4,5-trihydroxyphenyl group. At the 3-position, there is a 2,4,6-trihydroxyphenyl group. At the 4-position, there is a 2,4,6-trihydroxyphenyl group. At the 6-position, there is a 2,4,6-trihydroxyphenyl group. At the 7-position, there is a 2,4,6-trihydroxyphenyl group. At the 8-position, there is a 2,4,6-trihydroxyphenyl group. At the 9-position, there is a 2,4,6-trihydroxyphenyl group. At the 10-position, there is a 2,4,6-trihydroxyphenyl group.</p>	-10.70 ± 0.00
ZINC238744931	 <p>The chemical structure of ZINC238744931 is a complex molecule. It features a central chromane ring system. At the 2-position, there is a 3,4,5-trihydroxyphenyl group. At the 3-position, there is a 2,4,6-trihydroxyphenyl group. At the 4-position, there is a 2,4,6-trihydroxyphenyl group. At the 6-position, there is a 2,4,6-trihydroxyphenyl group. At the 7-position, there is a 2,4,6-trihydroxyphenyl group. At the 8-position, there is a 2,4,6-trihydroxyphenyl group. At the 9-position, there is a 2,4,6-trihydroxyphenyl group. At the 10-position, there is a 2,4,6-trihydroxyphenyl group.</p>	-10.58 ± 0.04

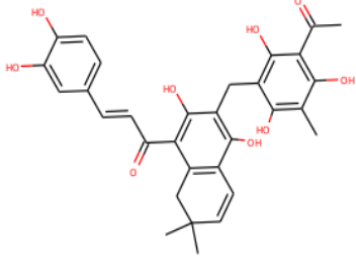
ZINC238753381		-9.80±0.00
---------------	--	------------

Table 10. Average binding affinities after molecular docking of Rottlerin and analogs to PKC δ . An average of five trials was taken for the binding affinities of each analog with corresponding standard deviation values.

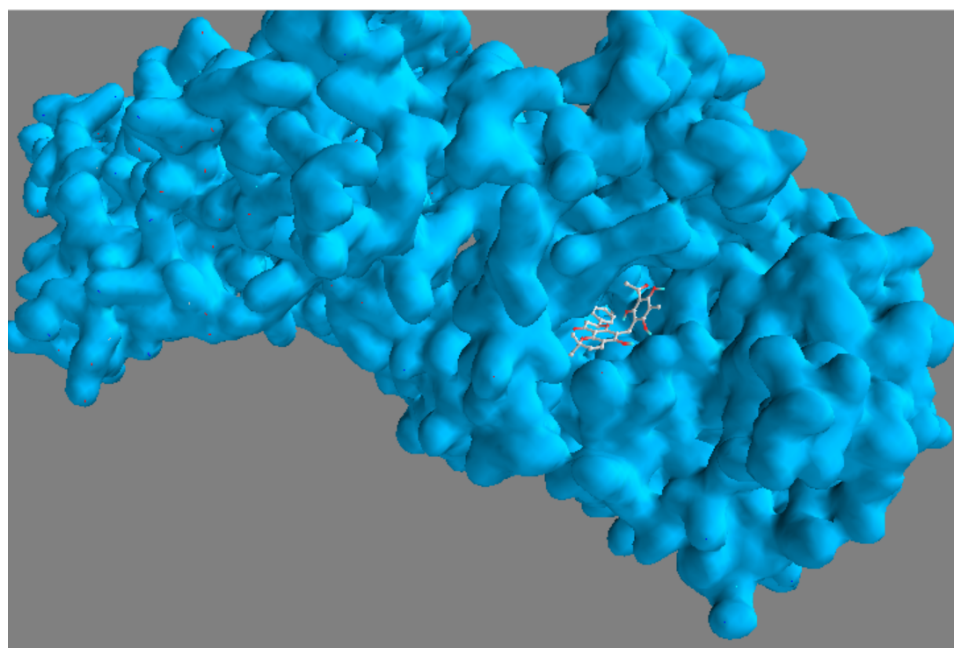


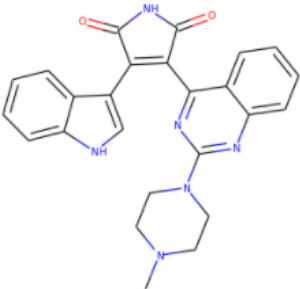
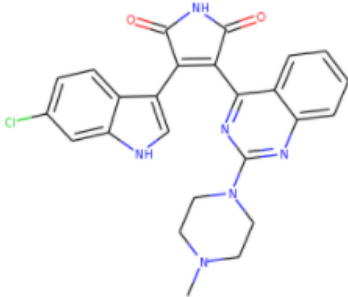
Figure 12. This image shows the analog ZINC33832041 (in the ball and stick model) interacting with PKC δ (shown in the molecular surface model).

The binding energy of Rottlerin to PKC δ was measured to be -9.3 kcal/mol over five trials. The analog that decreased binding energy the most was ZINC33832041 with an decrease of about 1.4 kcal/mol from that of Rottlerin. All analogs bound to PKC δ at the same binding site. The largest change in structure from Rottlerin to its analogs was the construction of a cyclohexane via a nucleophilic attack of an alkene by a hydroxyl group,

which was found in three of the analogs that increased binding affinities compared to Rottlerin.

PKC η Inhibitor: Sotrastaurin

We examined 26 analogs of sotrastaurin binding to PKC η . Below are the 5 analogs that caused the greatest decrease in binding energy compared to base sotrastaurin.

Inhibitor	Structure	Binding Energy (kcal/mol)
Sotrastaurin		-9.24 ± 0.09
Analog		
ZINC95571944		-10.0 ± 0.12

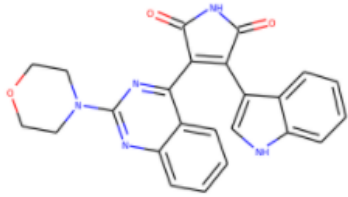
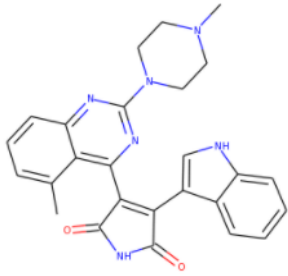
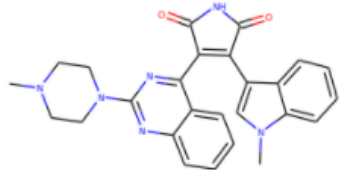
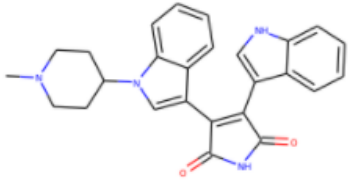
ZINC45318117		-9.64 ± 0.15
ZINC95574708		-9.62 ± 0.13
ZINC95578909		-9.94 ± 0.09
ZINC13489990		-10.58 ± 0.13

Table 11. Average binding affinities after molecular docking of Sotrastaurin and analogs to PKC η . An average of five trials was taken for the binding affinities of each analog with corresponding standard deviation values.

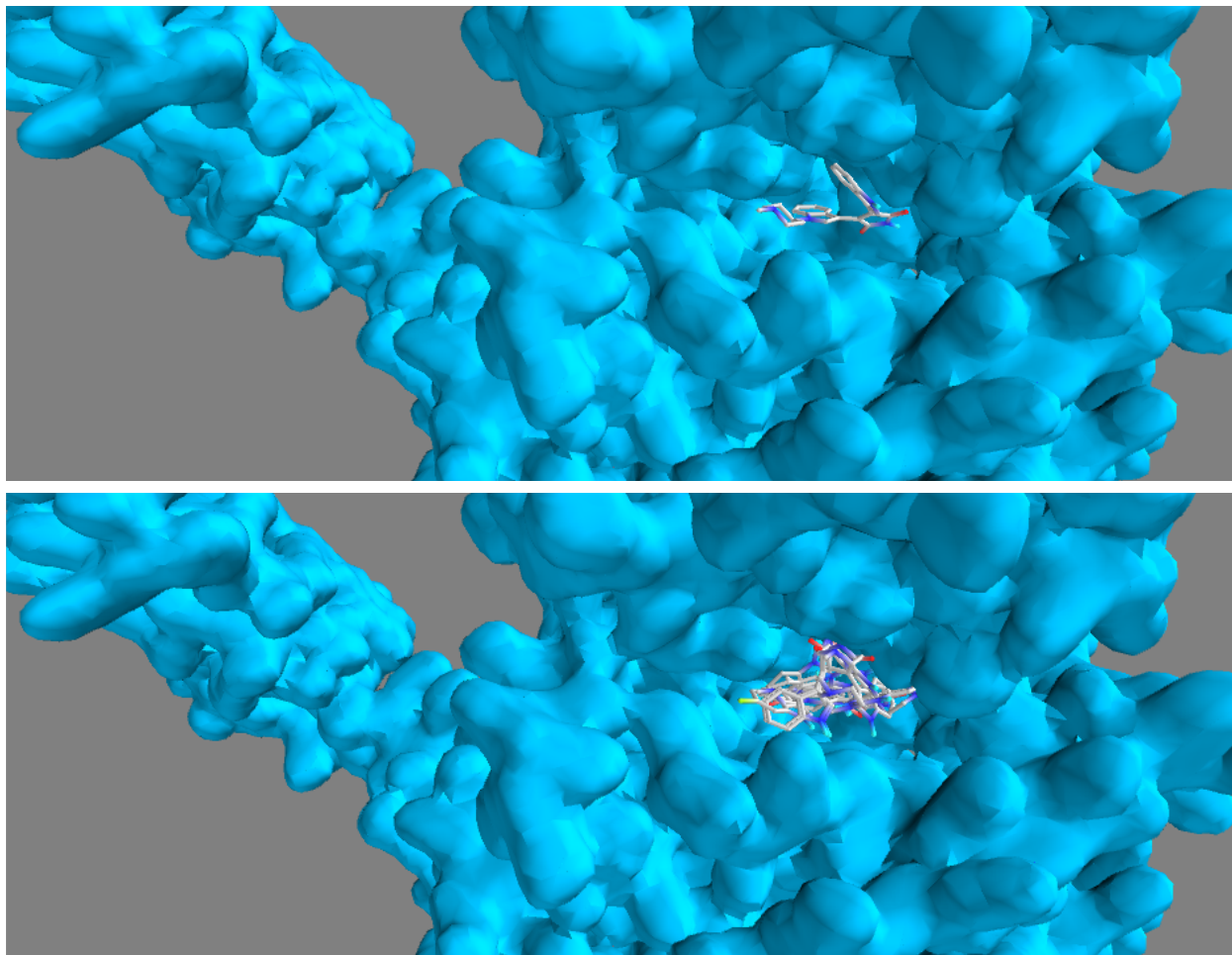


Figure 13. Image to the top shows the binding of ZINC13489990, which had the lowest binding energy, on to PKC η . Image to the bottom shows the binding of all the compounds, Sotrastaurin and its examined analogs, on to PKC η .

Binding of sotrastaurin to PKC η was measured with a ΔG of -9.24 kcal/mol over 5 trials. The figures show that each analog of midostaurin, as well as midostaurin itself, bind to the same area on the PKC η molecule. The analog that decreased binding energy the most was ZINC13489990, which differs from base sotrastaurin in that it has a cyclohexane converted to a cyclopentane, as well as the loss of two nitrogen groups, as seen in Figure 13. This leads to a binding energy decrease of about -1.36 kcal/mol, from -9.24 kcal/mol for midostaurin to -10.58 kcal/mol for the analog.

PLC γ 1 Inhibitor: U73122

We examined 26 analogs of U73122 from the ZINC Database. Of these 26 analogs, there were three analogs with lower binding energies upon docking with PLC γ 1 than that of U73122.

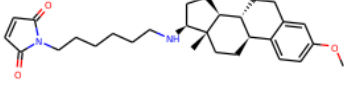
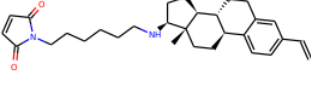
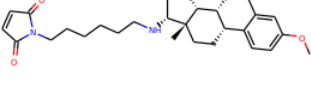
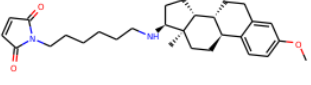
Inhibitor	Structure	Binding Energy (kcal/mol)
U73122		$- 8.63 \pm 0.47$
Analog		
ZINC575440631		$- 9.10 \pm 0.43$
ZINC145390416		$- 8.66 \pm 0.87$
ZINC31356813		$- 8.64 \pm 0.62$

Table 12. Average binding energies after molecular docking of U73122 and analogs to PLC γ 1. An average of five trials was taken for the binding energies of the analogues.

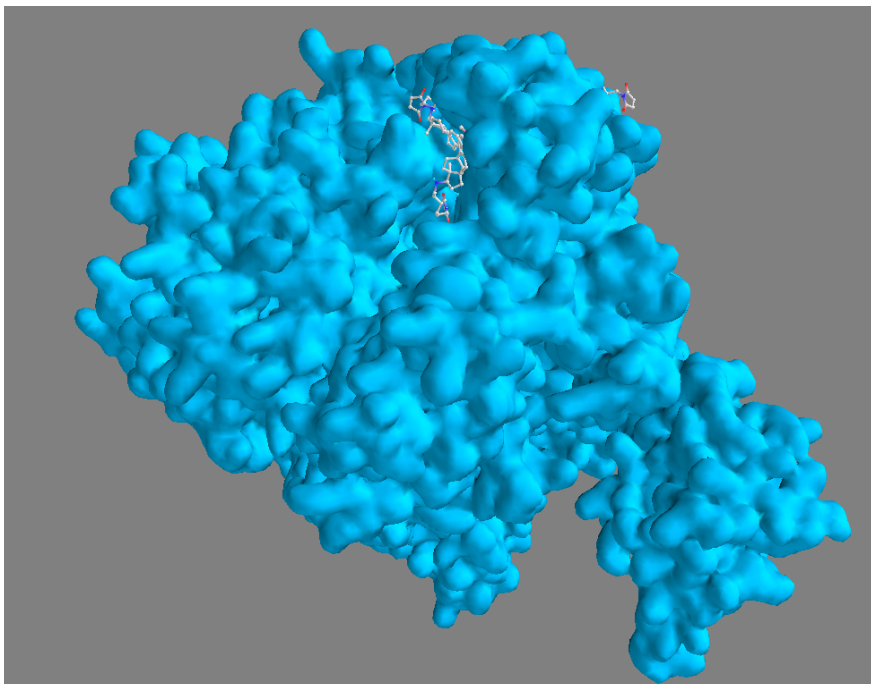


Figure 14. This image shows the analogs ZINC575440631, ZINC145390416, and ZINC31356813 (in the ball and stick model) interacting with PLC γ 1 (shown in the blue molecular surface model).

Binding of U73122 to PLC γ 1 was measured with a ΔG of $- 8.63 \pm 0.47$ kcal/mol over eleven trials. Binding of U73122 analogs to PLC γ 1 were measured across five trials. As shown in figure 14, analogs ZINC145390416 and ZINC31356813 bind to the same binding pocket of the PLC γ 1 molecule. The ZINC575440631 analog was predicted to be bound at a different location of the signaling molecule as its primary binding mode. The analog that was measured to have the lowest binding energy to PLC γ 1 was ZINC575440631 which differs from base U73122 structure with respect to the presence of an alkene, as seen in table 12. This resulted in a binding energy change of about -0.47 kcal/mol, from $- 8.63 \pm 0.47$ kcal/mol for U73122 to $- 9.10 \pm 0.43$ kcal/mol for the analog. The analog with the second lowest binding energy with PLC γ 1, among 26 analogs tested, was ZINC145390416 which differs from base U73122 in

stereochemistry, as seen in Table 12. This resulted in a binding energy change of about -0.03 kcal/mol, from $- 8.63 \pm 0.47$ kcal/mol for U73122 to $- 8.66 \pm 0.87$ kcal/mol for the analog. The analog with the third lowest binding energy with PLC γ 1, among 26 analogs tested, was ZINC145390416 which also differs from base U73122 in stereochemistry, as seen in table X. This resulted in a binding energy change of about -0.01 kcal/mol, from $- 8.63 \pm 0.47$ kcal/mol for U73122 to $- 8.64 \pm 0.62$ kcal/mol for the analog.

PLC γ 2 Inhibitor: U73122

We examined 26 analogs of U73122 from the ZINC Database. Of these 26 analogs, there was one analog with a decreased binding energy upon docking with PLC γ 2 than that of U73122.

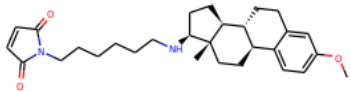
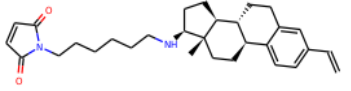
Inhibitor	Structure	Binding Energy (kcal/mol)
U73122		$- 8.18 \pm 0.32$
Analog		
ZINC575440631		$- 8.46 \pm 0.31$

Table 13. Average binding energies after molecular docking of U73122 and analogs to PLC γ 1. An average of five trials was taken for the binding energies of the analogues.

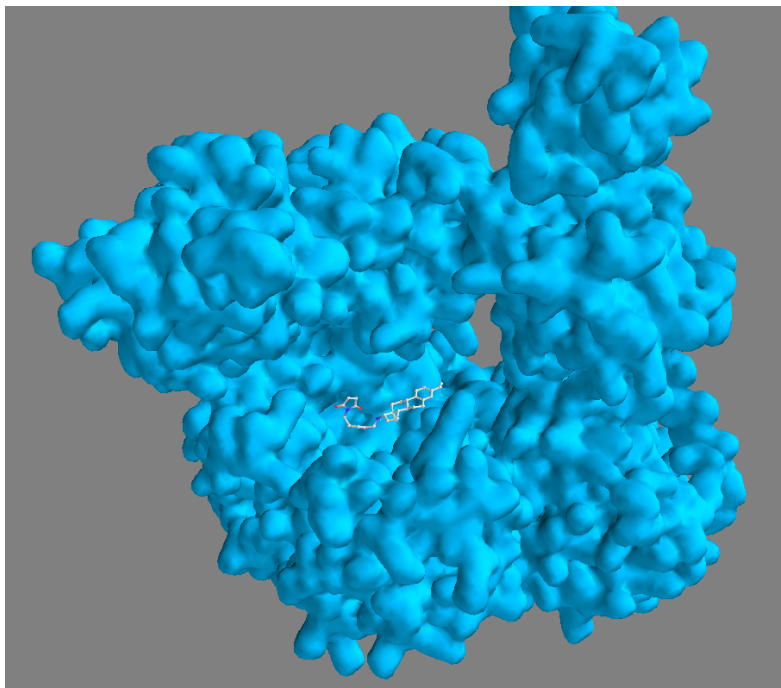


Figure 15. This image shows the analog ZINC575440631 (in the ball and stick model) interacting with PLC γ 2 (shown in the blue molecular surface model).

Binding of U73122 to PLC γ 2 was measured with a ΔG of $- 8.18 \pm 0.316$ kcal/mol over eleven trials. Binding of U73122 analogs to PLC γ 2 were measured across five trials. The ZINC575440631 analog binds to the same binding pocket of the PLC γ 2 signaling molecule as established inhibitor U73122. ZINC575440631, which differs from the base U73122 structure with respect to the presence of an alkene, was the only analog of the 26 screened that was predicted to have decreased binding energy to PLC γ 2 than U73122. The screening software predicted a binding energy change of about -0.28 kcal/mol, from $- 8.18 \pm 0.316$ kcal/mol for U73122 to $- 8.46 \pm 0.313$ kcal/mol for the analog.

Discussion

Once the binding energy of a ligand and each of its analogs to the target protein was calculated, analogs were ranked by how they changed binding affinity. Some analogs introduced structural changes that greatly enhanced binding to the target protein, as evidenced by a much more negative ΔG of interaction compared to the original ligand structures. The analogs that increased binding affinity were selected, and their binding fit was observed in PyRx. This was done by loading the file with the modelling results for one analog into PyRx with the target protein structure. This allowed direct visualization of the predicted best binding sites on the target protein that PyRx found for each ligand and analog. From here, it can be observed the molecular character of the binding site, such as the regions of hydrophobicity, polarity, and aromaticity, based on which amino acid residues comprise the binding site. It can be observed which parts of the ligand bind to each amino acid in the binding site, as well as how a ligand analog binds differently in the binding site. This allowed characterization of how each structural change afforded by each analog improved certain electrostatic interactions that contributed to the overall increase in binding affinity.

Our findings suggest that there are many novel and existing molecules that can be used to reduce the release of histamines and cytokines responsible for the allergic response, and further modification of these molecules may increase their inhibition capacities. In general, each inhibitor used as a ligand for each protein macromolecule had at least two analogs that increased binding to that protein. In some cases the binding affinity of the ligand's analog increased by over 1 kcal/mol compared to the ligand,

corresponding to at least a tenfold increase in ligand affinity for the protein. This indicates that there is much room for improvement of existing inhibitors for these proteins, and modifications can easily be made to them to reach analog structures. Such a large increase in affinity observed by the analog bindings indicates that these potential inhibitors can be made much more effective and reach the status of potent drug inhibition. Analog acquisition can be done several ways: by chemical synthesis or through purification from biological organisms.

Between inhibitors and their analog structures, there was also a pattern of some intermolecular forces always being retained. The binding sites of these proteins were very specific in character, often containing regions of high aromaticity, and of negative, positive, and neutral charge. Likewise, these potential inhibitors bound so well to their respective proteins because they also contained complementary regions to the protein binding sites. Even if analogs changed some structure of the inhibitors, these main intermolecular interactions between protein and inhibitor were maintained, and contributed to the bulk of the free energy of binding. Specific breakdowns of each inhibitor and its analogs can be found below.

PI3K - Wortmannin

By examining the structures we found that the Wortmannin analogs with the most negative binding energy, ZINC257519889 and ZINC144119389, differed from Wortmannin's structure by a change in the stereochemistry. A change of the ether substituent from a wedge to a dash made the analog bind more strongly. In ZINC144119389, having both the ether and ketone substituents moved from a wedge to a

dash led to decreased binding energy. The results suggest that changes in stereochemistry were effective at increasing the binding of Wortmannin to PI3K. The binding site of ZINC8035078, ZINC144119389, and ZINC71789745 were the same and were a different binding site than ZINC257519889 and ZINC3875294. Both of these analogs were bound at two different sites on PI3K. Studies have shown that there are at least five different binding pockets in PI3K which can all allow for inhibition, including allosteric inhibition (Miller et al., 2017).

PI3K - ZSTK474

The PI3K binding area that ZSTK474 and its examined analogs bound to was conserved, as they all bound to the same pocket. By examining their structures, it was found that the ZSTK474 analogs with the most negative binding energy, ZINC1772653009, ZINC73160255, and ZINC1243947389, differed in structure through changes to the triazine ring or its substituents which may have led to their higher binding affinities. In ZINC73160255, there is a pyrimidine instead of the triazine ring which may have made the analog bind more strongly as it became bound deeper within the PI3K binding area. In ZINC1772653009, the morpholine substituent on the triazine ring has been changed to an aminopiperidine, which may have made the analog bind more strongly. In ZINC1243947389, the morpholine substituent on the triazine ring has been changed to a tetrahydropyridine, which may have led to increased binding energy, the highest amongst the set of ZSTK474 analogs tested. The substituent changes on the analogs are interestingly on the part of the ZSTK474 inhibitor that protrudes out of the binding area pocket of PI3K.

PKC β 1 - Enzastaurin

By examining the structures we found that the analogs with the most negative binding energies differed from Enzastaurin's structure by a substitution of the nitrogen in the benzene ring for a carbon, which made the molecule less charged/polar, and by a change in the stereochemistry. A change of the ether substituent from a wedge to a dash made the analog bind more strongly. Because Enzastaurin is already a good inhibitor of PKC β (IC₅₀ of 50 nM), the analogs didn't need to have major modifications in order to demonstrate stronger binding affinities.

PKC β 1 - Ruboxistaurin

There were several structural changes that resulted in decreased binding energy. These changes mainly involve stereochemistry and substituent substitutions. The analog with the strongest binding energy, ZINC3825435, substituted the tertiary amine with a hydroxyl group. This group protrudes out of the binding area pocket of PKC β 1. Similarly, the analog with the second highest binding energy, ZINC13604307, substituted the same tertiary amine with an amino group. The analog was attached to the same binding pocket on the PKC β 1 protein as ZINC3825435. However, the amino group did not protrude outwards like the hydroxyl group. The other analogs had changes in either stereochemistry, other substitutions, or a combination of both. These findings suggest that the change to Ruboxistaurin with the most significance when binding PKC β 1 is the substitution of the tertiary amine with a hydroxyl or amine group.

PKC β 1 - Midostaurin

The PKC β 1 binding area that midostaurin and all of its analogs bound to was conserved, as evidenced by the figures, and had several particular characteristics. There was a region with many aromatic amino acids pointing into the pocket, and another region that had many negatively charged amino acids and oxygens. For all of the analogs, there was always some interaction between the aromatic area of the ligand and the aromatic amino acids of the PKC β 1 binding pocket, indicating that this interaction was very important to the binding energy of midostaurin and its analogs to PKC β 1. For midostaurin, the ligand oriented itself so that its aromatic region was as close to all of the aromatic amino acids in the pocket as possible. There was very little interaction with the negatively charged amino acids of the binding pocket. In the analog ZINC253614774, the change in stereochemistry led to the observance of an extra aromatic interaction between the lone end benzene on the left of the molecule and the binding pocket, which likely resulted in the observed decrease in binding energy is probably a big reason for binding energy decrease between ligand and protein. The change in stereochemistry caused the analog ZINC100080802 to orient differently in the binding pocket than midostaurin. Despite the additional chloride group, the analog ZINC27326075 took the same conformation in the binding pocket as ZINC253614774, so it is unclear why it has the highest affinity for PKC β 1 out of all the tested midostaurin analogs. In the analog ZINC1569989194, methylation caused the ligand to take a different conformation in the binding pocket than other analogs, with the aromatic region pointing outwards, and this was also the case for ZINC584567048, which had an extra carbonyl group on the pentane

near the aromatic region of the ligand. It is noticeable that most of the analogs, and midostaurin itself, prefer to orient with their aromatic regions overlapping that of the protein. For most of the analogs as well, there was not very clear engagement of the negatively charged region of the PKC β 1 binding pocket, and it did not interact visibly with the ligands.

PKC β 2 - Enzastaurin

Through examination of the structures, the analogs with the most negative binding energies differed from Enzastaurin's structure either in a substitution of an atom or by ring size. The ZINC13489985 analog has a carbon in the benzene ring instead of the nitrogen that was present in Enzastaurin, which made the ligand less polar. The ZINC13489987 analog has replaced a cyclohexane with a cyclopentane leading to a newly formed stereocenter, which may have contributed to the increased binding affinity to PKC β 2.

PKC β 2 - Sotrastaurin

Of the two high affinity potential inhibitors, the analog with the highest affinity, ZINC36477833, differed from Sotrastaurin structure through the lack of a methyl group on a cyclic nitrogen. Changes in the structure from a methyl to a hydrogen is a contribution of the stronger binding affinity, likely due to increased hydrogen bond capacity. While the second analog, ZINC955736, did have an increased binding affinity as well, major changes in its structure were only responsible for a 0.54 kcal/mol improvement in binding affinity. These changes included the addition of three fluorines, the removal of two cyclic structures, and the addition of an ester, which made the

molecule more polar overall. Therefore, the small change of the methyl-group removal appears to have a much greater impact than the many major adjustments found on ZINC955736.

PKC δ - Sotrastaurin

The central maleimide group on Sotrastaurin forms a hydrogen bond with ASN478 in the PKC δ binding pocket. This interaction is important for ligand binding to PKC δ because the maleimide group is conserved across all the analogues that had higher binding affinities compared to Sotrastaurin. Two analogues differed from Sotrastaurin by the addition of a chlorine substituent on the indoline group. The added chlorine substituent on these analogues may improve binding by steric or electronic effects. The chlorine atom fills up a large volume, and may provide a tighter fit to the residues in the binding pocket. The large size of the chlorine atom may also contribute to van der Waal interactions between the chlorine and nonpolar residues during binding.

PKC δ - Rottlerin

By examining the structures we found that the analogs with the lowest binding energy, ZINC33832041 and ZINC238744931, differed from Rottlerin's structure by the attack of the existing alkene by the hydroxyl within Rottlerin's structure to form a novel ring. From there, ZINC33832041 and ZINC238744931 alter stereochemistry by adjusting to a dash or wedge onto the phenyl group, which may decrease binding energy. Furthermore, Rottlerin contains a hydroxyl group on one benzene whereas in ZINC238744931 it has been exchanged for a methyl group. It is unclear if this leads to lower binding energy since the analog with the lowest binding energy, ZINC33832041,

contains the hydroxyl. Finally, ZINC238753381 does not contain the newly formed cyclohexane, yet the decreased binding energy may come from the change in constituents, two hydroxyls added which increase hydrogen bonding capacity.

PKC η - Sotrastaurin

The main binding site for sotrastaurin and its analogs on PKC η is conserved, as observed by the figures. Inspection of this binding site on PKC η in PyRx reveals that it contains a region of aromatic amino acids, as well as a region of nonpolar and region of negatively charged amino acids. Within all of the analogs of sotrastaurin, it appears that the amine group on the pentane ring at the top of the molecule always forms a hydrogen bond with a section of the binding pocket of PKC η , so this is probably a large factor in the free energy of ligand-protein interaction. The aromatic section of the binding pocket does not appear to interact strongly with sotrastaurin at all, as the ligand and all its analogs are separated by a large physical space from the aromatic amino acids of PKC η . In the analog ZINC95571944, the addition of a chlorine group caused the substrate to orient differently in the binding pocket than normal sotrastaurin, which might have been part of the increased affinity of the ligand-protein in. In ZINC45318117, the replacement of a nitrogen with an oxygen leads to an electrostatic interaction with a PKC η amine group in the binding pocket. The analogs ZINC95574708 and ZINC95578909 both added methyl groups in different places of the ligand, which changed the orientation of the analog of sotrastaurin binding to the pocket. As stated before, the analog with the highest increase in binding affinity, ZINC13489990, differs from base sotrastaurin in that it has a cyclohexane converted to a cyclopentane, as well as the loss of two nitrogen groups,

leading to a different conformation in the PKC η binding pocket. The aromatic residues of the binding pocket did not play a major, observable role in binding for any of these analogs. The addition of minor substituent groups to the sotrastaurin ligand to make nearly identical analogs still caused large changes in the conformation of the ligand in the protein binding pocket, indicating that binding is flexible many different modes of binding can occur.

PLC γ 1 - U73122

Upon examination of the structures of these low binding energy analogues, we observed that the analog with the highest affinity to PLC γ 1 amongst the set of U73122 analogs tested was ZINC575440631. It differed from U73122's structure through a change to one of its substituents. In this analogue, the ether substituent bound to an aromatic carbon has been changed to an alkene. Analogs ZINC145390416 and ZINC31356813 differed from the structure of U73122 simply by a change in stereochemistry. Changes in the structure from wedges to dashes resulted in the analogs binding more strongly.

PLC γ 2 - U73122

Upon examination of the structure of ZINC575440631, the lowest binding energy analog amongst the set of U73122 analogs tested, we observed that it differs from U73122's structure through a change to one of its substituents. In this analog, the ether substituent bound to an aromatic carbon has been changed to an alkene. Notably, this analog was also predicted to have the lowest binding energy, among the 26 analogs

tested, with PLC γ 1. This is indicative of the degree of low binding energy of this analog with PLC γ isoforms.

These findings might aid in the development of a new allergy medication, perhaps with more efficacy than ones currently on the market. For each of the inhibitors tested, there was at least one analog that bound more tightly to the target protein than the inhibitor itself. These analogs can be easily synthesized for future testing. Furthermore, treatments targeting the molecules we examined have the potential to be administered prophylactically, and still be useful even after exposure to allergens

Future Directions

The first thing that can be done with these results is to test a combination of analog modifications. The research conducted in this project identified analogs to existing inhibitors for proteins of the mast cell degranulation pathway. These analogs are discrete and most of them do not overlap, so the modifications made from the base inhibitor to create them can be combined. In this way, beneficial changes can be combined to make a potential inhibitor that would be even more potent than any of the analogs individually.

The structures of the analogs that increased binding affinity the most could be combined in an effort to further boost ligand-protein binding by putting together individually beneficial structural changes. This can be done by importing the structure of each ligand into a molecular editing software like PYMOL. Once within PYMOL, the structure of the ligand could be changed and then saved as a separate file. In this way, the molecular changes of multiple analogs could be combined to create new potential structures to test. The affinity of these new structures would then be modelled in PyRx to see if the summation of the molecular changes was truly beneficial. The analog combination can be repeated with several different structural variants in an attempt to find an optimized ligand structure. In addition, user-suggested changes could be implemented based on observations of the character of the primary binding site on the protein that the ligand attached to. If a binding site was rich in aromatic amino acid residues, then a custom modification of the ligand could be made in PYMOL outside of those provided by the analogs of ZINC database, such as an addition of a benzene or naphthalene ring to the ligand structure. However, any and all of these structural

modifications shared the same underlying principle of enhancing the observed intermolecular interaction between the ligand and protein at the main binding site, so any favorable analog combinations or custom structures would be made with the intent of optimizing at least one of these interactions in an attempt to improve the overall ΔG of binding.

These “custom” potential inhibitors can also be modified based on the observed characteristics of the binding site on the protein. For example, the binding pocket of PKC β 1 had many negatively charged amino acids that midostaurin did not interact with, and the binding pocket of PKC η had a region of aromaticity that sotrastaurin did not interact with as well. The information gained from this project with regard to combining analogs and tailoring inhibitors to their binding sites would be very useful in future creation of better inhibitors for these proteins. An example of this is the structure the custom sotrastaurin analog shown below:

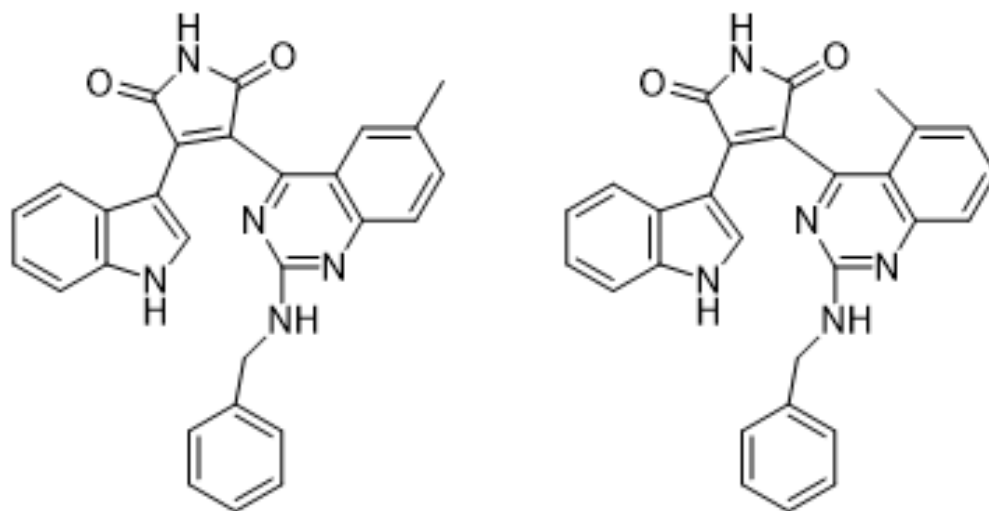


Figure 16: Structure of two custom analogs modelled off sotrastaurin and optimized to maximize interactions with the PKC η binding pocket.

Both of these sotrastaurin analogs were designed based on the research done in this study. They combine multiple beneficial traits of sotrastaurin analogs from the ZINC database, such as methylation and removal of nitrogen in selective locations. They also are designed with the binding pocket structure of PKC η considered. The addition of an aromatic group rather than a cyclohexane is intended to help drug binding to aromatic residues in the binding pocket and enhance overall total affinity. Similar structural modifications can be made to other potential inhibitors targeting other proteins based on the research result of this study, which will enhance drug design by allowing scientists to better understand and optimize the intermolecular forces between proteins and their inhibitors.

The results compiled from this project are purely theoretical, so the next step after theoretical drug design would be to actually synthesize the ligands with the highest affinity for proteins. The protein modelling in PyRx yielded analogs to several known inhibitors that are predicted to have a higher free energy release upon binding their target proteins. These potential inhibitor analogs have not yet been made though, so it would be recommended to use the existing inhibitors as a base to make their analogs. Once the analogs are made, they can then be tested in actual analytical devices to see if their free energy of binding to the target proteins match the PyRx predictions. This could be done using analytical devices like NMR (nuclear magnetic resonance) and ITC (isothermal titration calorimetry). Determining the actual strength of binding of the potential inhibitor analogs compared to the existing inhibitors would be very useful to verify the results gained from PyRx models.

Because our current data is based on computer modeling, we suggest a next step would be *in vitro* experimentation using a mast cell line to determine the efficacy of potential inhibitors in a cellular environment. To accomplish this a MC/9 mast cell line can be used, which are mouse liver mast cells that express FcεR1 and will release histamine when exposed to antigens after incubating with anti-Fc-receptor antibodies (ATCC® CRL-8306™). These cells are commonly used in degranulation assays because they can be induced into degranulation, which is the main context of measurement for this study.

In order to measure said degranulation accurately, it will also be necessary to collect control data of degranulation in known conditions. The first most important test would be a negative control to determine how much histamine and other degranulatory substances are released naturally when the cells are at rest and not being induced to degranulate. As a positive control, degranulation can be induced using the addition of IgE. Degranulation can be assayed using enzyme linked immunosorbent assay (ELISA) or flow cytometry. Relative intensities of degranulation and concentrations of degranulatory metabolites can be measured to see if relative mast cell degranulation is lower in solutions with the inhibitor analog present compared to the existing inhibitor and simple uninhibited mast cells. If degranulation is actually reduced with the analog ligands, they can finally be put into testing for novel anti-allergic drugs. Following cellular assays, future experimentation can be conducted on murine models to model the effects of the therapeutic in a mammalian system. If time permits, future experimentation

within murine models will be conducted in order to understand and minimize negative effects on other bodily functions.

Another possible avenue for future research is to determine how to best target these potential therapeutics to mast cells. One popular method of targeted drug delivery is using nanoparticles. Currently, nanoparticles are being used to encapsulate and deliver antigen-specific immunotherapy and DNA vaccines (Pohlit et al., 2017). Nanoparticles confer several advantages over traditional drug delivery systems: protection against degradation, targeted delivery, and higher concentrations at the delivery site for increased effectiveness. These can also be biodegradable or nonbiodegradable and their surfaces can be highly customized to target specific cells (Pohlit et al., 2017).. Nanoparticles are a promising method of delivering our identified drug targets to mast cells to suppress histamine release. The future direction outlined here would be crucial to further understanding the efficacy and safety of the potential inhibitors.

Equity Impact Report

Using the *Racial Equity Impact Assessment*, we assessed our research on the basis of several factors: identifying the stakeholders in our research, examining the causes, considering adverse impacts, and examining alternatives and improvements. This framework was posed by *race forward*—the center for racial justice innovation and it provides a guide to address questions of equity. In this report, we discuss the impact of our research on various racial/ethnic and socioeconomic groups and provide recommendations for equitable next steps of our research.

Defining Equity in Healthcare

Our team first defined the difference between equity and equality, as defining the distinction between these two terms was important for our consideration of equity in our research. Equality does not take into account disparities in need while equity does. Equity can be thought of as synonymous with justice and it has three aims: focus, inclusion, and narrowing gaps (World Health Organization, 2000). The focus is on the health of the vulnerable population and thus our policy should focus on improving the health of the most vulnerable. We should consider the inclusivity of our study to ensure that no communities are left out. Finally, our research policy should narrow the current gaps in health.

According to the World Health Organization (2000), equity in health is aimed to minimize avoidable disparities in health and its determinants and to have an equitable distribution of health care resources. In order to have equitable access, the distribution of health services must take into account the social, economic, and demographic

characteristics and need. Thus, to discuss equitable access to our allergy therapeutic we must understand the needs of the demographics whom our research will impact.

Who Our Research Serves: Identifying Stakeholders

Throughout the years, the field of medicine has evolved to consider various socioeconomic and cultural factors that shape a person's health. Research highlights certain groups that are more prone to allergies than others and those that struggle with symptom management.

Susceptibility to allergies is partly based on race. A study on young children aged 1-8, including Afro-American and Caucasian children, investigated the effects of strong risk factors of allergy, including going to daycare more often and exposure to secondhand tobacco smoke. (Sun & Sundell, 2011). African American children of the study were found more likely to have a positive skin prick test (diagnostic test for allergens) and elevated allergen-specific and total IgE which mediates the allergic response. These differences persisted even after standardizing for income, education, environmental exposures, and many other lifestyle factors that differed between races (Wegienka et al., 2011). Black women are also 2.5 times more likely to be sensitized to at least 3 allergens compared to white women (Wegienka et al., 2011). It is also known that people with multiple food allergies are at greater risk of severe food-induced reactions (Bilaver et al., 2016). Lastly, Black children under 18 years old have double the diagnoses for allergic disease compared to white children (Wegienka et al., 2011). Black patients are also at an increased risk of having severe food-induced anaphylaxis (Warren et al., 2021). Asian children have higher odds of developing food allergies compared to white children,

whereas Hispanic children are less likely to develop food allergies than white children (Bilaver et al., 2016). Further research needs to be conducted to determine if these disparities are caused by genetics or lifestyle.

Among those who have allergies, socioeconomic factors affect disparities in diagnosis, treatment, and prevention. It is known that low income children who meet the criteria for food allergy were not diagnosed by a physician as often as high income children (Warren et al., 2021). Population studies on families with children who have food allergies have shown that the lowest income families spend 2.5 times more money on emergency department visits and hospitalization (Bilaver et al., 2016). On the other hand, families with a higher household income spent more on out-of-pocket medications and specialist visits and that epinephrine auto-injectors, one of the primary treatments for anaphylactic shock, has placed an economic burden on low-income families. Patients on Medicaid receive less follow up care than patients who can afford private insurance, which can help prevent recurrence of severe symptoms (Warren et al., 2021). This suggests that children from families with a higher socioeconomic status are more likely to receive adequate treatments and preventative care that lowers their risk for serious symptoms.

It is also important to consider racial inequities in access to medical care. Some factors include access to transportation, income, insurance coverage, and medical trust/physician cultural competency, among others (Warren et al., 2021). For example, it's been shown that black children are less likely to have a food allergy diagnosis by a physician, attesting to structural barriers to medical care (Warren et al., 2021). Overall,

barriers faced by racial and socioeconomic minority groups need to be overcome so that our proposed therapeutics can help treat these patient populations.

Examining the Causes of Inequities and Considering Adverse Impacts

Research that is conducted with the best intentions can often be misused for different applications. In our study, we identified potential drug targets to be proposed to pharmaceutical companies for further testing and drug development. Our hope is that these medications can be distributed equitably to those with allergies. Unfortunately, there are barriers to universal access to medication that will curtail the potential impact of this research.

One issue that provides barriers to vulnerable populations is accessibility to the medication. The paper *Measuring Equity in Access to Pharmaceutical Services Using Concentration Curve* establishes a model to score access to pharmaceuticals. This measure takes into account several access indicators with a score of 100 to prescriptions that are available in any pharmacy to a score of one to prescribed medicines that are not available at all. A score of 90 was given if a patient has to change to an alternate drug and scores of 60 and 50 are given if patients have to make a trip to a larger city to have availability to the drug (Davari et al., 2015). The proposed methodology then includes scores for socioeconomic status by providing a ranking for income, occupation, education, home status and family size. The sum of these scores is used to determine the socioeconomic status of the individual which can be used to access the barrier they might face to receiving pharmaceutical treatments. This study provided a method for measuring

socioeconomic status and pharmaceutical equity. Future research into the development of our proposed therapeutic should follow this framework to assess accessibility.

Disparities in access to medication can affect how our proposed treatments are distributed. Areas with a high percentage of minorities have less pharmacy density and communities with a low average income level, low employment, and high crime rates are less likely to have access to home medication delivery services (Chisholm-Burns et al., 2017). In addition, uninsured patients are four times more likely to not take medications for financial reasons, and patients with lower income who have higher out of pocket medication costs are at much greater risk of cost-related medication nonadherence (Chisholm-Burns et al., 2017). These patients are not able to afford medications at the inflated prices set by pharmaceutical companies. Currently, the pharmaceutical industry is controlled by the free market, where supposedly high prices are a result of high research and development costs (Spinello, 1992). If a company has a monopoly on a certain type of drug, they can control the prices, and in our capitalistic society, the goal is often to obtain higher profits at the expense of accessibility/equity in distribution (Spinello, 1992). Medication nonadherence due to financial reasons leads to poorer health and increased hospitalizations, which are also expensive, perpetuating the cycle of inequity (Chisholm-Burns et al., 2017).

Recommendations

Our team needs to advocate for groups that may lack access to our proposed drug by encouraging pharmaceutical companies to be more equitable in their drug pricing policies. This could be achieved by lobbying for more governmental regulation over the

pharmaceutical industry (Spinello, 1992). We also can recommend that the pharmaceutical company that produces our drug should follow the proposed methodology of Davari et al. (2015) to ensure that the drug will be equitably distributed. This way, treatment can go to the groups who actually require it the most and our medication will help the most vulnerable populations and close gaps in health care

Additionally, once the drug is developed it must undergo clinical trial testing to ensure its safety and efficiency (Mbuagbaw et al., 2017). This is another opportunity to focus on vulnerable populations. The PROGRESS Plus acronym provides a framework to include the determinants of health within the design of a clinical trial. It stands for Place of residence, Race/ethnicity/culture/language, Occupation, Gender, Religion, Education, Socio-economic status, and Social capita (Mbuagbaw et al., 2017). The rationale for including place of reference makes the study designer consider how different areas, for example rural versus urban may impact the study results. This will be particularly important for us since allergies can be directly caused by environmental factors. The role of minority groups in the trial must be considered as well as language and level of education. The paper suggests not excluding participants based on their english skills for example and over translations of the trial to ensure inclusivity. Additionally, gender can be linked to inequalities as well and so clinical trial designers should consider ensuring that recruitment efforts are identical to include various gender identities. In total, these are a few key considerations that must be made to ensure that the clinical trial is inclusive and thus provides evidence on the effects of a diverse population, especially those of

vulnerable groups who are disproportionately impacted by allergies as discussed previously in this report.

Through conducting our Gemstone research, we have been able to contribute to the field of immunology and allergy research by identifying targets for drug development and provided recommendations for an equitable framework for pharmaceutical development and distribution. Through this project, we have committed to providing a new therapeutic to those who suffer from allergies to provide a new, effective and affordable option to patients that need it. By keeping these questions of equity at the forefront of our research we have been able to complete a project that not only advances scientific knowledge but also the needs of our society.

Appendices

Appendix A - Glossary

Definitions are from Oxford Dictionary unless otherwise cited. Other definitions originate from various sources in order to find the most concise or accurate definition of relevant terms.

Adaptive immunity - immunity that has memory and occurs after exposure to an antigen either from a pathogen or a vaccination (Molnar & Gair, 2013).

Agglutination - (with reference to bacteria or red blood cells) clumping together.

Allergy-specific immunotherapy (SIT) - administration of allergen extracts to achieve clinical tolerance of allergens that cause symptoms in patients with allergic conditions (Frew, 2010).

Anaphylactic shock - an extreme, often life-threatening allergic reaction to an antigen to which the body has become hypersensitive.

Antibody - a blood protein produced in response to counter a specific antigen.

Antigen - a toxin or other foreign substance which induces an immune response in the body, such as the production of antibodies.

Antigen-presenting cell (APC) - any cell that assists in the production of immune responses by presenting antigen; especially any of several types of cell with monocytic lineage that present antigen in association with class II MHC molecules, to helper T lymphocytes.

B cell - a lymphocyte not processed by the thymus gland, and responsible for producing antibodies. Also known as B lymphocyte.

Basophil - a basophilic white blood cell.

Corticosteroid - any of a group of steroid hormones produced in the adrenal cortex or made synthetically. There are two kinds: glucocorticoids and mineralocorticoids. They have various metabolic functions and some are used to treat inflammation.

Cytidine deaminase (AID) - enzyme that in humans is encoded by the *CDA* gene (Kuhn, 1993)

Cytokine - any of a number of substances, such as interferon, interleukin, and growth factors, which are secreted by certain cells of the immune system and have an effect on other cells.

Decongestant - used to relieve nasal congestion.

Degranulation - (of a cell) lose or release granules of a substance, typically as part of an immune reaction.

ELISA (enzyme-linked immunosorbent assay) - a laboratory technique that uses antibodies linked to enzymes to detect and measure the amount of a substance in a solution, such as serum. The test is done using a solid surface to which the antibodies and other molecules stick. In the final step, an enzyme reaction takes place that causes a color change that can be read using a special machine. There are many different ways that an enzyme-linked immunosorbent assay can be done. Enzyme-linked immunosorbent assays may be used to help diagnose certain diseases. (“NCI Dictionary of Cancer Terms”, n.d.).

FcεR1 - the high affinity Immunoglobulin E receptor which is a tetrameric membrane protein complex expressed on mast cells and basophils which belongs to the family of immunoreceptors involved in antigen recognition (Type I 2018).

Histamine - a compound which is released by cells in response to injury and in allergic and inflammatory reactions, causing contraction of smooth muscle and dilation of capillaries.

Humoral immune response - antibodies produced by B cells cause the destruction of extracellular microorganisms and prevent the spread of infections (Janeway, 2001).

Immunoglobulin (IgE, IgG, IgM, IgD, IgA) - any of a class of proteins present in the serum and cells of the immune system, which function as antibodies.

Interferon- γ (IFN- γ) - an interferon that is produced by T cells, regulates the immune response, and in a form produced by recombinant DNA technology is used especially to control infections due to inability of white blood cells to destroy certain bacteria and fungi (Merriam-Webster).

Leukotriene - any of a group of biologically active compounds, originally isolated from leukocytes. They are metabolites of arachidonic acid, containing three conjugated double bonds.

Major histocompatibility complex (MHC) - major histocompatibility complex (MHC), group of genes that code for proteins found on the surfaces of cells that help the immune system recognize foreign substances. Also known as the human leukocyte antigen (HLA) system.

Mast cell - a cell filled with basophil granules, found in numbers in connective tissue and releasing histamine and other substances during inflammatory and allergic reactions.

Opsonization - making (a foreign cell) more susceptible to phagocytosis.

Phagocytosis - the ingestion of bacteria or other material by phagocytes and amoeboid protozoans.

Pharmacotherapy - medical treatment by means of drugs.

Proinflammatory - that promotes inflammation (Ex. When the lesions are traumatized, or rubbed firmly, the cutaneous mast cells may release *proinflammatory* mediators, causing edema, erythema, and even vesicle formation.) (Merriam-Webster, 2007)

Prostaglandin - any of a group of compounds with varying hormone-like effects, notably the promotion of uterine contractions. They are cyclic fatty acids.

T cell - a lymphocyte of a type produced or processed by the thymus gland and actively participating in the immune response.

Tyrosine - a hydrophilic amino acid which is a constituent of most proteins and is important in the synthesis of some hormones.

Appendix B - Supplemental Figures

Binding Site (macromolecule)	Known Inhibitors (ligand)	Binding Energy (ΔG)	Standard Deviation	K_d
PKC-eta (η)	Miltefosine	-4.863636364	0.4365151252	2.70E-04
PKC-eta (η)	Sotrastaurin	-9.027272727	0.2453198284	2.38E-07
PKC-eta (η)	Staurosporine	-10.1	1.385640646	3.88E-08
PKC-eta (η)	GSK-690693	-7.645454545	0.1809068067	2.45E-06
PKC-eta (η)	A-674563	-7.881818182	0.376346069	1.65E-06
PKC-delta (Δ)	Miltefosine	-5.481818182	0.2676497032	9.50E-05
PKC-delta (Δ)	Sotrastaurin	-10.01818182	0.6750084175	4.46E-08
PKC-delta (Δ)	Rottlerin	-9.363636364	0.09244162777	1.35E-07
PKC-delta (Δ)	Ingenol Mebuate	-6.363636364	4.843195789	2.14E-05
PKC-theta (θ)	Miltefosine	-5.318181818	0.437762908	1.25E-04
PKC-theta (θ)	Sotrastaurin	-9.33	0.5375872022	1.43E-07
PKC- β 1	Miltefosine	-5.045454545	0.3559877424	1.99E-04
PKC- β 1	Sotrastaurin	-9.681818182	0.6997402115	7.87E-08
PKC- β 1	Midostaurin	-9.633333333	0.05773502692	8.54E-08
PKC- β 1	Enzastaurin	-10.15454545	0.3830499611	3.54E-08
PKC- β 1	Ruboxistaurin	-8.736363636	1.80403588	3.89E-07
PKC- β 2	Miltefosine	-4.818181818	0.3124681802	2.91E-04
PKC- β 2	Sotrastaurin	-8.981818182	0.460039524	2.57E-07
PKC- β 2	Midostaurin	-9.3	0.1	1.50E-07
PKC- β 2	Enzastaurin	-9.4	0.3130495168	1.27E-07
PKC- β 2	Ruboxistaurin	-9.009090909	0.1921173884	2.45E-07
PI3K	Wortmannin	-7.627272727	0.3608071759	2.53E-06
PI3K	LY294002	-7.527272727	0.09045340337	3.00E-06
PI3K	ZSTK474	-8.427272727	0.1793929156	6.55E-07
PI3K	Nobiletin	-6.363636364	0.1858640755	2.14E-05
PLC- γ 1	GDP	-7.8375	0.3020761493	1.77E-06
PLC- γ 1	Resveratrol	-7.590909091	0.5300085763	2.69E-06
PLC- γ 1	Piceatannol	-7.681818182	0.430855386	2.31E-06
PLC- γ 1	U73122	-8.6	0.4546060566	4.89E-07
PLC- γ 1	Nicotinamide	-5.254545455	0.1213559752	1.39E-04
PLC- γ 2	GDP	-7.3125	0.2167124494	4.31E-06

PLC- γ 2	Resveratrol	-7.236363636	0.05045249791	4.90E-06
PLC- γ 2	Piceatannol	-7.409090909	0.1578261414	3.66E-06
PLC- γ 2	U73122	-8.209090909	0.3144981572	9.47E-07
PLC- γ 2	Nicotinamide	-5.2	0.04472135955	1.53E-04

Appendix C - Structure Analysis and Comparison

PI3K

1. Errat Server Comparison

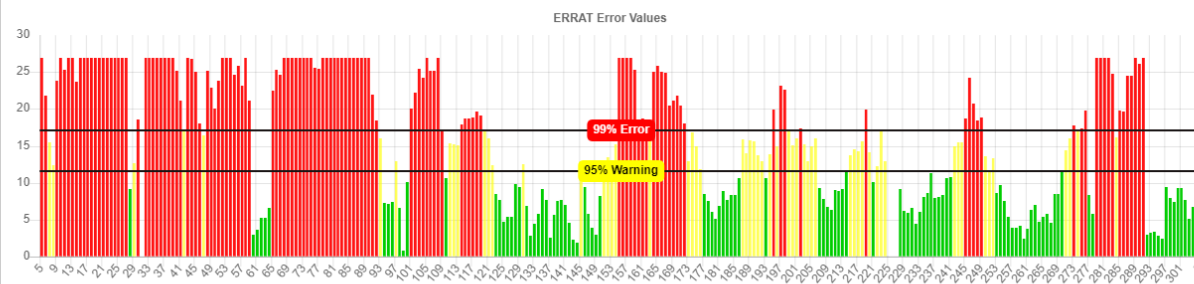
a. PHYRE2 PDB

Completed at 8:03 am | [View Structure](#)

Input: (PI3K_construction.pdb)

Moleman is used to identify chains and separate into files. Each pdb chain file is linked below for each plot. For an explanation on how the chains were found, here is the moleman logfile

Quality Factor: A: 36.2416 | [PDF](#) | [PostScript](#) | [Log](#) | [PDB chain file used](#)



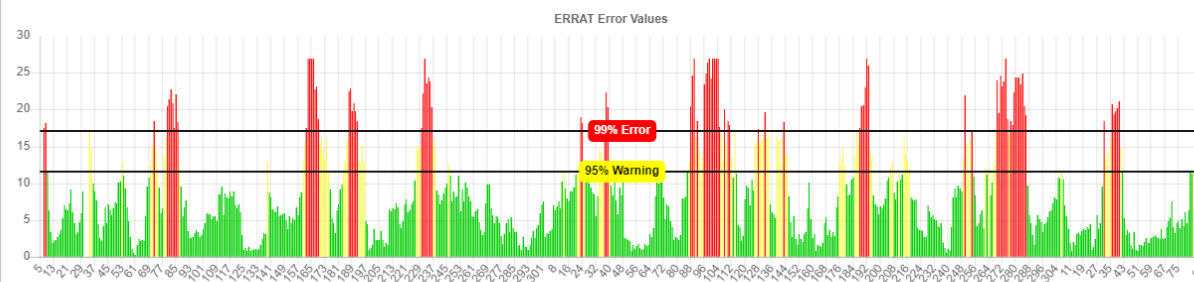
b. Refinement with ModRefiner

Completed at 8:03 am | [View Structure](#)

Input: (PI3K.pdb)

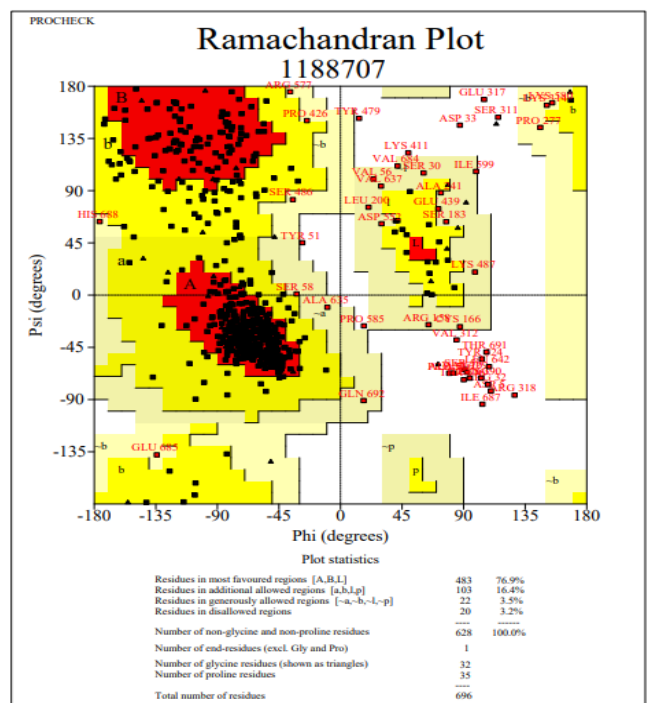
Moleman is used to identify chains and separate into files. Each pdb chain file is linked below for each plot. For an explanation on how the chains were found, here is the moleman logfile

Quality Factor: A: 72.6208 | [PDF](#) | [PostScript](#) | [Log](#) | [PDB chain file used](#)

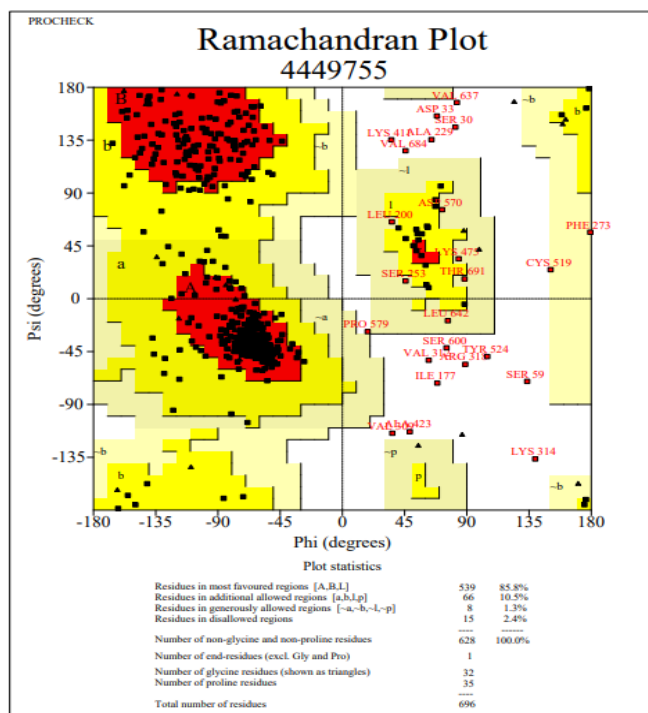


2. ProCheck Ramachandran Plots

a. PHYRE2 PDB

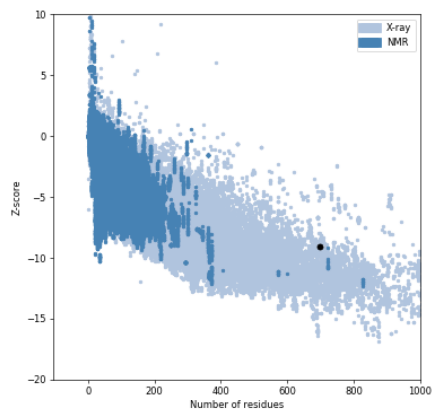
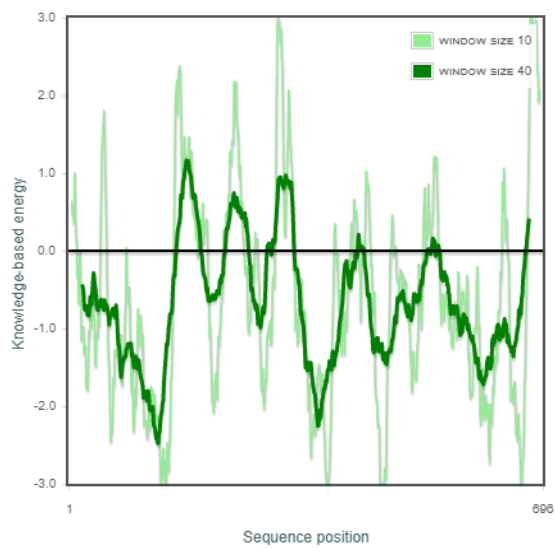


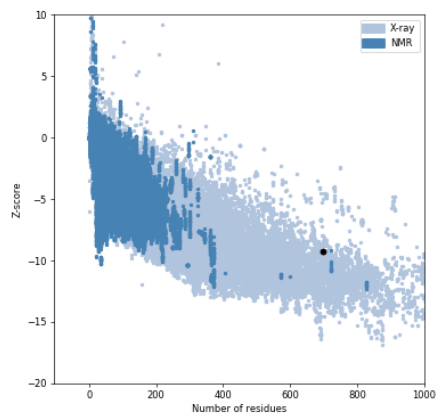
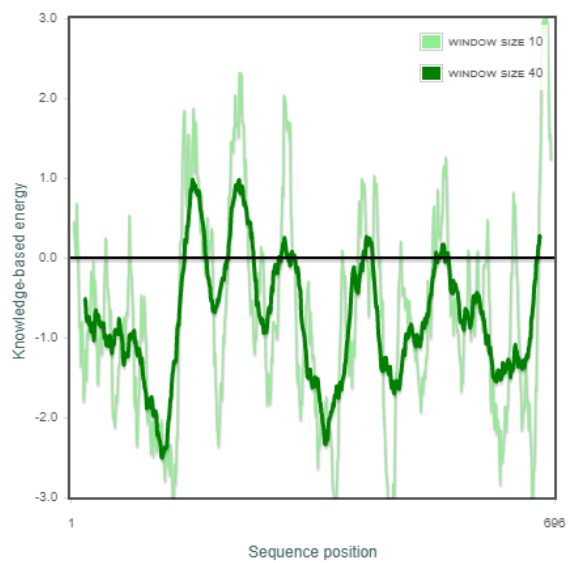
b. Refinement with ModRefiner



3. ProSa Comparison

a. PHYRE2 PDB

Results for PI3K_construction.pdb, chain *blank* (696 aa)**Overall model quality** [HELP](#)Z-Score: **-9.05****Local model quality** [HELP](#)**b. Refinement with ModRefiner**

Results for PI3K.pdb, chain *blank* (696 aa)**Overall model quality** [HELP](#)Z-Score: **-9.3****Local model quality** [HELP](#)**PKC- α (PRKCA)**

1. Errat Server Comparison

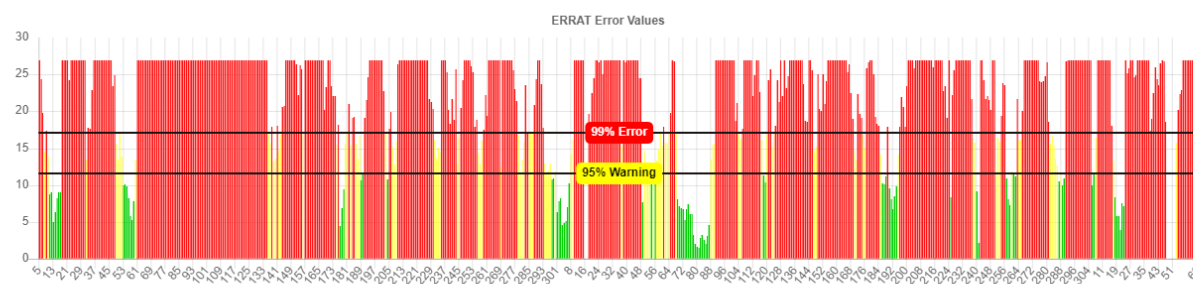
a. PHYRE2 PDB

Completed at 8:16 am | [View Structure](#)

Input: (PRKCA_construction.pdb)

Moleman is used to identify chains and separate into files. Each pdb chain file is linked below for each plot. For an explanation on how the chains were found, here is the moleman logfile

Quality Factor: A: 12.3288 | [PDF](#) | [PostScript](#) | [Log](#) | [PDB chain file used](#)



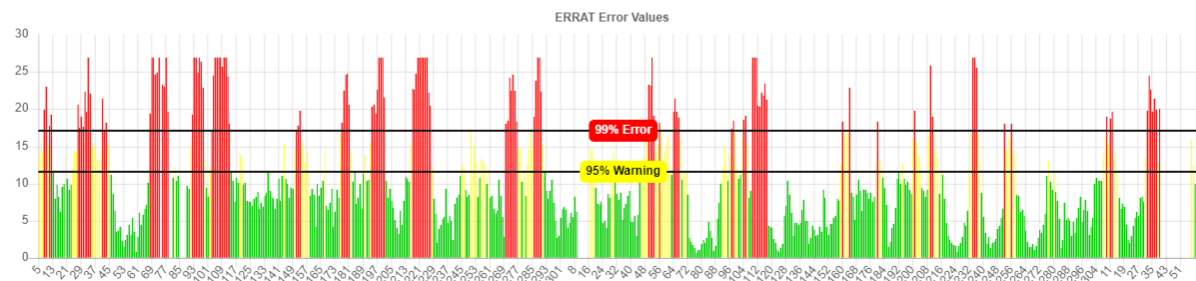
b. Refinement with ModRefiner

Completed at 8:17 am | [View Structure](#)

Input: (PRKCA.pdb)

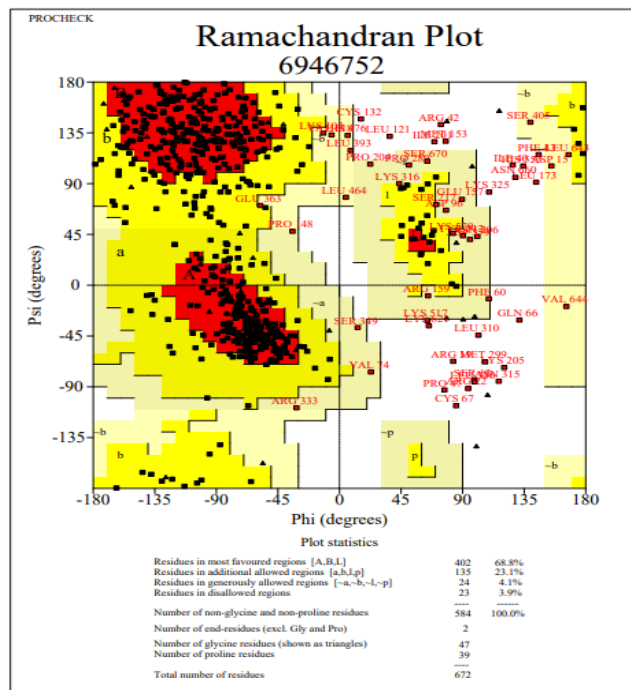
Moleman is used to identify chains and separate into files. Each pdb chain file is linked below for each plot. For an explanation on how the chains were found, here is the moleman logfile

Quality Factor: A: 60.3476 | [PDF](#) | [PostScript](#) | [Log](#) | [PDB chain file used](#)

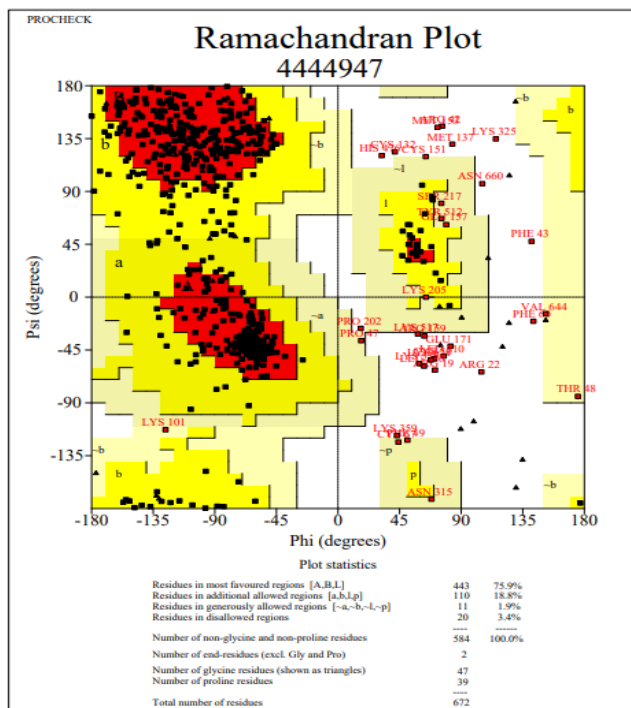


2. ProCheck Ramachandran Plots

a. PHYRE2 PDB

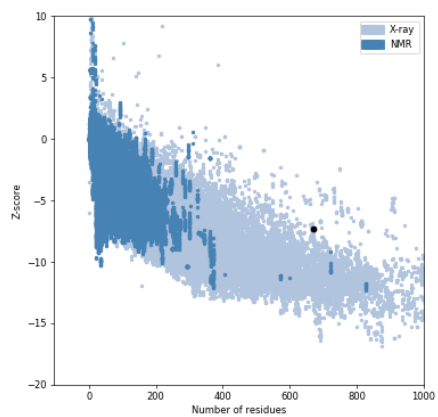
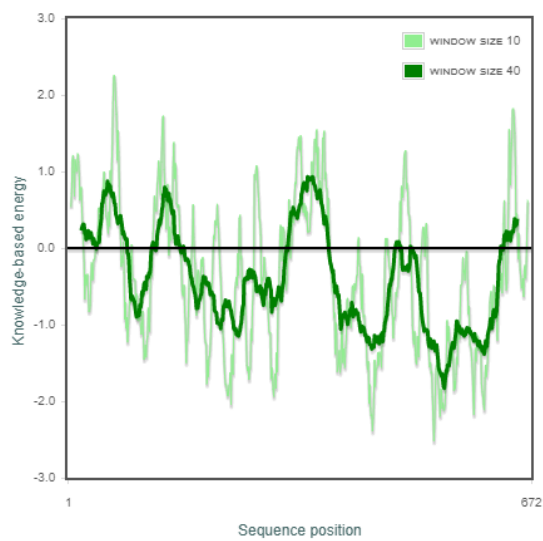


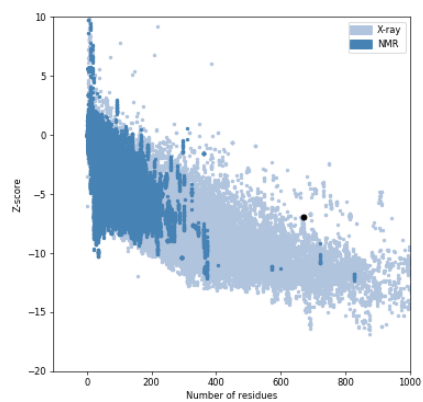
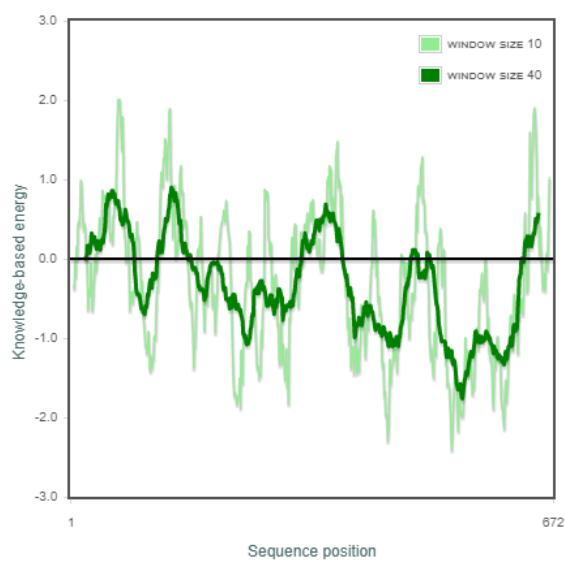
b. Refinement with ModRefiner



3. ProSA Comparison

a. PHYRE2 PDB

Results for PRKCA_construction.pdb, chain *blank* (672 aa)**Overall model quality** [HELP](#)Z-Score: **-7.35****Local model quality** [HELP](#)**b. Refinement with ModRefiner**

Results for PRKCA.pdb, chain *blank* (672 aa)**Overall model quality** [HELP](#)Z-Score: **-6.96****Local model quality** [HELP](#)**PKC- β 1 (PRKCB1)****1. Errat Server Comparison**

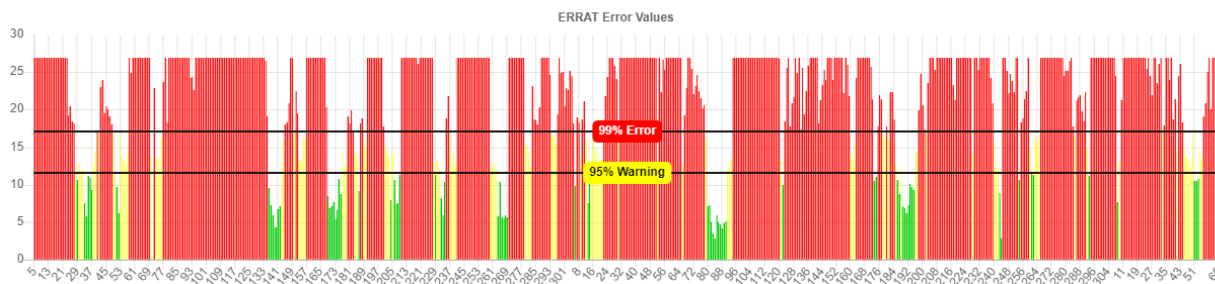
a. PHYRE2 PDB

Completed at 7:30 am | [View Structure](#)

Input: (PRKCB1_construction.pdb)

Moleman is used to identify chains and separate into files. Each pdb chain file is linked below for each plot. For an explanation on how the chains were found, here is the moleman logfile

Quality Factor: A: 11.3293 | [PDF](#) | [PostScript](#) | [Log](#) | [PDB chain file used](#)



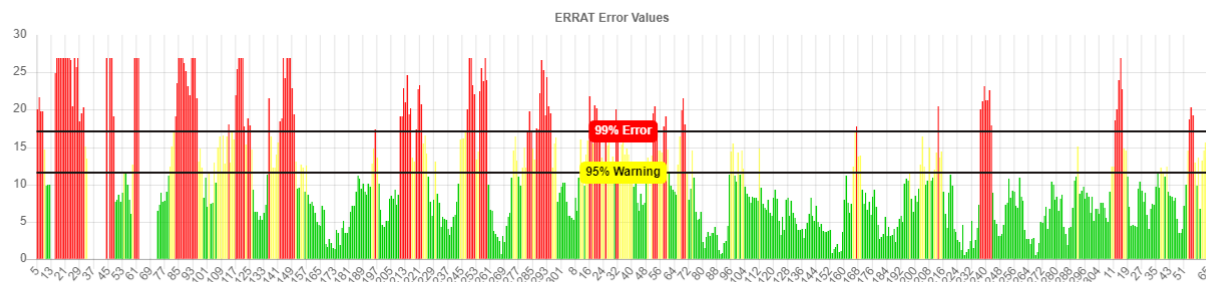
b. Refinement with ModRefiner

Completed at 7:31 am | [View Structure](#)

Input: (PRKCB1.pdb)

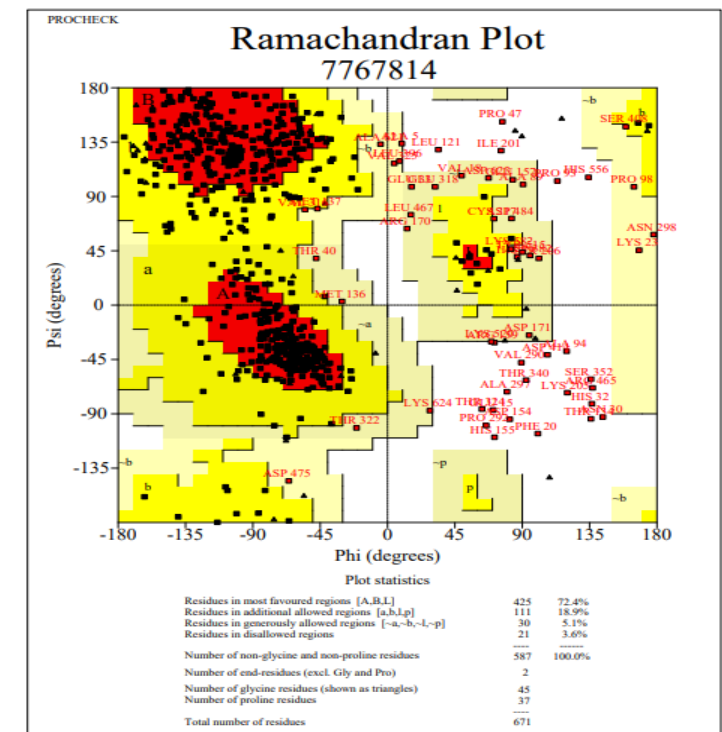
Moleman is used to identify chains and separate into files. Each pdb chain file is linked below for each plot. For an explanation on how the chains were found, here is the moleman logfile

Quality Factor: A: 60.7199 | [PDF](#) | [PostScript](#) | [Log](#) | [PDB chain file used](#)

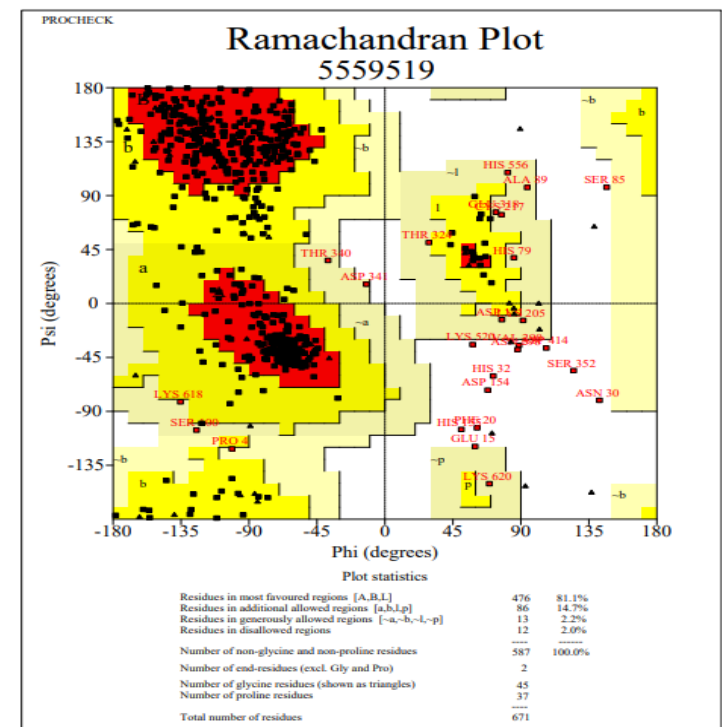


2. ProCheck Ramachandran Plots

a. PHYRE2 PDB

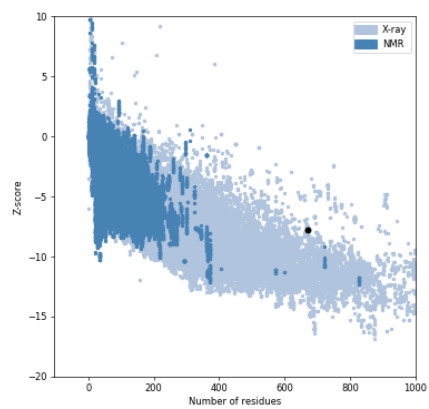
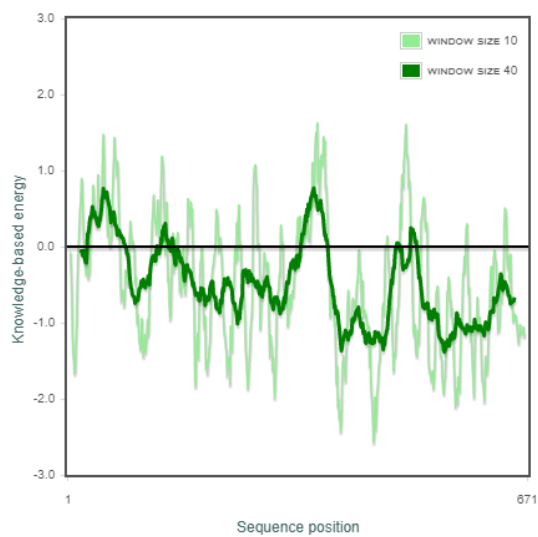


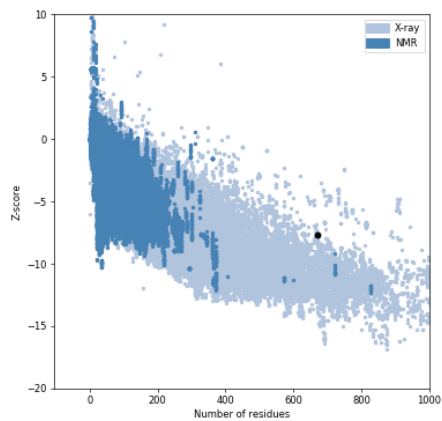
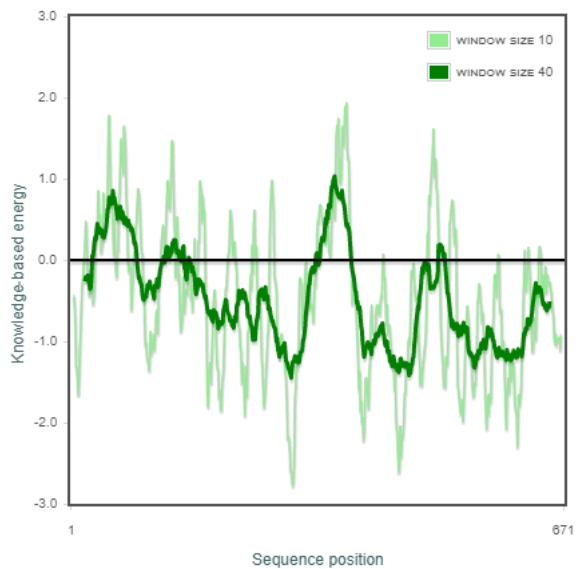
b. Refinement with ModRefiner



3. ProSA Comparison

a. PHYRE2 PDB

Results for PRKCB1_construction.pdb, chain *blank* (671 aa)**Overall model quality** [HELP](#)Z-Score: **-7.82****Local model quality** [HELP](#)**b. Refinement with ModRefiner**

Results for PRKCB1.pdb, chain *blank* (671 aa)**Overall model quality** [HELP](#)Z-Score: **-7.72****Local model quality** [HELP](#)**PKC- β 2 (PRKCB2)**

1. Errat Server Comparison

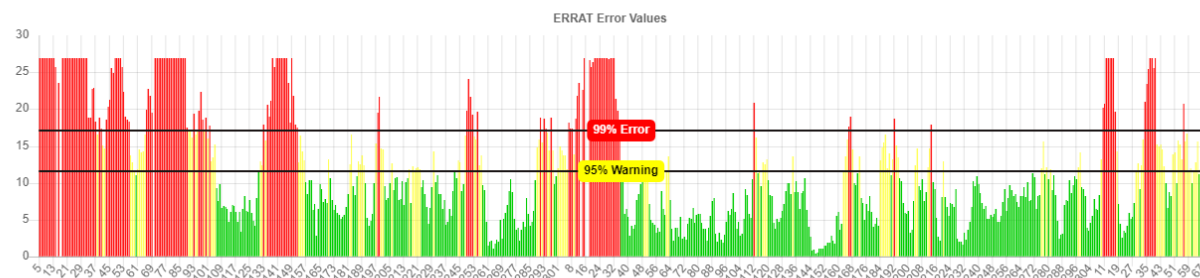
a. PHYRE2 PDB

Completed at 7:47 am | [View Structure](#)

Input: (PRKCB2_construction.pdb)

Moleman is used to identify chains and separate into files. Each pdb chain file is linked below for each plot. For an explanation on how the chains were found, here is the moleman logfile

Quality Factor: A: 57.5114 | [PDF](#) | [PostScript](#) | [Log](#) | [PDB chain file used](#)



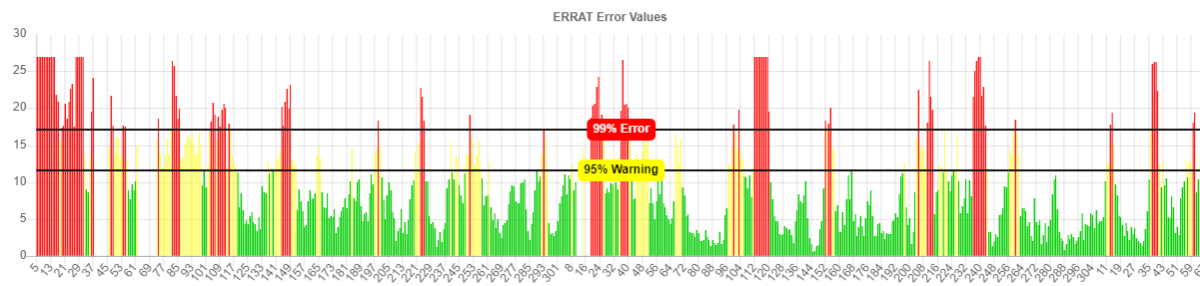
b. Refinement with ModRefiner

Completed at 7:47 am | [View Structure](#)

Input: (PRKCB2.pdb)

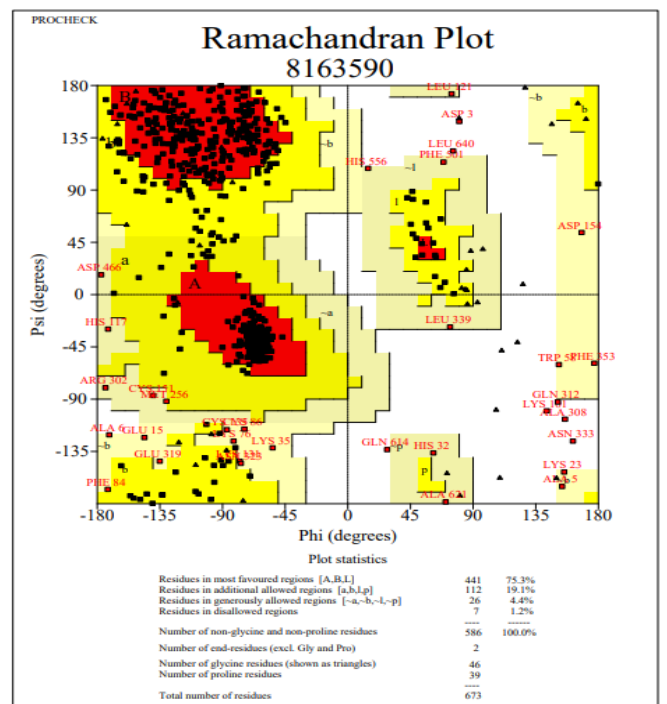
Moleman is used to identify chains and separate into files. Each pdb chain file is linked below for each plot. For an explanation on how the chains were found, here is the moleman logfile

Quality Factor: A: 63.125 | [PDF](#) | [PostScript](#) | [Log](#) | [PDB chain file used](#)

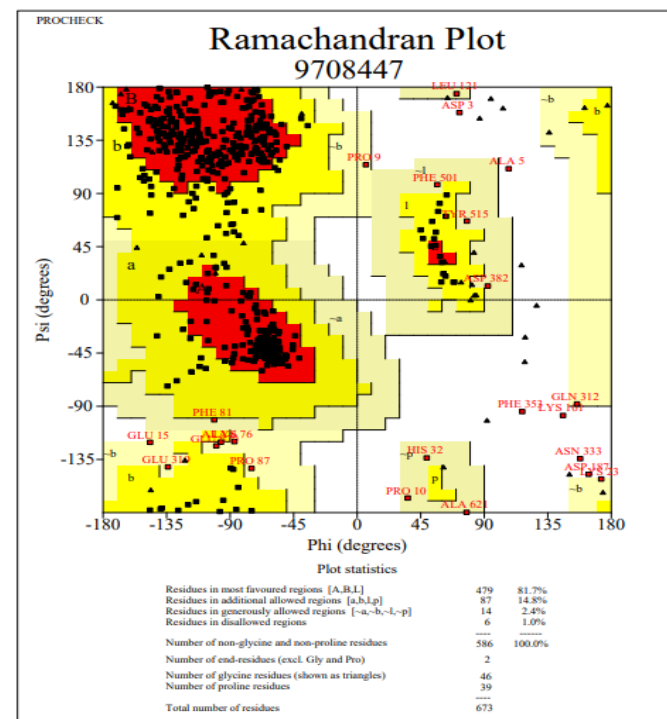


2. ProCheck Ramachandran Plots

a. PHYRE2 PDB

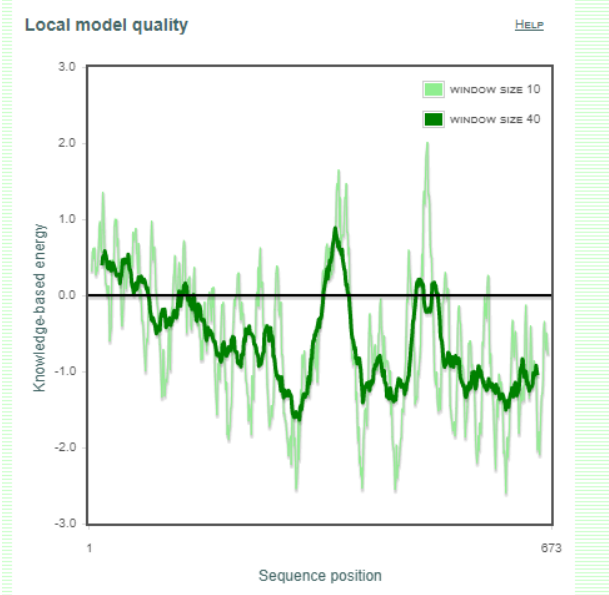
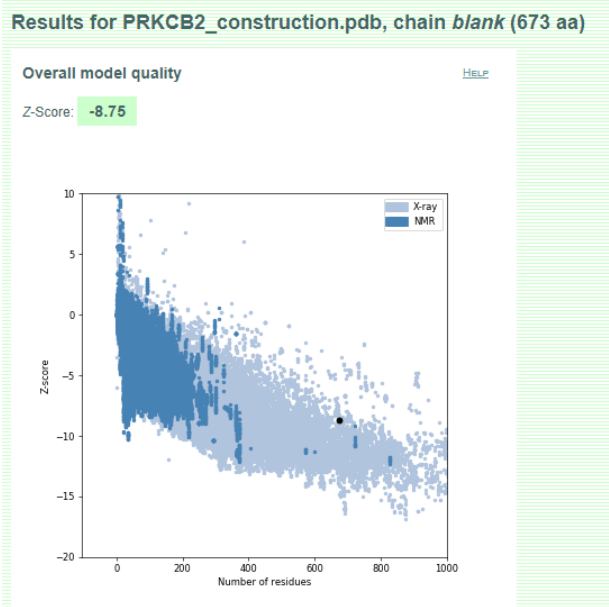


b. Refinement with ModRefiner



3. ProSA Comparison

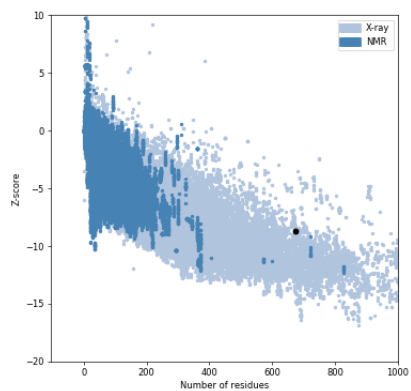
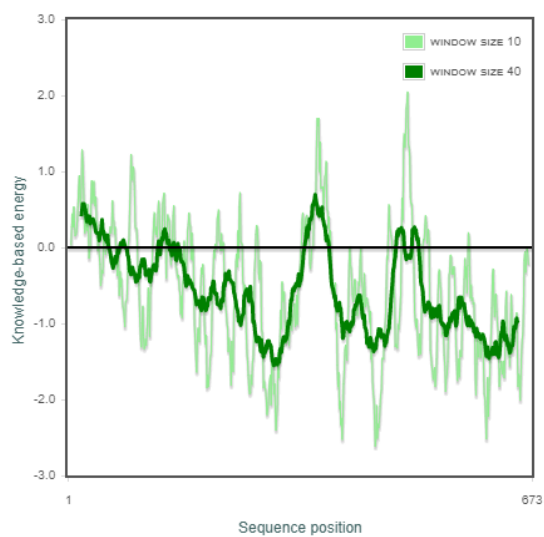
a. PHYRE2 PDB



b. Refinement with ModRefiner

Results for PRKCB2.pdb, chain *blank* (673 aa)Overall model quality [HELP](#)

Z-Score: -8.66

Local model quality [HELP](#)**PKC- δ (PRKCD)**

1. Errat Server Comparison

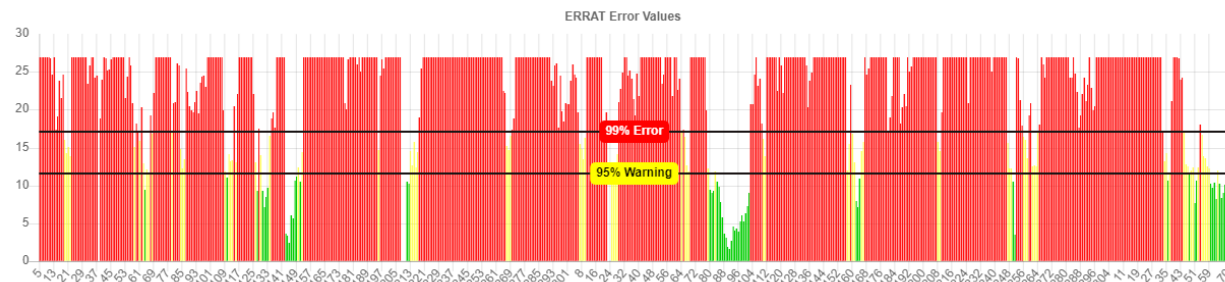
a. PHYRE2 PDB

Completed at 9:48 pm | [View Structure](#)

Input: (PRKCD_construction.pdb)

Moleman is used to identify chains and separate into files. Each pdb chain file is linked below for each plot. For an explanation on how the chains were found, here is the moleman logfile

Quality Factor: A: 8.45921 | [PDF](#) | [PostScript](#) | [Log](#) | [PDB chain file used](#)



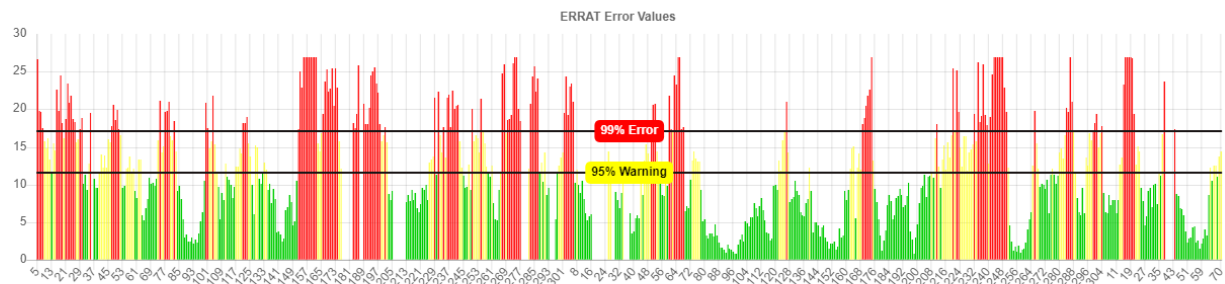
b. Refinement with ModRefiner (Zhang Lab)

Completed at 9:48 pm | [View Structure](#)

Input: (PRKCD.pdb)

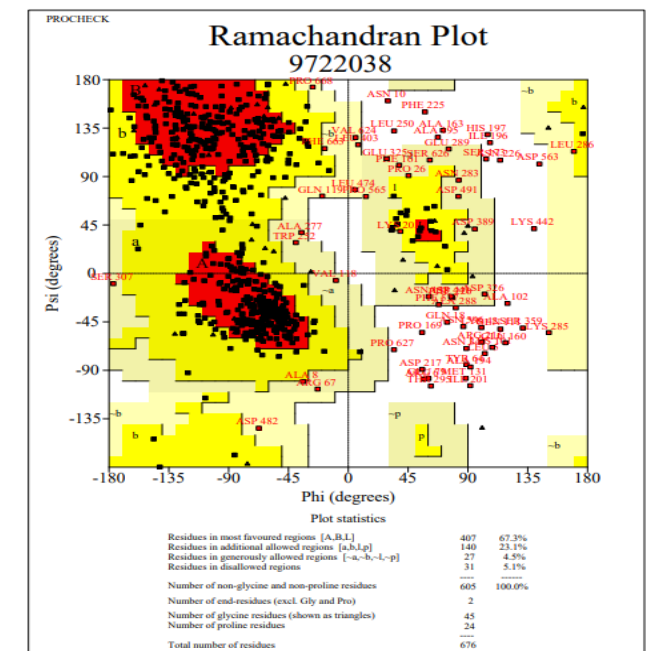
Moleman is used to identify chains and separate into files. Each pdb chain file is linked below for each plot. For an explanation on how the chains were found, here is the moleman logfile

Quality Factor: A: 49.361 | [PDF](#) | [PostScript](#) | [Log](#) | [PDB chain file used](#)

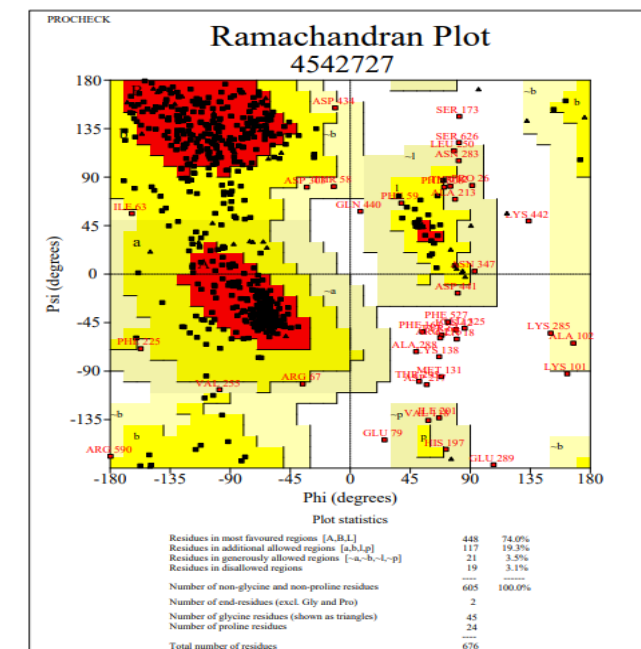


2. ProCheck Ramachandran Plots

a. PHYRE2 PDB

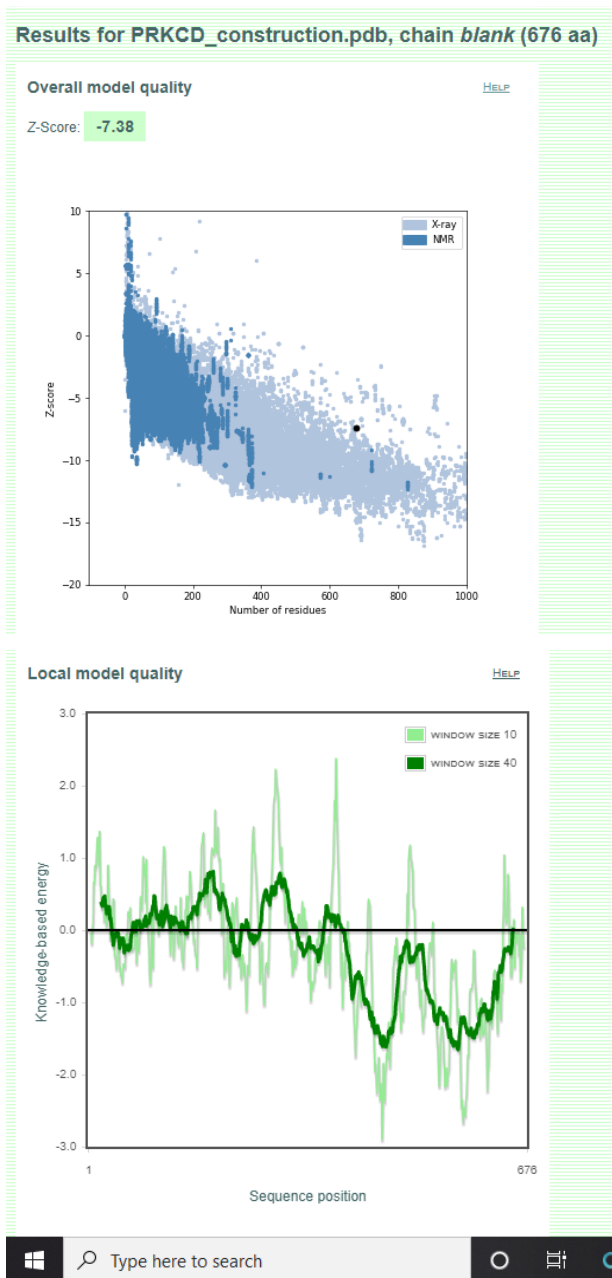


b. Refinement with ModRefiner (Zhang Lab)

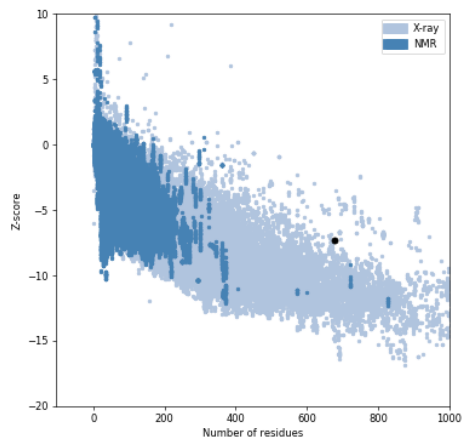
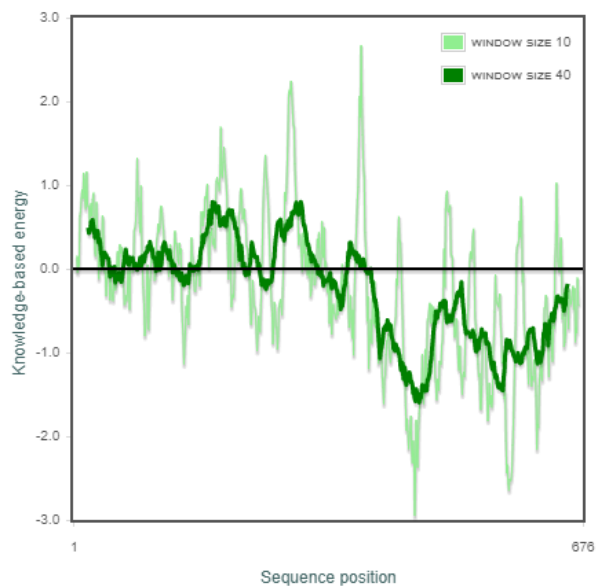


3. ProSA Comparison

a. PHYRE2 PDB



b. Refinement with ModRefiner (Zhang Lab)

Results for PRKCD.pdb, chain *blank* (676 aa)Overall model quality [HELP](#)Z-Score: **-7.3**Local model quality [HELP](#)

PKC- η (PRKCH)

1. Errat Server Comparison

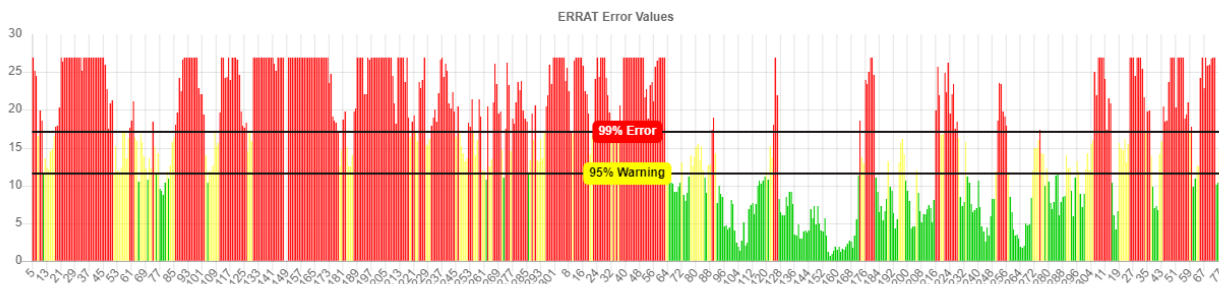
a. PHYRE2 PDB

Completed at 9:14 pm | [View Structure](#)

Input: (PRKCH_construction.pdb)

Moleman is used to identify chains and separate into files. Each pdb chain file is linked below for each plot. For an explanation on how the chains were found, here is the moleman logfile

Quality Factor: A: 28.2318 | [PDF](#) | [PostScript](#) | [Log](#) | [PDB chain file used](#)



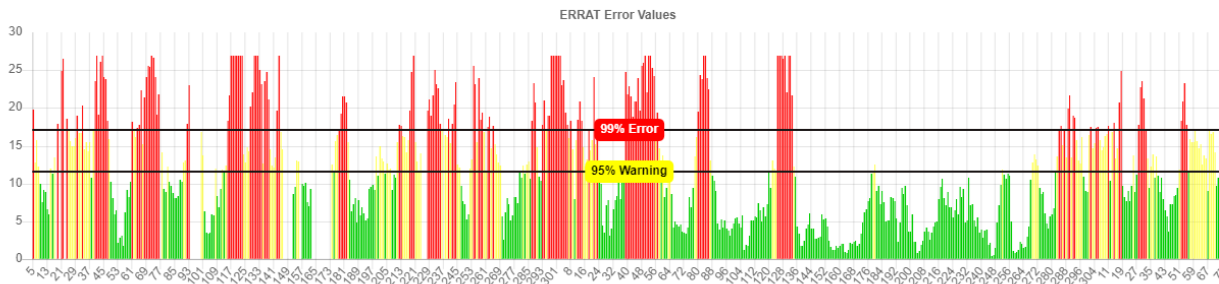
b. Refinement with ModRefiner (Zhang Lab)

Completed at 9:14 pm | [View Structure](#)

Input: (PRKCH.pdb)

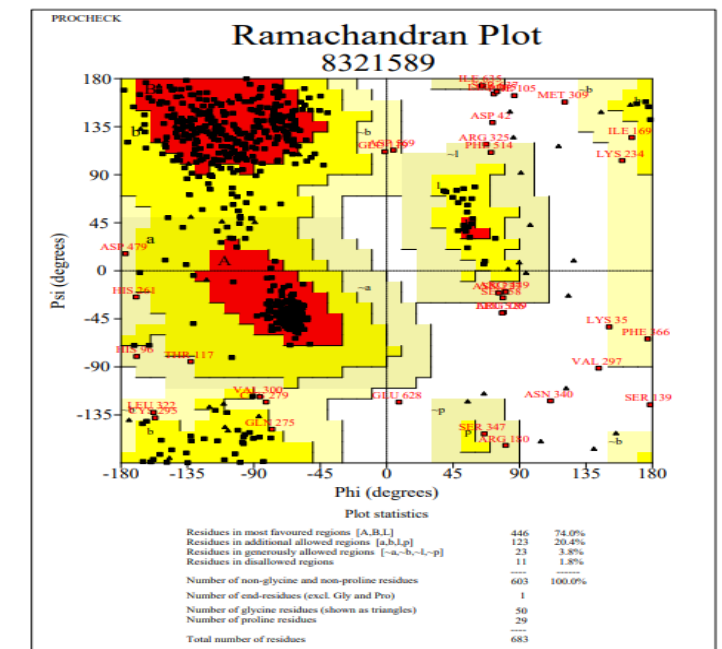
Moleman is used to identify chains and separate into files. Each pdb chain file is linked below for each plot. For an explanation on how the chains were found, here is the moleman logfile

Quality Factor: A: 51.1664 | [PDF](#) | [PostScript](#) | [Log](#) | [PDB chain file used](#)

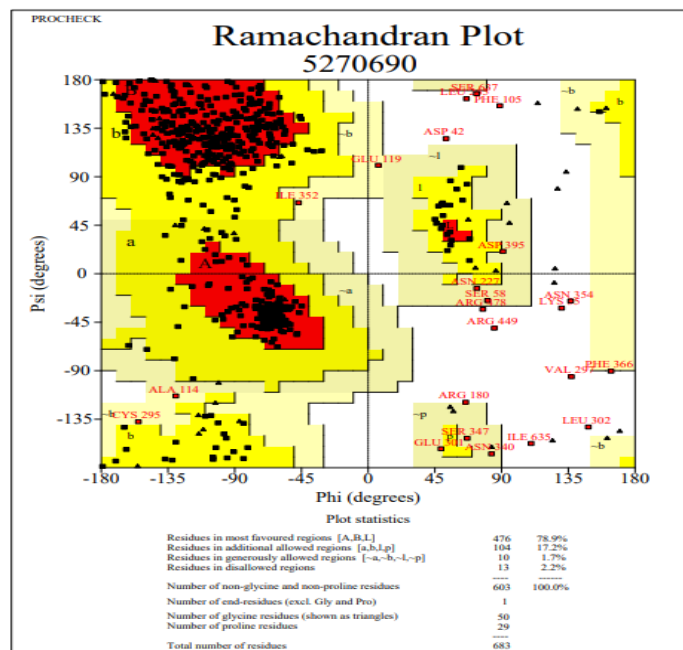


2. ProCheck Ramachandran Plots

a. PHYRE2 PDB

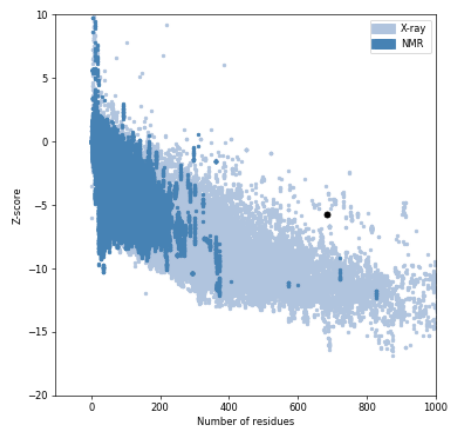
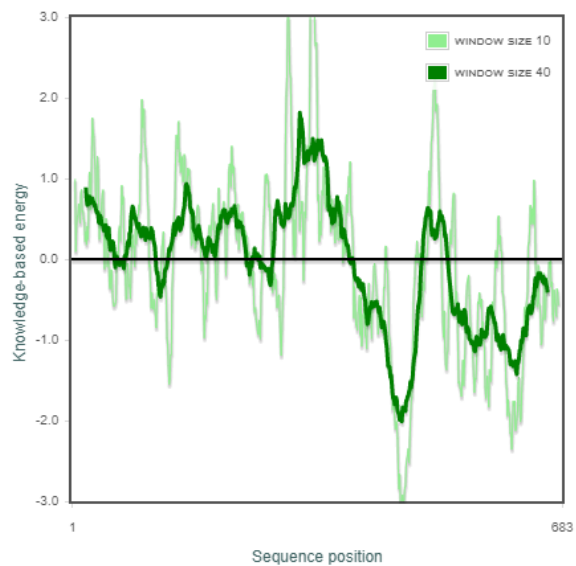


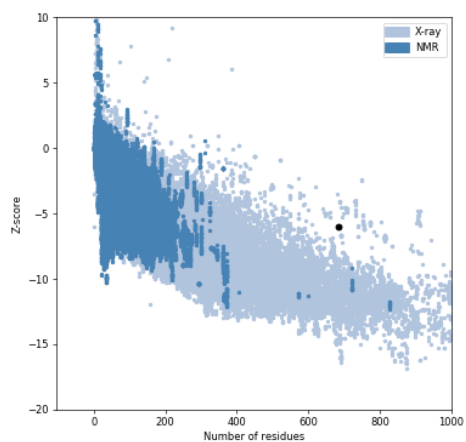
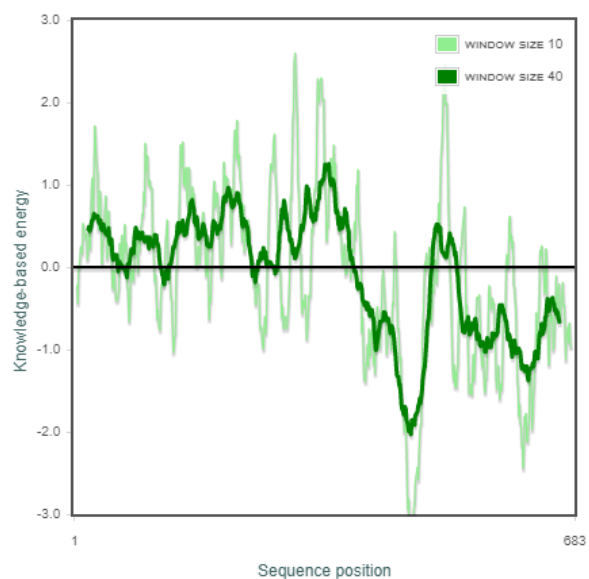
b. Refinement with ModRefiner (Zhang Lab)



3. ProSA Comparison

a. PHYRE2 PDB

Results for PRKCH_construction.pdb, chain *blank* (683 aa)**Overall model quality** [HELP](#)Z-Score: **-5.75****Local model quality** [HELP](#)**b. Refinement with ModRefiner (Zhang Lab)**

Results for PRKCH.pdb, chain *blank* (683 aa)**Overall model quality**[HELP](#)Z-Score: **-6.04****Local model quality**[HELP](#)**PKC-θ (PRKCQ)**

1. ERRAT Server Comparison

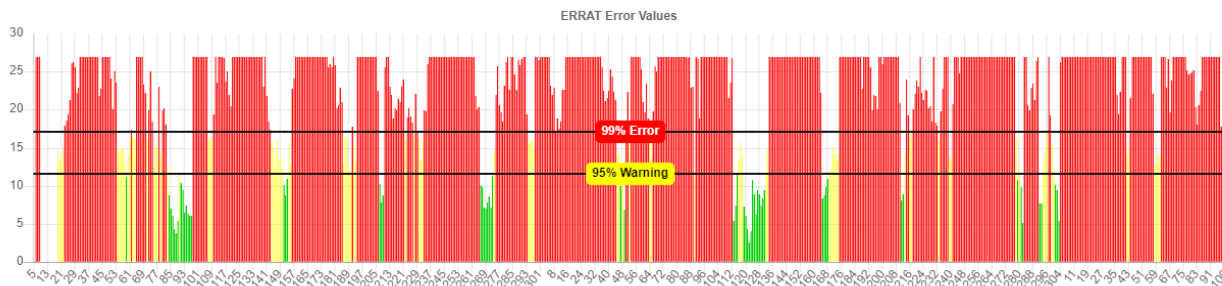
a. PHYRE2 PDB

Completed at 8:28 pm | [View Structure](#)

Input: (PRKCQ_construction.pdb)

Moleman is used to identify chains and separate into files. Each pdb chain file is linked below for each plot. For an explanation on how the chains were found, here is the moleman logfile

Quality Factor: A: 8.73362 | [PDF](#) | [PostScript](#) | [Log](#) | [PDB chain file used](#)



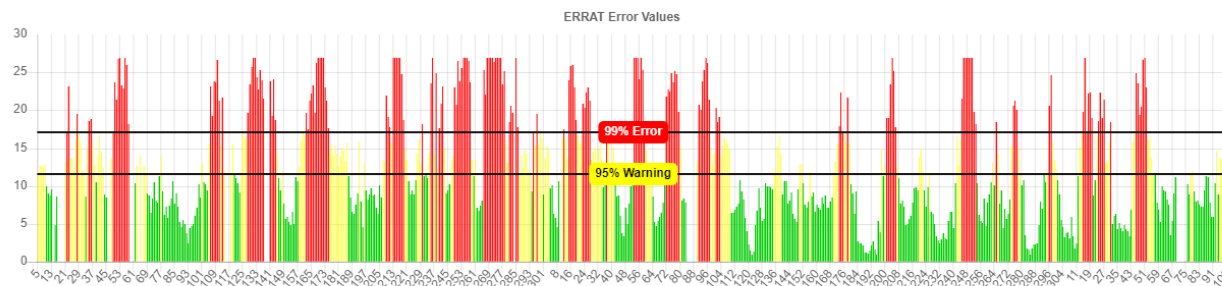
b. Refinement with ModRefiner (Zhang Lab)

Completed at 8:29 pm | [View Structure](#)

Input: (PRKCQ.pdb)

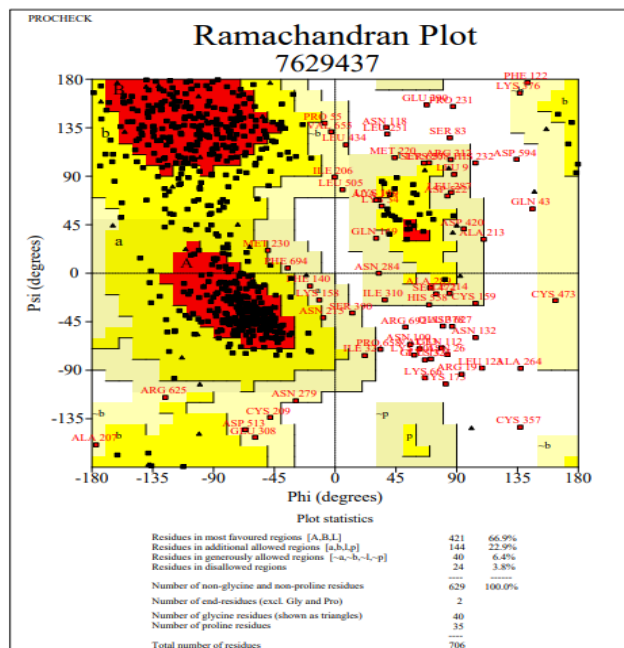
Moleman is used to identify chains and separate into files. Each pdb chain file is linked below for each plot. For an explanation on how the chains were found, here is the moleman logfile

Quality Factor: A: 47.7477 | [PDF](#) | [PostScript](#) | [Log](#) | [PDB chain file used](#)

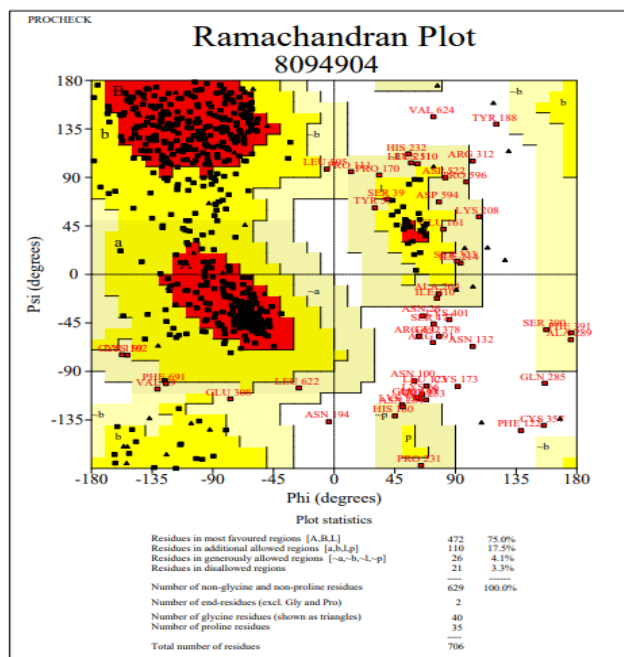


2. ProCheck Ramachandran Plots

a. PHYRE2 PDB

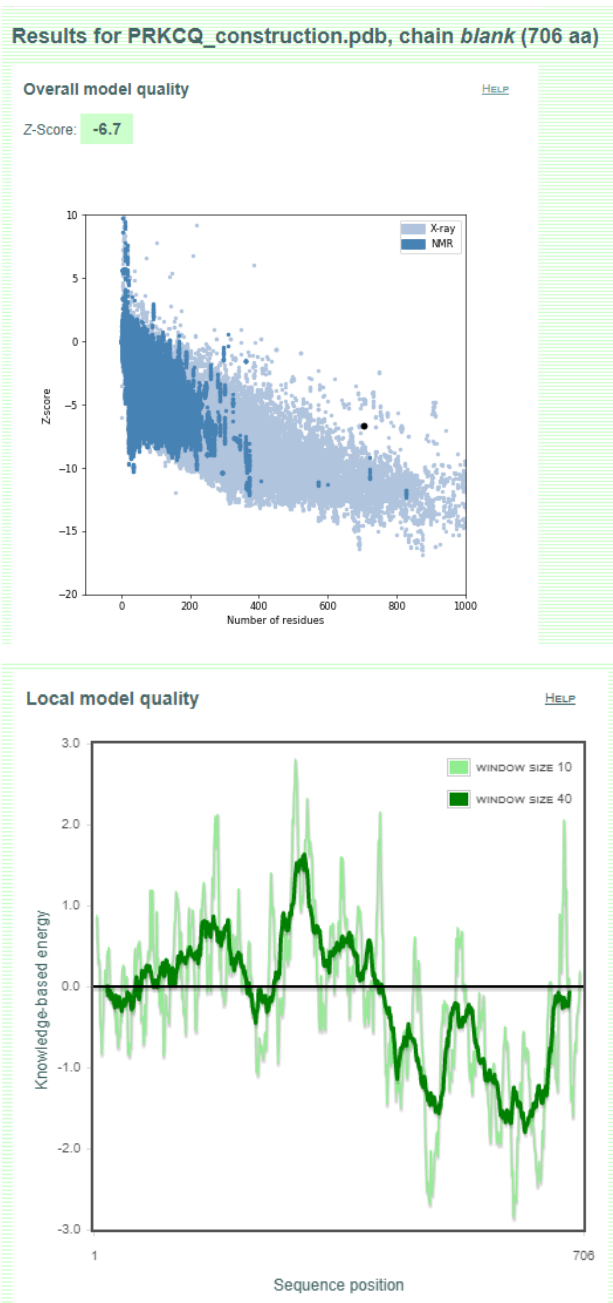


b. Refinement with ModRefiner (Zhang Lab)

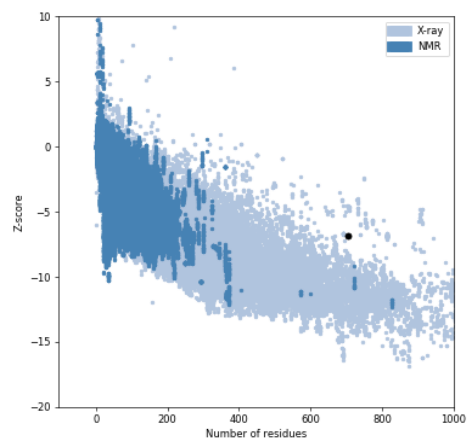
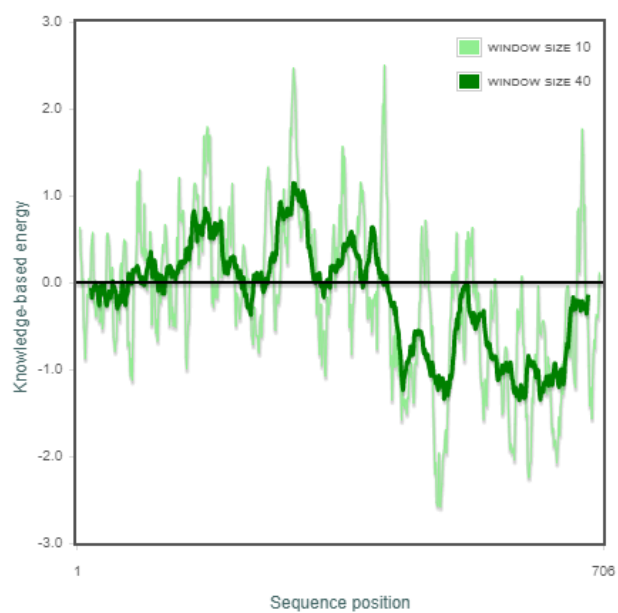


3. ProSA Comparison

a. PHYRE2 PDB



b. Refinement with ModRefiner (Zhang Lab)

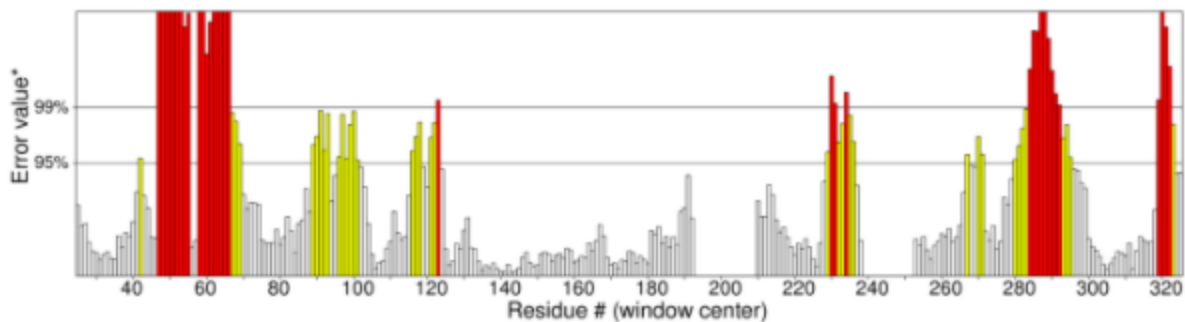
Results for PRKCQ.pdb, chain *blank* (706 aa)**Overall model quality**[HELP](#)Z-score: **-6.86****Local model quality**[HELP](#)

PLCG1

1. Errat Server Comparison

a. PHYRE2 PDB

Program: ERRAT2
 File: PLCG1_construction.pdb
 Chain#:
 Overall quality factor**: 87.397

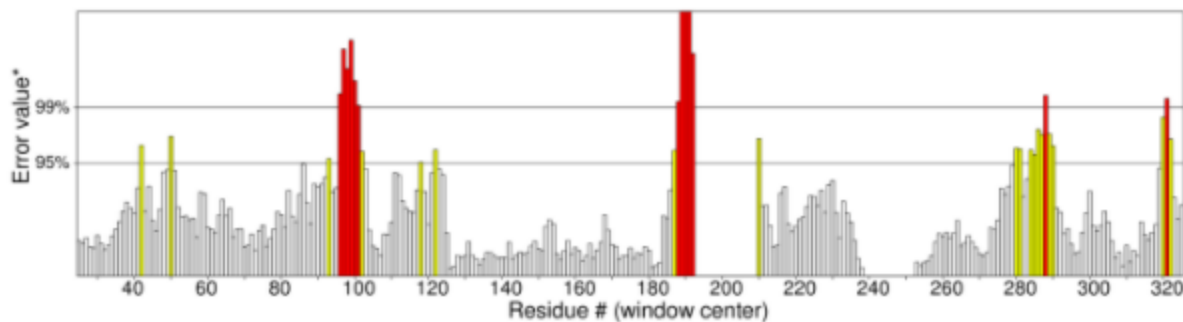


*On the error axis, two lines are drawn to indicate the confidence with which it is possible to reject regions that exceed that error value.

**Expressed as the percentage of the protein for which the calculated error value falls below the 95% rejection limit. Good high resolution structures generally produce values around 95% or higher. For lower resolutions (2.5 to 3Å) the average overall quality factor is around 91%.

b. Refinement with ModRefiner

Program: ERRAT2
 File: PLCG1.pdb
 Chain#:
 Overall quality factor**: 83.487

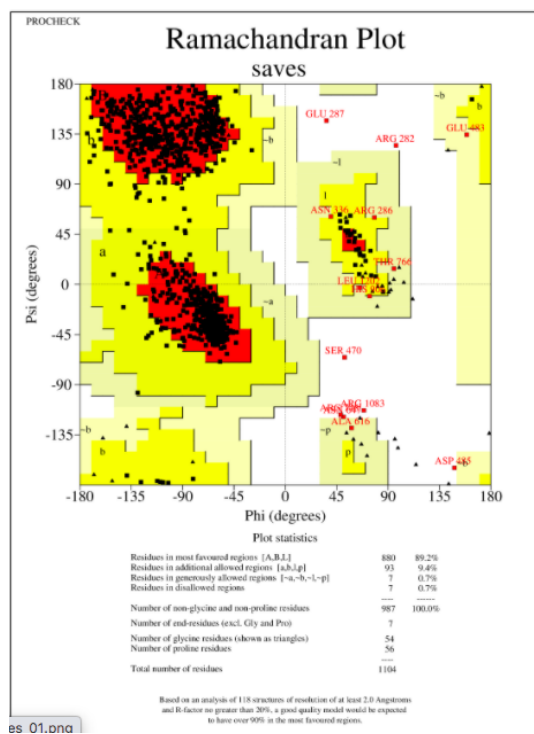


*On the error axis, two lines are drawn to indicate the confidence with which it is possible to reject regions that exceed that error value.

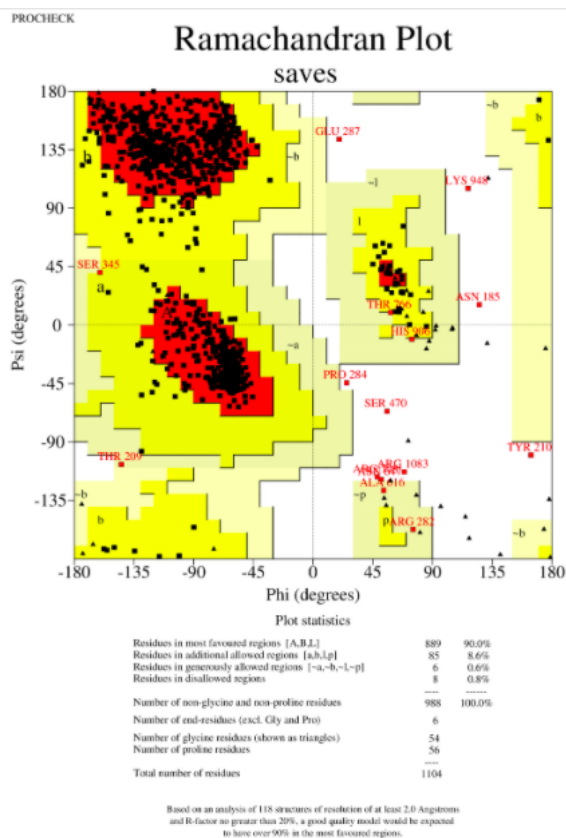
**Expressed as the percentage of the protein for which the calculated error value falls below the 95% rejection limit. Good high resolution structures generally produce values around 95% or higher. For lower resolutions (2.5 to 3Å) the average overall quality factor is around 91%.

2. ProCheck Ramachandran Plots

a. PHYRE2 PDB

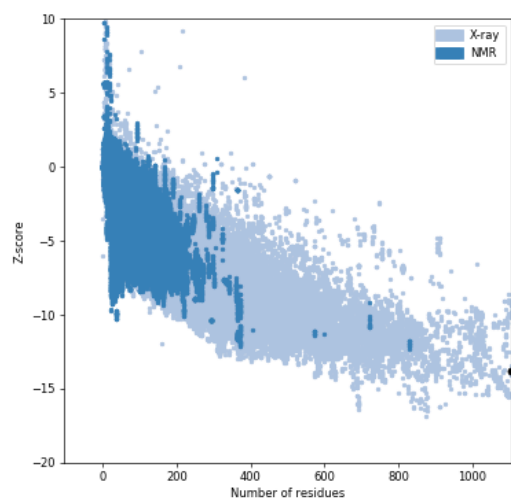
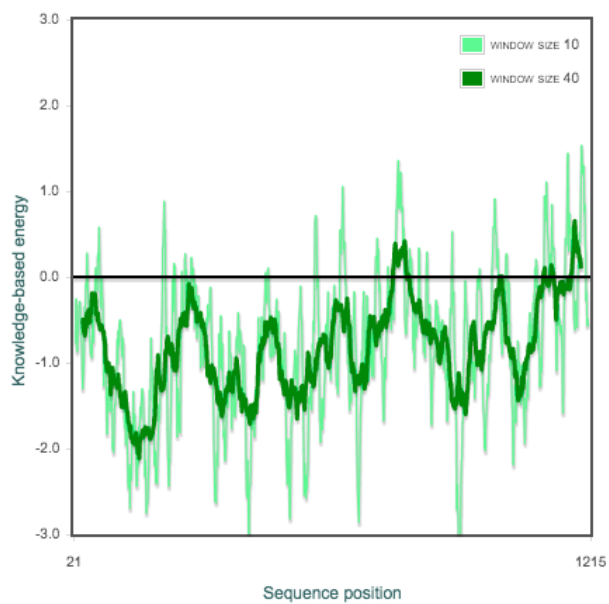


b. Refinement with ModRefiner

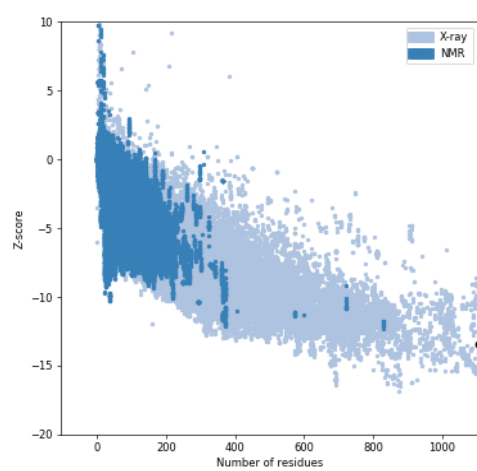


3. ProSa Comparison

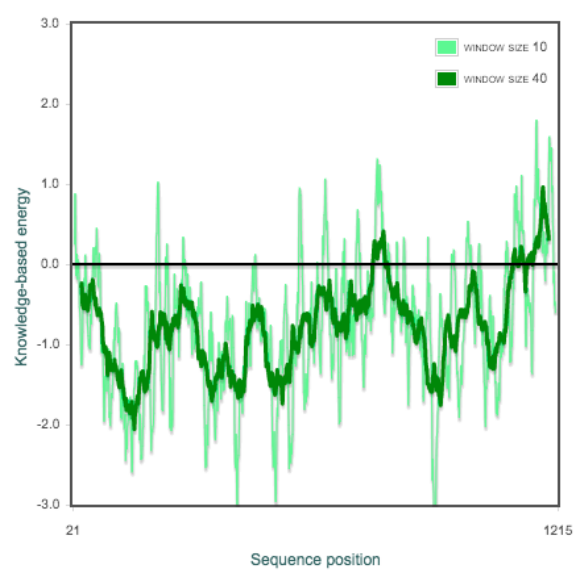
a. PHYRE2 PDB

Overall model quality[HELP](#)Z-Score: **-13.82****Local model quality**[HELP](#)**b. Refinement with ModRefiner**

Overall model quality

[HELP](#)Z-Score: **-13.44**

Local model quality

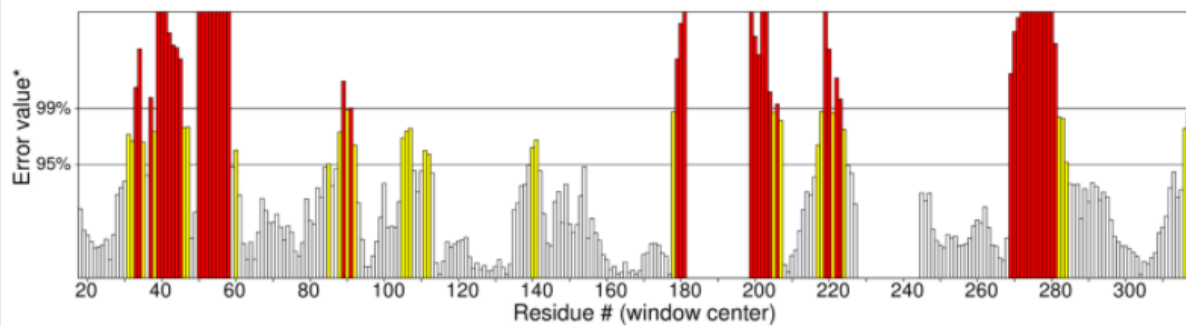
[HELP](#)

PLCG2

1. Errat Server Comparison

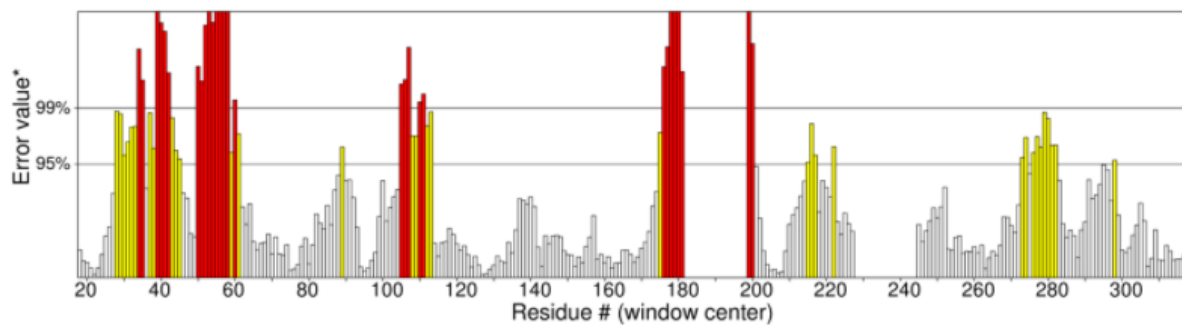
a. PHYRE2 PDB

Program: ERRAT2
File: PLCG2_construction.pdb
Chain#:
Overall quality factor**: 64.968



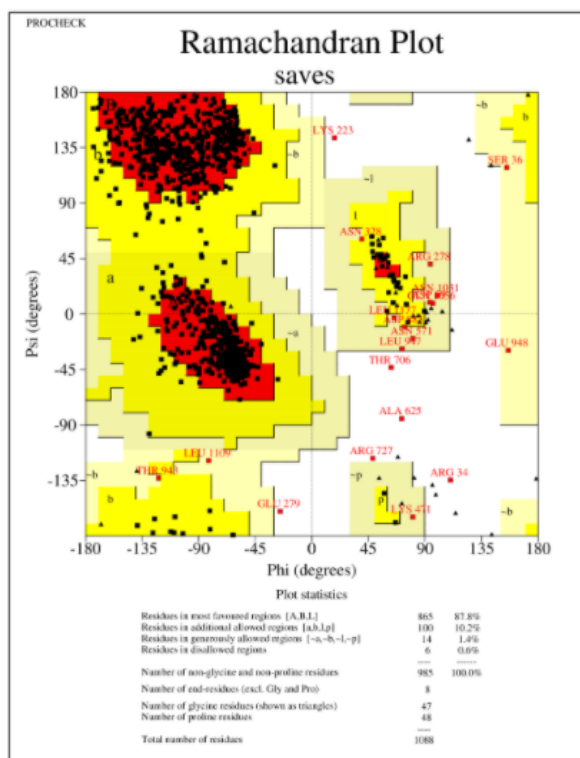
b. Refinement with ModRefiner

Program: ERRAT2
File: PLCG2.pdb
Chain#:
Overall quality factor**: 72.449

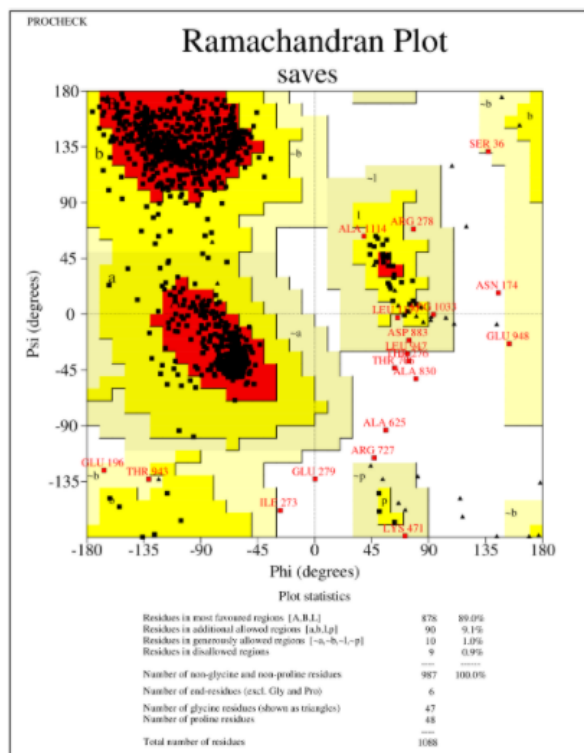


2. ProCheck Ramachandran Plots

a. PHYRE2 PDB

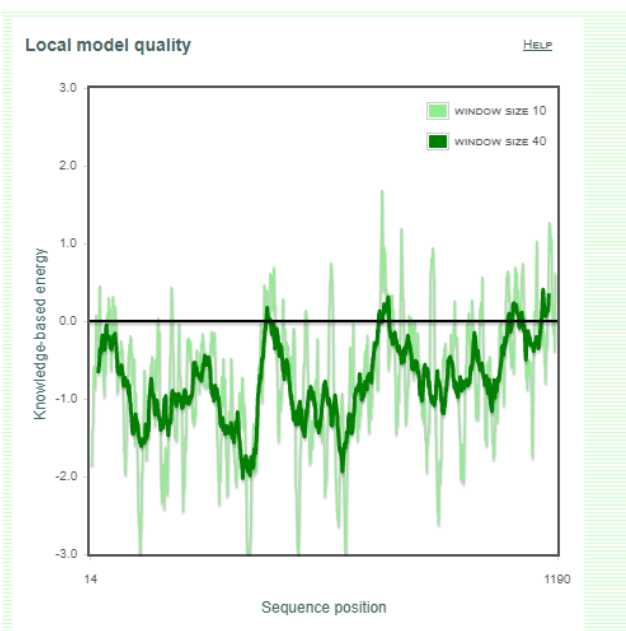
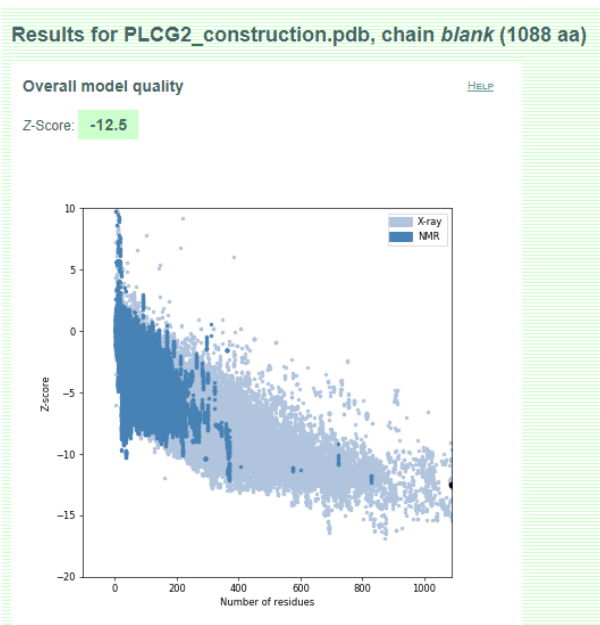


b. Refinement with ModRefiner

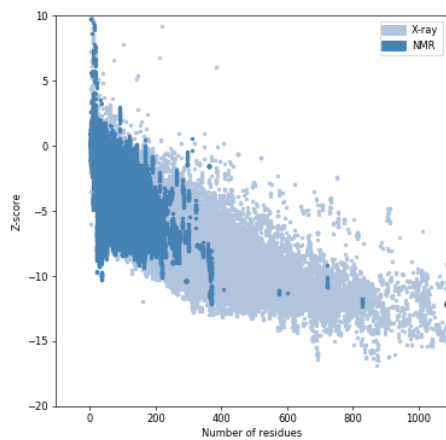
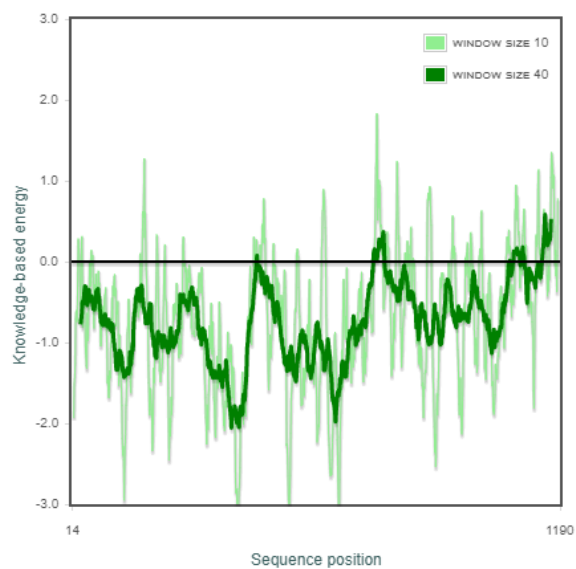


3. ProSa Comparison

a. PHYRE2 PDB



b. Refinement with ModRefiner

Results for PLOG2.pdb, chain *blank* (1088 aa)**Overall model quality**[HELP](#)Z-Score: **-12.17****Local model quality**[HELP](#)

References

- Akdis, M. (2014). New treatments for allergen immunotherapy. *The World Allergy Organization Journal*, 7(1), 23. doi:10.1186/1939-4551-7-23
- Alberts, B., Johnson, A., Lewis, J., Raff, M., Roberts, K., Walter, P. (2002). B cells and antibodies. *Molecular Biology of the Cell* (4th ed.). New York: Garland Science. Retrieved from: <https://www.ncbi.nlm.nih.gov/books/NBK26884/>
- American College of Allergy, Asthma, and Immunology (2014). Who has allergies and why. *American College of Allergy, Asthma, and Immunology*. Retrieved from: <https://acaai.org/allergies/who-has-allergies/children-allergies>
- Bagnasco, D., Ferrando, M., Varricchi, G., Passalacqua, G., & Canonica, G.W. (2016). A Critical Evaluation of anti-IL-13 and anti-IL-4 strategies in severe asthma. *International Archives of Allergy and Immunology*, 170, 122-13. doi: 10.1159/000447692
- Barker, S.A., Caldwell, K.K., Hall, A., Martinez, A.M., Pfeiffer, J.R., Oliver, J.M., & Wilson, B.S. (1995). Wortmannin blocks lipid and protein kinase activities associated with PI3-kinase and inhibits a subset of responses induced by FcεRI cross-linking. *Molecular Biology Cell*, 6, 1145–1158. Retrieved from: <https://www.ncbi.nlm.nih.gov/pmc/articles/PMC301273/>
- Beaven, M. A., Jacobsen, S., & Horáková, Z. (1972). Modification of the enzymatic isotopic assay of histamine and its application to measurement of histamine in

tissues, serum and urine. *Clinica Chimica Acta*, 37, 91-103.

doi:10.1016/0009-8981(72)90419-6

Becker, K. P., & Hannun, Y. A. (2005). Protein kinase C and phospholipase D: intimate interactions in intracellular signaling. *Cellular and Molecular Life Sciences CMLS*, 62(13), 1448-1461. doi:10.1007/s00018-005-4531-7

Bell, K.S., et al. (2015). The role of individual protein kinase C isoforms in mouse mast cell function and their targeting by the immunomodulatory parasitic worm product. *Immunology Letters*, 168(1). 31–40. doi:10.1016/j.imlet.2015.09.001

Bilaver, L. A., Kester, K. M., Smith, B. M., & Gupta, R. S. (2016). Socioeconomic Disparities in the Economic Impact of Childhood Food Allergy. *Pediatrics*, 137(5). <https://doi.org/10.1542/peds.2015-3678>

Blank, U. (n.d). Type I high affinity IgE receptor (FcεRI). Retrieved October 18, 2018, from <http://www.mastcell-basophil.net/wiki/wiki-start/type-i-high-affinity-ige-receptor-fceri/>

Bonilla, F.A. & Oettgen, H.C. (2010). Adaptive immunity. *Journal of Allergy and Clinical Immunology*, 125(2), 33-40. Retrieved from <https://www.sciencedirect.com/science/article/pii/S0091674909014055?via=ihub>.

Bubnoff, D.V., Geiger, E., & Bieber, T. (2001). Antigen-presenting Cells in Allergy. *Journal of Allergy and Clinical Immunology*, 108(3), 329-339. <https://doi.org/10.1067/mai.2001.117457>

- Cazzolli, R., Shemon, A. N., Fang, M. Q., & Hughes, W. E. (2006). Phospholipid signaling through phospholipase D and phosphatidic acid. *IUBMB Life*, 58(8), 457-461. <https://doi.org/10.1080/15216540600871142>
- Centers for Disease Control and Prevention. (2017). *Gateway to health communication & social marketing practice*. Retrieved from <https://www.cdc.gov/healthcommunication/ToolsTemplates/EntertainmentEd/Tips/Allergies.html>
- Chisholm-Burns, M. A., Spivey, C. A., Gatwood, J., Wiss, A., Hohmeier, K., & Erickson, S. R. (2017). Evaluation of racial and socioeconomic disparities in medication pricing and pharmacy access and services. *American Journal of Health-System Pharmacy*, 74(10), 653–668. <https://doi.org/10.2146/ajhp150872>
- Colovos, C., & Yeates, T. O. (1993). Verification of protein structures: Patterns of nonbonded atomic interactions. *Protein Science*, 2(9), 1511-1519. doi:10.1002/pro.5560020916
- Cosconati S, Forli S, Perryman AL, Harris R, Goodsell DS, Olson AJ. Virtual Screening with AutoDock: Theory and Practice. *Expert Opin Drug Discov*. 2010 Jun 1;5(6):597-607. doi: 10.1517/17460441.2010.484460. PMID: 21532931; PMCID: PMC3083070.
- Cruse, G., Gilfillan, A.M., & Smrz, D. (2015). Flow cytometry-based monitoring of mast cell activation. *Methods in Molecular Biology*, 1220, 365-379.

https://doi.org/10.1007/978-1-4939-1568-2_23

Dallakyan S, Olson AJ. Small-molecule library screening by docking with PyRx.

Methods Mol Biol. 2015;1263:243-50. doi: 10.1007/978-1-4939-2269-7_19.

PMID: 25618350.

Davari, Majid et al. "Measuring Equity in Access to Pharmaceutical Services Using

Concentration Curve; Model Development." *Iranian journal of pharmaceutical research : IJPR* vol. 14,4 (2015): 1317-26.

Demo, S.D., Masuda, E., Rossi, A.B., Thronset, B.T., Gerard, A.L., Chan, E.H., ... &

Scheller, R.H. (1999). Quantitative measurement of mast cell degranulation using a novel flow cytometric annexin-V binding assay. *Cytometry: The Journal of the International Society for Analytical Cytology*, 36(4), 340-348.

[https://doi.org/10.1002/\(SICI\)1097-0320\(19990801\)36:4<340::AID-CYTO9>3.0.CO;2-C](https://doi.org/10.1002/(SICI)1097-0320(19990801)36:4<340::AID-CYTO9>3.0.CO;2-C)

Dima A. Sabbah, Jonathan L. Vennerstrom, and Haizhen A. Zhong *Journal of Chemical Information and Modeling* 2012 52 (12), 3213-3224. DOI: 10.1021/ci3003057

Dykstra, M., Cherukuri, A., Sohn, H. W., Tzeng, S., & Pierce, S. K. (2003) Location is everything: lipid rafts and immune cell signaling. *Annual Review of Immunology*. 21(1), 457-481. <https://doi.org/10.1146/annurev.immunol.21.120601.141021>

Easthope, S. & Jarvis, B. (2001). Omalizumab. *Drugs*, 61(2), 253-261.

<https://doi.org/10.2165/00003495-200161020-00008>

English Oxford Living Dictionaries (n.d.). Retrieved from

<https://en.oxforddictionaries.com/>

Faustino-Rocha, A.L., Ferreira, R., Gama, A., Oliviera, P.A., & Ginja, M. (2017).

Antihistamines as promising drugs in cancer therapy. *Life Sciences*, *172*, 27-41.

doi:10.1016/j.lfs.2016.12.008Celine

Forli, S., Huey, R., Pique, M.E., Sanner, M.F., Goodsell, D.S. & Olson, A.J. (2016)

Computational protein-ligand docking and virtual drug screening with the

AutoDock suite. *Nature Protocols*, *11*(6), 905-919. doi:10.1038/nprot.2016.051

Forthal, D.N. (2014). Functions of antibodies. *Microbiology Spectrum*, *2*(4), 1-17.

Retrieved from: <https://www.ncbi.nlm.nih.gov/pmc/articles/PMC4159104/>

Frew, A.J. (2010). Allergen immunotherapy. *Journal of Allergy and Clinical Immunology*,

125(2). doi:10.1016/j.jaci.2009.10.064

Fukuishi, N., Murakami, S., Ohno, A., Yamanaka, N., Matsui, N., Fukutsuji, K., . . .

Akagi, M. (2014). Does β -Hexosaminidase Function Only as a Degranulation

Indicator in Mast Cells? The Primary Role of β -Hexosaminidase in Mast Cell

Granules. *The Journal of Immunology*, *193*(4), 1886-1894.

doi:<https://doi.org/10.4049/jimmunol.1302520>

Galli, S.J., Tsai, M., & Piliponsky, A. M. (2008). The development of allergic

inflammation. *Nature*, *454*(7203), 445-454. doi:

<https://doi.org/10.1038/nature07204>

Gericke, A., Leslie, N.R., Lösche, M., & Ross, A.H. (2013). PtdIns(4,5)P₂-mediated cell

signaling: emerging principles and PTEN as a paradigm for regulatory

mechanism. *Advances in Experimental Medicine and Biology*, 991, 85-104.

https://doi.org/10.1007/978-94-007-6331-9_6

Gilfillan, A.M. & Tkaczyk, C. (2006). Integrated signalling pathway for mast cell activation. *Nature Reviews Immunology*, 6, 218-230. doi:10.1038/nri1782

Gu, H., Saito, K., Klaman, L.D., Shen, J., Fleming, T., Wang, Y., ... , & Neel, B.G.

(2001) Essential role for Gab2 in the allergic response. *Nature*, 412, 186. doi:

<https://doi.org/10.1038/35084076>

Hamza, A., Wei, N., & Zhan, C. (2012). Ligand-Based Virtual Screening Approach Using a New Scoring Function. *J. Chem. Inf. Model.* 52(4), 963–974.

<https://doi.org/10.1021/ci200617d>

Hart, T.K., Blackburn, M.N., Brigham-Burke, M., Dede, K., Al-Mahdi, N.,

Zia-Amirhosseini, P., & Cook, R.M. (2002). Preclinical efficacy and safety of

pascalizumab (SB 240683): a humanized anti-interleukin-4 antibody with

therapeutic potential in asthma. *Clinical and Experimental Immunology*, 130(1),

93-100. doi:10.1046/j.1365-2249.2002.01973.x

He, J., Narayanan, S., Subramaniam, S., Qi Ho, W., Lafaille, J., & Curotto de Lafaille, M.

(2015). Biology of IgE Production: IgE Cell Differentiation and the Memory of

IgE Responses. *Current Topics in Microbiology and Immunology*, 388, 1-19.

doi:10.1007/978-3-319-13725-4_1.

Hemmings, B.A. & Restuccia, D.F. (2012). PI3K-PKB/Akt pathway. *Cold Spring Harbor*

Perspectives in Biology, 4(9). doi:10.1101/cshperspect.a011189

- Hiemstra, P.S. & Daha, M.R. (1998). Opsonization. *Encyclopedia of Immunology (Second Edition)*, 1885-1888. doi:10.1006/rwei.1999.0475
- Holgate, S.T. (2014). New strategies with anti-IgE in allergic diseases. *World Allergy Organization Journal*, 7(17), 1-6. doi:10.1186/1939-4551-7-17
- Huang, K. (1989). The mechanism of protein kinase C activation. *Trends in Neurosciences*, 12(11) 425–432., doi:10.1016/0166-2236(89)90091-x.
- Incorvaia, C. & Mauro, M. (2015). Evolution of anti-IgE treatment. *Cellular & Molecular Immunology*,13(3), 409-410. doi:10.1038/cmi.2015.14
- Incorvaia C., Riario-Sforzo G., Ridolo E. (2017). IgE depletion in severe asthma: what we have and what could be added in the near future. *Ebiomedicine*. 17. 16-17, doi:10.1016/j.ebion.2017.02.007.
- Janeway, C.A. Jr., Travers, P., Walport, M., et al. (2001). Immunobiology: The Immune System in Health and Disease. *New York: Garland Science*. 5. Retrieved from: <https://www.ncbi.nlm.nih.gov/books/NBK27144/>
- Jean, S., & Kiger, A.A. (2014). Classes of phosphoinositide 3-kinases at a glance. *Journal of cell science*, 127(5), 923-8. <https://dx.doi.org/10.1242/jcs.093773>
- Kau, A.L. & Korenblat, P.E. (2014). Anti-Interleukin 4 and 13 for asthma treatment in the era of endotypes. *Current Opinion in Allergy and Clinical Immunology*, 14(6), 570–575. <http://doi.org/10.1097/ACI.0000000000000108>
- Kawano, Y., Noma, T., Kou, K., Yoshizawa, I., & Yata, J. (1995). Regulation of human IgG subclass production by cytokines: human IgG subclass production enhanced differentially by interleukin-6. *Immunology*, 84(2), 278–284.

- Kelley LA, Mezulis S, Yates CM, Wass MN, Sternberg MJ. The Phyre2 web portal for protein modeling, prediction and analysis. *Nat Protoc.* 2015 Jun;10(6):845-58. doi: 10.1038/nprot.2015.053. Epub 2015 May 7. PMID: 25950237; PMCID: PMC5298202.
- Kim, H. & Fischer, D. (2011). Anaphylaxis. *Allergy, Asthma, and Clinical Immunology*, 7(1). Retrieved from 10.1186/1710-1492-7-S1-S6.
- Kim, M. J., Kim, E., Ryu, S. H., & Suh, P. (2000). The mechanism of phospholipase C- γ 1 regulation. *Experimental & Molecular Medicine*, 32(3), 101-109. doi:10.1038/emm.2000.18
- Kim, M.S., Rådinger, M., & Gilfillan, A. M. (2008). The multiple roles of phosphoinositide 3-kinase in mast cell biology. *Trends in immunology*, 29(10), 493-501.
- Koyasu, S. (2003). The role of PI3K in immune cells. *Nature*, 4(4). 313-319. <https://doi.org/10.1038/ni0403-313>
- Kuhn K., Bertling, W.M., Emmrich, F. (1993). Cloning of a functional cDNA for human cytidine deaminase (CDD) and its use as a marker of monocyte/macrophage differentiation. *Biochem Biophys Res Commun.* 190(1), 1–7. doi:10.1006/bbrc.1993.1001. PMID 8422236.
- Laffleur, B., Debeaupuis, O., Dalloul, Z., & Cogné, M. (2017). B cell intrinsic mechanisms constraining IgE memory. *Frontiers in Immunology*, 8, 1277. <http://doi.org/10.3389/fimmu.2017.01277>

- Lanser, B.J., Wright, B.L., Orgel, K.A., Vickery, B.P., & Fleischer, D.M. (2015). Current options for the treatment of food allergy. *Pediatric Clinics of North America*, 62(6), 1531–1549. <http://doi.org/10.1016/j.pcl.2015.07.015>
- Laskowski, R.A., Rullmann, J.A.C., MacArthur, M.W. et al. AQUA and PROCHECK-NMR: Programs for checking the quality of protein structures solved by NMR. *J Biomol NMR* 8, 477–486 (1996).
<https://doi.org/10.1007/BF00228148>
- Lavecchia A., Di Giovanni C. (2013). Virtual screening strategies in drug discovery: a critical review. *Curr Med Chem*, 20(23), 2839-2860. doi: 10.2174/09298673113209990001.
- Lionta, E., Spyrou, G., Vassilatis, D. K., & Cournia, Z. (2014). Structure-based virtual screening for drug discovery: principles, applications and recent advances. *Current topics in medicinal chemistry*, 14(16), 1923–1938.
<https://doi.org/10.2174/1568026614666140929124445>
- Liu, M., & Yokomizo, T. (2015). The role of leukotrienes in allergic diseases. *Allergology International*, 64(1), 17-26. doi:10.1016/j.alit.2014.09.001
- Maceyka M., Harikumar K.B., Milstien S., & Spiegel S. (2011). Sphingosine-1-phosphate signaling and its role in disease. *Trends in Cell Biology*. 22(1), 50-60.
- Macmillan, D., & McCarron, J.G. (2010). The phospholipase C inhibitor U-73122 inhibits Ca(2+) release from the intracellular sarcoplasmic reticulum Ca(2+) store

by inhibiting Ca(2+) pumps in smooth muscle. *British journal of pharmacology*, 160(6), 1295–1301. <https://doi.org/10.1111/j.1476-5381.2010.00771.x>

Maddaly, R., Pai, G., Balaji, S., Sivaramakrishnan, P., Srinivasan, L., Shyama Sunder, S., & Paul, S.F.D. (2010). Receptors and signaling mechanisms for B-lymphocyte activation, proliferation and differentiation – Insights from both in vivo and in vitro approaches. *FEBS Letters*. 584(24), 4883-4894.
<https://doi.org/10.1016/j.febslet.2010.08.022>

Marple, B. F., Fornadley, J. A., Patel, A. A., Fineman, S. M., Fromer, L., Krouse, J. H., . . . Penna, P. (2007). Keys to successful management of patients with allergic rhinitis: Focus on patient confidence, compliance, and satisfaction. *Otolaryngology-Head and Neck Surgery*, 136(6_suppl).
doi:10.1016/j.otohns.2007.02.031

Mbuagbaw, L., Aves, T., Shea, B., Jull, J., Welch, V., Taljaard, M., ... & Tugwell, P. (2017). Considerations and guidance in designing equity-relevant clinical trials. *International journal for equity in health*, 16(1), 1-9.

Merriam-Webster. (2007, December 20). *pro-inflammatory*. Retrieved from <https://www.merriam-webster.com/medical/pro-inflammatory>

Metcalf, D.D., Peavy, R.D., & Gilfillan, A.M. (2009) Mechanisms of mast cell signaling in anaphylaxis. *Journal of Allergy and Clinical Immunology*. 124, 639-646.
doi:10.1016/j.jaci.2009.08.035

- Metz, M., Brockow, K., Metcalfe, D.D., & Galli, S.J. (2008). Mast cells, basophils, and mastocytosis. *Clinical Immunology*, 4, 284-297.
doi:10.1016/B978-0-323-04404-2.10022-3
- Miller, M. S., Maheshwari, S., McRobb, F. M., Kinzler, K. W., Amzel, L. M., Vogelstein, B., & Gabelli, S. B. (2017). Identification of allosteric binding sites for PI3K α oncogenic mutant specific inhibitor design. *Bioorganic & Medicinal Chemistry*, 25(4), 1481–1486. <https://doi.org/10.1016/j.bmc.2017.01.012>
- Mizugishi, K., Yamashita, T., Olivera, A., Miller, G.F., Spiegel, S., & Proia, R.L. (2005). Essential role for sphingosine kinases in neural and vascular development. *Molecular and Cell Biology*, 25, 11113–11121. doi: 10.1128/MCB.25.24.11113-11121.2005
- Molnar, C. & Gair, J. (2013). 23.2. Adaptive immune response. In *Concepts of Biology-1st Canadian Edition* (1st ed.). Retrieved from <https://opentextbc.ca/biology/chapter/23-2-adaptive-immune-response/>
- Nagai, H., Teramachi, H., & Tuchiya, T. (2006). Recent Advances in the development of anti-allergic drugs. *Allergology International*, 55(1), 35-42.
doi:10.2332/allergolint.55.35
- NCI Dictionary of Cancer Terms. (n.d.). Retrieved from <https://www.cancer.gov/publications/dictionaries/cancer-terms/def/enzyme-linked-immunosorbent-assay>

- Noris, M. & Remuzzi, G. (2013). Overview of Complement Activation and Regulation. *Seminars in Nephrology*, 33(6), 479-492. doi:10.1016/j.semnephrol.2013.08.001
- Nyborg, A. et al. (2015). Development of an antibody that neutralizes soluble IgE and eliminates IgE expressing B cells. *Cellular & Molecular Immunology*, 13(3), 391-400. doi:10.1038/cmi.2015.19
- Oettgen, H.C. & Burton, O.T. (2015). IgE Receptor Signaling in Food Allergy Pathogenesis. *Current Opinion in Immunology*, 36, 109-114. doi: 10.1016/j.coi.2015.07.007
- Olivera, A., Kohama, T., Edsall, L., Nava, V., Cuvillier, O., Poulton, S., & Spiegel, S. (1999). Sphingosine kinase expression increases intracellular sphingosine-1-phosphate and promotes cell growth and survival. *The Journal of Cell Biology*, 147(3), 545-558. doi: 10.1083/jcb.147.3.545
- Olivera, A. & Rivera, J. (2005). Sphingolipids and the balancing of immune cell function: lessons from the mast cell. *J. Immunol*, 174(3), 1153–1158. <https://doi.org/10.4049/jimmunol.174.3.1153>
- Orengo, J. M., Radin, A. R., Kamat, V., Badithe, A., Ben, L. H., Bennett, B. L., . . . Yancopoulos, G. D. (2018). Treating cat allergy with monoclonal IgG antibodies that bind allergen and prevent IgE engagement. *Nature Communications*, 9(1), 1421. doi:10.1038/s41467-018-03636-8
- Oskeritzian, C.A., Milstien, S., & Spiegel, S. (2007). Sphingosine-1-phosphate in allergic responses, asthma and anaphylaxis. *Pharmacol Ther*, 115(3), 390-9. doi: 10.1016/j.pharmthera.2007.05.011

"Overview of ELISA", (n.d.). *Thermo Fisher Scientific*. Retrieved from

<https://www.thermofisher.com/us/en/home/life-science/protein-biology/protein-biology-learning-center/protein-biology-resource-library/pierce-protein-methods/overview-elisa.html>

Parravicini, V., Gadina, M., Kovarova, M., Odom, S., Gonzalez-Espinosa, C., Furumoto, Y., ... & Rivera, J. (2002). Fyn kinase initiates complementary signals required for IgE-dependent mast cell degranulation. *Nature Immunology*, 3(8), 741-748. doi: 10.1038/ni817

Peng, Z. & Beaven, M.A. (2005). An essential role for phospholipase D in the activation of protein kinase C and degranulation in mast cells. *The Journal of Immunology*, 174(9), 5201–5208. doi:10.4049/jimmunol.174.9.5201

Pohlit, H., Bellinghausen, I., Frey, H., & Saloga, J. (2017). Recent advances in the use of nanoparticles for allergen-specific immunotherapy. *Allergy*, 72(10), 1461–1474. <https://doi.org/10.1111/all.13199>

Rivera, J. & Gilfillan, A. M. (2006). Molecular regulation of mast cell activation. *Molecular Mechanisms in Allergy and Clinical Immunology*, 117(6), 1214-1225. doi:10.1016/j.jaci.2006.04.015

Satoh, T., Moroi, R., Aritake, K., Urade, Y., Kanai, Y., Sumi, K., Nakamura, M. et al. (2006). Prostaglandin D2 plays an essential role in chronic allergic inflammation of the skin via CRTH2 receptor. *The Journal of Immunology*, 177(4), 2621-2629. doi:10.4049/jimmunol.177.4.2621

Schroeder, H.W. & Cavacini, L. (2010). Structure and function of immunoglobulins.

Journal of Allergy and Clinical Immunology, 125(202), S41–S52.

doi:10.1016/j.jaci.2009.09.046

Serra-Pages, M., Olivera, A., Torres, R., Picado, C., de Mora, F., & Rivera, J. (2012).

E-prostanoid 2 receptors dampen mast cell degranulation via

cAMP/PKA-mediated suppression of IgE-dependent signaling. *Journal of*

Leukocyte Biology, 92(6), 1155-1165.

Siddiqi, A.R., Srajer, G.E., & Leslie, C.C. (2000). Regulation of human PLD1 and PLD2

by calcium and protein kinase C. *Biochimica Et Biophysica Acta (BBA) -*

Molecular Cell Research, 1497(1), 103–114.

doi:10.1016/s0167-4889(00)00049-5.

Silwal, P., Shin, K., Choi, S., Kang, S.W., Park, J.B., Lee, H., . . . Park, S.K. (2015).

Adenine suppresses IgE-mediated mast cell activation. *Molecular Immunology*,

65(2), 242-249. doi:10.1016/j.molimm.2015.01.021

Singer, W.D., Brown, H.A., Jiang, X., & Sternweis, P.C. (1996). Regulation of

phospholipase D by protein kinase C is synergistic with ADP-ribosylation factor

and independent of protein kinase activity. *Journal of Biological Chemistry*,

271(8). 4504–4510. doi:10.1074/jbc.271.8.4504.

Spinello, R. A. (1992). Ethics, Pricing and the Pharmaceutical Industry. *Journal of*

Business Ethics, 11, 617–626. <https://doi.org/10.1007/BF00872273>

- Stavnezer, J., Guikema, E.J., & Schrader, C.E. (2008). Mechanism and regulation of class switch recombination. *Annual Review of Immunology*, 26, 261-292. doi: 10.1146/annurev.immunol.26.021607.090248
- Stavnezer, J. & Schrader, C.E. (2014). Ig heavy chain class switch recombination: mechanism and regulation. *Journal of Immunology*, 193(11), 5370–5378. <http://doi.org/10.4049/jimmunol.1401849>
- Stone, K.D., Prussin, C., & Metcalfe, D.D. (2010). IgE, Mast Cells, Basophils, and Eosinophils. *Journal of Allergy and Clinical Immunology*, 125(2), 73-80. doi:10.1016/j.jaci.2009.11.017
- Sun, W.Y. & Bonder, C.S. (2012). Sphingolipids: a potential molecular approach to treat allergic inflammation. *Journal of Allergy*, 2012, doi:10.1155/2012/154174
- Sun, Y., & Sundell, J. (2011). Life style and home environment are associated with racial disparities of asthma and allergy in Northeast Texas children. *Science of The Total Environment*, 409(20), 4229–4234. <https://doi.org/10.1016/j.scitotenv.2011.07.011>
- Trott, O., Olson, A.J., AutoDock Vina: improving the speed and accuracy of docking with a new scoring function, efficient optimization and multithreading, *Journal of Computational Chemistry* 31 (2010) 455-461
- Vanhaesebroeck, B., Guillermet-Guibert, J., Graupera, M., & Bilanges, B. (2010). The emerging mechanisms of isoform-specific PI3K signalling. *Nature Reviews Molecular Cell Biology*, 11, 329–341. doi: 10.1038/nrm2882

- Vidarsson, G., Dekkers, G., & Rispens, T. (2014). IgG subclasses and allotypes: from structure to effector functions. *Frontiers in Immunology*, 4, 1-17.
doi:10.3389/fimmu.2014.00520
- Walker, E.H., Pacold, M.E., Perisic, O., Stephens, L., Hawkins, P.T., Wymann, M.P., & Williams, R.L. (2000). Structural determinants of phosphoinositide 3-kinase inhibition by wortmannin, LY294002, quercetin, myricetin, and staurosporine. *Molecular Cell*, 6(4), 909-919. doi:10.1016/S1097-2765(05)00089-4
- Warren, C. M., Turner, P. J., Chinthrajah, R. S., & Gupta, R. S. (2021). Advancing Food Allergy Through Epidemiology: Understanding and Addressing Disparities in Food Allergy Management and Outcomes. *The journal of allergy and clinical immunology. In practice*, 9(1), 110–118.
<https://doi.org/10.1016/j.jaip.2020.09.064>
- Warrington, R., Watson, W., Kim, H. L., & Antonetti, F.R. (2011). An introduction to immunology and immunopathology. *Allergy, Asthma, & Clinical Immunology*, (7), 1-8. doi:10.1186/1710-1492-7-S1-S1
- Wegienka, G., Havstad, S., Joseph, C. L., Zoratti, E., Ownby, D., Woodcroft, K., & Johnson, C.
C. (2011). Racial disparities in allergic outcomes in African Americans emerge as early as age 2 years. *Clinical & Experimental Allergy*, 42(6), 909–917.
<https://doi.org/10.1111/j.1365-2222.2011.03946>.
- Wiederstein, M., & Sippl, M. J. (2007). ProSA-web: Interactive web service for the recognition

of errors in three-dimensional structures of proteins. *Nucleic Acids Research*, 35(Web Server). doi:10.1093/nar/gkm290

World Allergy Organization (WAO) White Book on Allergy. Edited by: Pawankar R, Canonica GW, Holgate ST, Lockey RF. 2011, Milwaukee, WI: WAO

World Health Organization. Equity in access to public health-report and documentation of the

technical discussions. No. SEA-HSD-240. WHO Regional Office for South-East Asia, 2000.

Xu, D., & Zhang, Y. (2011). Improving the physical realism and structural accuracy of PROTEIN models by a Two-Step ATOMIC-LEVEL energy minimization.

Biophysical Journal, 101(10), 2525-2534. doi:10.1016/j.bpj.2011.10.024